

UNCLASSIFIED

AD NUMBER

ADB008942

LIMITATION CHANGES

TO:

Approved for public release; distribution is unlimited.

FROM:

Distribution authorized to U.S. Gov't. agencies only; Test and Evaluation; 01 MAR 1975. Other requests shall be referred to Aeronautical Systems Division, ATTN: ASD/XRG, Wright-Patterson AFB, OH 45433.

AUTHORITY

ASD ltr dtd 11 Jun 1980

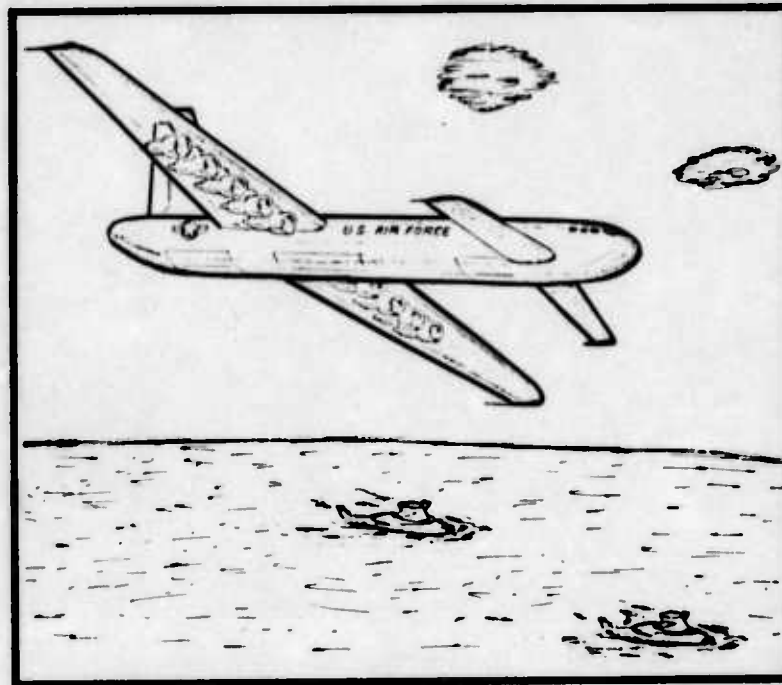
THIS PAGE IS UNCLASSIFIED

THIS REPORT HAS BEEN DELIMITED
AND CLEARED FOR PUBLIC RELEASE
UNDER DOD DIRECTIVE 5200.20 AND
NO RESTRICTIONS ARE IMPOSED UPON
ITS USE AND DISCLOSURE.

DISTRIBUTION STATEMENT A

APPROVED FOR PUBLIC RELEASE;
DISTRIBUTION UNLIMITED.

NUCLEAR AIRCRAFT FEASIBILITY STUDY
VOLUME II. APPENDICES



AD B 0 0 8 9 4 2

1975
GRADUATE CLASS
OF
SYSTEMS ENGINEERING

MARCH 1975

SCHOOL OF ENGINEERING
AIR FORCE INSTITUTE OF TECHNOLOGY
WRIGHT-PATTERSON AIR FORCE BASE, OHIO

AD No.
DDC FILE COPY

B B C
RECEIVED
FEB 5 1976
RECEIVED
A

NOTICE

This effort was accomplished for the purposes of illuminating problem areas in the context of a total weapon system concept and assessing the impact of different propulsion system design approaches upon the total aircraft system weight and performance. It was performed as a thesis research effort by AFIT students, and the resultant weapon system design concept is the product of the design constraints selected by the students. The influences of two of these constraints, the fuselage volume allotted per crew member, and the design wing loading are such that the resulting aircraft system size, weight, and power requirements are considerably larger than those obtained during previous in-house studies or those reported by other competent investigators examining similar mission requirements. Thus, it is important to note that the design constraints, subsystem tradeoffs, aircraft configuration selection and subsystem integration tasks were totally accomplished by the students and are, therefore, not to be construed in any way as reflecting the opinion or thinking of the Air Force or the Deputy for Development Planning.

Dr. Larry W. Noggle
ASD/XR (AFSC)
Wright-Patterson AFB OH 45433

SEARCHED	INDEXED
SERIALIZED	FILED
<i>Letter on file</i>	
B	

REPORT DOCUMENTATION PAGE		READ INSTRUCTIONS BEFORE COMPLETING FORM
1. REPORT NUMBER GSF/SE/75-1-Vol-2	2. GOVT ACCESSION NO.	3. RECIPIENT'S CATALOG NUMBER
4. TITLE (and Subtitle) NUCLEAR AIRCRAFT FEASIBILITY STUDY, (VOL II) Volume II. Appendices.		5. TYPE OF REPORT & PERIOD COVERED MASTERS THESIS
7. AUTHOR(s) M. W. AMOS, J. S. BUTT, B. L. CAMPBELL, R. G. DIEHL, W. J. FANNING, JR., G. M. LACY, R. J. LUCZAK, E. M. MOORMAN, JR., J. W. SHATTUCK, V. K. WILKINSON		8. CONTRACT OR GRANT NUMBER(s) 1287p
9. PERFORMING ORGANIZATION NAME AND ADDRESS AIR FORCE INSTITUTE OF TECHNOLOGY (AFIT/EN) WRIGHT-PATTERSON AFB OH 45433		10. PROGRAM ELEMENT, PROJECT, TASK AREA & WORK UNIT NUMBERS P. E. 6 3737F
11. CONTROLLING OFFICE NAME AND ADDRESS AERONAUTICAL SYSTEMS DIVISION (ASD/XR) WRIGHT-PATTERSON AFB OH 45433		12. REPORT DATE March 1975
14. MONITORING AGENCY NAME & ADDRESS (if different from Controlling Office) Distribution limited to U.S. Gov't. agencies only Test and Evaluation; 1 MAR 75. Other requests for this document.		13. NUMBER OF PAGES 88
16. DISTRIBUTION STATEMENT (of this Report) Prepared to [redacted] approval of ASD/XR Wright-Patterson AFB OH 45433. (9) Rept. for 1 Mar 74 - 7 Feb 75		15. SECURITY CLASS. (of this report) UNCLASSIFIED
17. DISTRIBUTION STATEMENT (of the abstract entered in Block 20, if different from Report) Approved for public release; distribution unlimited.		15.1. DECLASSIFICATION/DOWNGRADING SCHEDULE
18. SUPPLEMEN (10) Michael W. /Amos, James S. /Butt, Bruce L. /Campbell, Richard G. /Diehl William J. /Fanning, Jr		
19. KEY WORDS (Continue on reverse side if necessary and identify by block number) Nuclear propulsion, fault tree analysis, event tree analysis, heat transfer, life cycle cost, nuclear aircraft, weight estimation, anti-submarine, reactor power, large aircraft design, long endurance aircraft, nuclear safety, helium cooled reactor, liquid-metal cooled reactor.		
20. ABSTRACT (Continue on reverse side if necessary and identify by block number) The objective of this study was to assess the feasibility of applying nuclear propulsion to aircraft in performance of the Air Force mission. This was accomplished by using a systems approach with the system divided into six areas: (1) Mission Selection, (2) Required Mission Avionics, (3) Aircraft Design, (4) Propulsion System Design, (5) Public Safety, and (6) Cost. The overriding constraint of the study was the assumption that technology would limit an aircraft gross weight to 2,000,000 lbs in the 1990s. At this		

UNCLASSIFIED

SECURITY CLASSIFICATION OF THIS PAGE(When Data Entered)

gross weight, an aircraft built using conventional construction methods and powered by a liquid metal cooled nuclear reactor, but using only chemical fuel for takeoff, would have a negative payload of 120,000 lbs. If the aircraft were constructed using advanced composites and a liquid metal cooled reactor with chemical augmentation for takeoff, the payload would be 470,000 lbs. By switching the liquid metal reactor for a similarly constructed helium cooled reactor, the payload would drop from 470,000 lbs to 210,000 lbs. For each individual in the U.S., the risk of being killed by the radioactive particles associated with one of the airborne 574 MW reactors, would be 9.34×10^{-8} per year, which is less risk than that of being struck by lightning. The 52,000 hr airframe life cycle cost was estimated to be \$26.4 billion for 60 aircraft.

UNCLASSIFIED

SECURITY CLASSIFICATION OF THIS PAGE(When Data Entered)

PREFACE

This report was prepared by the 1975-M Graduate Systems Engineering Class (GSE-75M) at the Air Force Institute of Technology (AFIT), Wright-Patterson AFB, Ohio, in partial fulfillment of requirements for the Master of Science degree. This is not an official Air Force Design Study. The work was sponsored by the Propulsion and Energy Division, Deputy for Development Planning, Aeronautical Systems Division, Air Force Systems Command, Wright-Patterson AFB, Ohio. Authors of this report are the following 10 members of the AFIT GSE-75M class:

- Capt. Michael W. Amos, USAF
- Maj. James S. Butt, USAF
- Lt. Bruce L. Campbell, USAF
- Capt. Richard G. Diehl, USAF
- Maj. William J. Fanning, Jr., USAF
- Capt. George M. Lacy, Jr., USAF
- Capt. Ralph J. Luczak, USAF
- Maj. Edwin M. Moorman, Jr., USAF
- Capt. Julian W. Shattuck, USAF
- Maj. Vance K. Wilkinson, USAF

AFIT faculty members who advised and assisted the class are:

- Dr. D. Wallace Breuer
- Dr. Charles J. Bridgman
- Capt. James T. Karam, Jr., USAF
- Maj. Louis T. Montulli, USAF
- Dr. Lynn E. Wolaver
- Dr. Norman K. Womer

Technical work was conducted during the period 1 March 1974 to 7 February 1975. The final report was submitted on 14 March 1975.

Special appreciation is given to Col. James H. Hall, Deputy for Development Planning, ASD, and Dr. Larry W. Noggle, Nuclear Propulsion Technology Program Manager, ASD, for their close support and cooperation in all phases of the study.

Special recognition is given to the following for their cooperation in providing technical assistance in all phases of the study:

- Mr. Gary Averill, Naval Air Development Center.
- Maj. George T. Babbitt, USAF
- Mr. & Mrs. William Bustard, AFIT
- Mr. George Eck, Naval Air Development Center
- Dr. William C. Elrod, AFIT
- Mr. Anthony R. Haki, Westinghouse Astronuclear Laboratory
- Dr. James E. Hitchcock, AFIT
- Prof. Harold C. Larsen, AFIT
- Capt. King L. Mills, III, USAF
- Mr. David Panetta, Naval Air Development Center.
- Mr. Robert E. Thompson, Westinghouse Astronuclear Laboratory
- Maj. Jack L. Wolff, USAF

The report consists of three volumes: Volume I, *Final Report*; Volume II, *Appendices*; and Volume III, *Classified Annex*.

TABLE OF CONTENTS

Appendix	Page
A.4 Aircraft	A.4-1
A.4.1 Sample Calculations	A.4-1
A.4.1.1 Structural Weight (Section 4.1.1)	A.4-1
A.4.1.2 Takeoff Thrust (Section 4.1.2.1)	A.4-2
A.4.1.3 Chemical Engine Weight (Section 4.1.2.2)	A.4-2
A.4.1.4 Chemical Fuel Weight (Section 4.1.3)	A.4-2
A.4.1.5 Fixed Equipment Weight (Section 4.1.4)	A.4-2
A.4.1.6 L/D Calculation (Section 4.1.5.1)	A.4-2
A.4.1.7 Nuclear Reactor System Weight (Section 4.1.5)	A.4-3
A.4.1.8 Payload (Section 4.1.6)	A.4-4
A.4.1.9 Takeoff Performance (Section 4.4.1)	A.4-4
A.4.1.10 Climb Performance (Section 4.4.2)	A.4-4
A.4.1.11 Cruise Performance (Section 4.4.4)	A.4-4
A.4.1.12 Descent Performance (Section 4.4.5)	A.4-5
A.4.1.13 Landing Performance (Section 4.4.6)	A.4-6
A.4.1.14 Aircraft Tires (Section 4.3.7.1)	A.4-6
A.4.1.15 Landing Gear Strut (Section 4.3.7.2)	A.4-7
A.4.1.16 Aircraft Component Size and Weight	A.4-7
A.4.1.17 Aircraft Weight and Balance (Section 4.3.8.1)	A.4-10
A.4.1.18 Wing Section Properties (Section 4.3.4.5)	A.4-11
A.4.1.19 Rib Spacing Calculation (Section 4.3.4.6)	A.4-12
A.4.1.20 Divergence Speed (Section 4.3.4.7)	A.4-12
A.4.1.21 Reactor Mounting Structure	A.4-13
A.4.2 Computer Program Logic Charts	A.4-15
A.4.2.1 Aircraft Parameter Logic	A.4-15
A.4.2.2 Wing Analysis Logic	A.4-21
A.4.3 Airfoil Characteristics	A.4-26
A.6 Engines	A.6-1
A.6.1 Reliability	A.6-1
A.6.2 Derivation of Optimum Equations for the Brayton Cycle	A.6-3
A.6.3 Methodology Used in Indirect Cycle Heat Exchanger Engine Analysis	A.6-5
A.6.4 Sample Calculation of the Heat Exchanger Turbofan Engine	A.6-7
A.6.5 Additional Graphs for the Heat Exchanger Turbofan Engine	A.6-12
A.6.6 Flow Diagram of Computer Program Used for the Direct Cycle	A.6-15
A.6.7 Sample Calculation for the Direct Cycle	A.6-16
A.7 Heat Transfer	A.7-1
A.7.1 Piping Calculations	A.7-1
A.7.2 Tube Length Calculation Computer Logic	A.7-4
A.8 Safety Analysis	A.8-1
A.8.0 Introduction	A.8-1

next
page

cont

TABLE OF CONTENTS (Continued)

A.8.1	Release Probability Data	A.8-1
A.8.1.1	Crash Data	A.8-1
A.8.1.2	Aircraft System Failure Rates	A.8-6
A.8.1.3	Nuclear System Data	A.8-7
A.8.1.4	Containment Vessel Impact Data	A.8-8
A.8.2	Reactor Safety Study Validation	A.8-11
A.8.2.1	Magnitude of Release	A.8-11
A.8.2.2	Dispersion Model	A.8-13
A.8.2.3	Population Model	A.8-17
A.8.2.4	Medical Effects	A.8-19
A.8.3	Computer Logic Diagrams	A.8-24
A.9	Life Cycle Cost	A.9-1
A.9.1	Reactor	A.9-1
A.9.2	Avionics	A.9-3

LIST OF FIGURES

Figure		Page
A.4.2.1-1	Aircraft Design Parameters	A.4-16
A.4.2.1-2	Aircraft Parameter Logic	A.4-17
A.4.2.2-1	Wing Design Variables	A.4-21
A.4.2.2-2	Wing Analysis Logic	A.4-22
A.4.3-1	Airfoil Shape Coordinates	A.4-26
A.4.3-2	Root Section Characteristics	A.4-27
A.4.3-3	Tip Section Characteristics	A.4-28
A.6.1-1	Reliability of Engine System Concepts and Combinations	A.6-2
A.6.3-1	Computer Logic for CARPET	A.6-6
A.6.3-2	Simplified Flow Diagram for CARPET	A.6-7
A.6.4-1	Stations in Nuclear Engine	A.6-8
A.6.5-1	Overall Engine Pressure Ratio vs Net Thrust	A.6-13
A.6.5-2	Horsepower Extracted vs Net Thrust	A.6-13
A.6.5-3	Horsepower Extracted vs Net Thrust	A.6-14
A.6.5-4	Overall Engine Pressure Ratio vs Net Thrust	A.6-14
A.6.6-1	Computer Logic for Direct Cycle Engine	A.6-15
A.7.1-1	Concentric Pipe Cross Section	A.7-1
A.8.1.4.2-1	Soil Impact Burial	A.8-10
A.8.2.2-1	Vertical Concentration Distribution	A.8-14
A.8.2.3-1	Dose vs Probability of Death	A.8-19
A.8.3-1	Fault Tree Logic	A.8-25
A.8.3-2	Event Tree Logic	A.8-26

LIST OF TABLES

Table		Page
A.4.1	Component Weights (Ref. 33, Ch. 4, p. 41)	A.4-8
A.8.1.1.1-1	Aircraft Crash Rates	A.8-2
A.8.1.1.1-2	K-S Test of Failure Rates	A.8-2
A.8.1.1.2-1	Airport Crash Impact Speeds	A.8-4
A.8.1.1.2-2	Cruise Crash Impact Speeds	A.8-4
A.8.1.1.3-1	Airport Crash Impact Angles	A.8-5
A.8.1.1.3-2	Cruise Crash Impact Angles	A.8-5
A.8.1.1.3-3	Crash Impact Angle Probability Distribution	A.8-5
A.8.1.2.1-1	Aircraft Electrical System Failure Rates	A.8-6
A.8.1.2.2-1	Engine Failure Rates	A.8-6
A.8.1.3-1	Nuclear System Failure Rates	A.8-7
A.8.1.4-1	Containment Vessel Impact Tests	A.8-8
A.8.1.4.2-1	Depth of Burial Probability Distribution	A.8-11
A.8.2.1-1	Set of Initial Activity of Fission Products Used in Model	A.8-12
A.8.2.1-2	Amount of Radioactive Isotopes Released when Fissionized UO ₂ Melts	A.8-13
A.8.2.2-1	Meteorological Parameters	A.8-15
A.8.2.3-1	Cumulative Propulation (Thousands) of Categories as Selected Distances for a 22½° Sector	A.8-18
A.8.2.4-1	Inhalation Dose Factors (REM/CI) x 10 ³	A.8-21
A.8.2.4-2	Average Decay Energies and Dose Factors for Ground Deposition and Cloud Shine	A.8-22
A.9.6-1	Avionics Cost vs Reliability for a 14 Day Mission	A.9-3

APPENDIX A.4 AIRCRAFT

A.4.1 SAMPLE CALCULATIONS

Section 4 presented the method used in designing the nuclear powered aircraft. A numerical example of calculations is now shown. The specifications are as follows:

- a) $GW = 2,000,000$ lbs
- b) $W/S = 60$ lbs/sq ft.
- c) $t/c = 0.18$ at the wing root
- d) $\lambda = 0.4$
- e) $AR = 9$
- f) Runway length = 10,000 ft
- g) Fuselage = 40 ft x 428 ft
- h) $C_{LMAX} = 2$ (Flaps)
- i) $C_{LMAX} = 1$ (No flaps)
- j) $\sigma = 0.926$
- k) $LF = 2.5$
- l) τ_a = allowable stress for 2024 aluminum
- m) E_c = modulus of elasticity in compression
 $E_c = 10.7 \times 10^6$ psi for 2024 aluminum
 $E_c = 29.0 \times 10^6$ psi for 4130 steel
- n) M_{MAC} = bending moment at wing MAC
 $= 21,800,000$ ft-lb
- o) P_{MAC} = shear load at wing MAC = 355,100 lbs
- p) h_{1MAC} = height of beam envelope at wing MAC = 8.06 ft
- q) l_{1MAC} = chordwise length of beam envelope at wing MAC = 34.15 ft

A.4.1.1 STRUCTURAL WEIGHT (SECTION 4.1.1):

By Eq. 4.1.1-1

$$\text{Structural weight} = \left[0.16 GW + \frac{9.8 GW}{(100/W/S)^{0.63} W/S} \right] K_{t/c} K_{AR} K_{\lambda}$$

$$K_{t/c} = 0.86$$

$$K_{AR} = 0.95 \quad (\text{Ref.33, Ch. 2, p. 32})$$

$$K_{\lambda} = 1.00$$

therefore: Structural Weight = 455,000 lbs

A.4.1.2 TAKEOFF THRUST (SECTION 4.1.2.1):

Takeoff distance = 10,000 ft

From Fig. 4.1.2.1-1, $K = 430$

$$C_{LTO} = 0.75 C_{LMAX} = 1.5$$

$$\text{Eq. 4.1.2-1, } K = (W/S)(W/T)(1/C_{LTO})(1/\sigma)$$

$$\text{therefore: } W/T = K C_{LTO} \sigma / (W/S)$$

$$W/T = 9.9$$

Available $W/T = 8.91$ (90% of W/T)

Takeoff thrust = 225,000 lbs

A.4.1.3 CHEMICAL ENGINE WEIGHT (SECTION 4.1.2.2): The aircraft must have the capability to complete takeoff if one chemical engine is lost during takeoff (Ref. 116, p. 13).

Use six 50,000 lb thrust engines.

$$\text{Eq. 4.1.2-2 Engine weight} = \text{EXP} \left[\frac{\ln(\text{thrust}) + 1.36}{1.349} \right]$$

Engine weight = 8,333 lbs/engine

Total weight = 50,000 lbs

A.4.1.4 CHEMICAL FUEL WEIGHT (SECTION 4.1.3): Fuel weight = 0.16 GW

Fuel weight = 320,000 lbs

A.4.1.5 FIXED EQUIPMENT WEIGHT (SECTION 4.1.4): Fixed equipment weight = 0.10 GW.

Fixed equipment weight = 200,000 lbs

A.4.1.6 L/D CALCULATION (SECTION 4.1.5.1): Let aircraft speed = 350 kts (mission requirement) at 30,000 ft.

$$\rho = 0.00089 \text{ slugs/cu ft}$$

$$V = 591 \text{ ft/sec}$$

$$S_w = GW/(W/S) = 33,333 \text{ sq ft}$$

$$\text{Eq. 4.1.5-3 } C_L = 2 \text{ GW}/(\rho S_W V^2)$$

$$C_L = 0.386$$

$$\text{Eq. 4.1.5-6 } F = 129 + 0.007 S_W + (0.0021)(\text{Number of engines})(T/\text{engine})^{0.7}$$

From A.4.1.3: Six 50,000 lb thrust engines required.

$$F = 387.$$

$$\text{Eq. 4.1.5-5 } C_{DP} = F/S_W$$

$$C_{DP} = 0.0116$$

$$\text{Eq. 4.1.5-7 } C_{DI} = C_L^2/(\pi AR e)$$

$$C_{DI} = 0.00659$$

$$C_{DC} = 0.002 \text{ (Ref. 33, Ch. 2, p. 44)}$$

$$\text{Eq. 4.1.5-4 } C_D = C_{DP} + C_{DI} + C_{DC}$$

$$C_D = 0.02019$$

$$\text{Eq. 4.1.5-2 } L/D = C_L/C_D$$

therefore: $L/D = 19.12$

A.4.1.7 NUCLEAR REACTOR SYSTEM WEIGHT (SECTION 4.1.5):

By Eq. 4.1.5-1: $T = \text{GW}/(L/D)$ and $\text{Power} = TV$

From A.4.1.6: $V = 581 \text{ ft/sec}$ and $L/D = 19.12$

therefore: $T = 105,000 \text{ lbs}$

$$\text{Power} = 61,820,000 \text{ ft-lb/sec} = 84 \text{ MW}$$

At 35% efficiency and 15% for additional power (Section 4.1.5.2)

$$\text{Reactor power} = (\text{Power})(1/.35)(1.15)$$

$$\text{Reactor power} = 275.4 \text{ MW}$$

From Figure 4.1.5.2-1 (Gas Reactor): Reactor system weight = 603,000 lbs

A.4.1.8 PAYLOAD (SECTION 4.1.6):

$$\text{Payload} = \text{GW} - (\text{Structural} + \text{Engine} + \text{Fuel} + \text{Fixed} + \text{Reactor})$$

$$\text{therefore: Payload} = 372,000 \text{ lbs}$$

A.4.1.9 TAKEOFF PERFORMANCE (SECTION 4.4.1):

$$\text{By Eq. 4.4.1-1 } V = (2 \text{ GW} / (\rho S_T C_{LTO}))^{1/2}$$

$$\text{Let } \rho = 0.00231 \text{ Slugs/cu ft (1,000 ft field elevation)}$$

$$C_{LMAX} = 2; C_{LTO} = 1.5$$

$$V = 186 \text{ ft/sec} = 110 \text{ kts}$$

A.4.1.10 CLIMB PERFORMANCE (SECTION 4.4.2):

$$R/C = 600 \text{ fpm} = 10 \text{ ft/sec (mission requirement) at sea level}$$

$$\rho = 0.002378 \text{ slugs/cu ft; } C_L = 0.4 \text{ (angle of attack function)}$$

$$\text{By Eq. 4.4.2-2: } T_C = \frac{\text{GW } R/C (\rho S_T C_L)^{0.5}}{(2 \text{ GW})^{0.5}}$$

$$\text{therefore: } T_C = 56,300 \text{ lbs additional thrust required at sea level}$$

$$\text{At service ceiling of 40,000 ft: } R/C = 100 \text{ fpm}$$

$$\rho = 0.0005857 \text{ slugs/cu ft}$$

$$\text{By Eq. 4.4.2-2: } T_C = 4700 \text{ lbs additional thrust required at service ceiling}$$

A.4.1.11 CRUISE PERFORMANCE (SECTION 4.4.4):

$$\text{Maximum L/D} = 20.30 \text{ (determined by iteration of L/D equation over a range of V)}$$

$$\text{Cruise L/D} = 0.8 \text{ Maximum L/D} = 16.24 \text{ (Refs. 9 and 94)}$$

$$\text{By Eq. 4.1.5-1: Cruise thrust} = \text{GW/Cruise L/D}$$

$$\text{Cruise thrust} = 123,000 \text{ lbs}$$

$$\text{By Eq. 4.4.4-1}$$

$$V = \left[\frac{\text{GW} \left\{ 1 + \left[1 - 4 (L/D)^2 \left(\frac{C_{DP} + C_{DC}}{2.51 AR} \right) \right]^{1/2} \right\}}{\rho S_T L/D (C_{DP} + C_{DC})} \right]^{1/2}$$

$$\rho = 0.000890 \text{ slugs/cu ft (30,000 ft)}$$

therefore: with data from A.4.1.6: $V = 640 \text{ ft/sec} = 379 \text{ kts}$

A.4.1.11.1 STALL SPEED/THRUST (SECTIONS 4.4.4.1 AND 4.4.4.2):

$$\text{By Eq. 4.4.1-1: } V = \left(\frac{2 \text{ GW}}{\rho S_T C_{LMAX}} \right)^{1/2}$$

$$\rho = .000890 \text{ slugs/cu ft}$$

$$V_{\text{STALL}} = 367 \text{ ft/sec} = 217 \text{ kts}$$

$$\text{By Eq. 4.4.4-2: Stall L/D} = \frac{C_{LMAX}}{C_{DP} + C_{DC} + \frac{C_{LMAX}^2}{\pi AR e}}$$

$$\text{Stall thrust} = \text{GW}/(\text{Stall L/D}) = 115,600 \text{ lbs}$$

since required cruise thrust is greater than required stall thrust.

$$\text{By Eq. 4.4.2-3: Total thrust} = \text{Climb thrust} + \text{MAX (Cruise thrust or Stall thrust)}$$

therefore: Total thrust = 138,000 lbs at 30,000 ft

A.4.1.11.2 MAXIMUM SPEED (SECTION 4.4.4.3):

$$\text{L/D at } V_{\text{MAX}} = \text{GW}/T_T = 14.49$$

therefore by Eq. 4.4.4-1 (above)

$$V = 777 \text{ ft/sec} = 460 \text{ kts} = \text{Mach } 0.78$$

A.4.1.12 DESCENT PERFORMANCE (SECTION 4.4.5):

Maximum R/D = 8000 fpm (mission requirement)

By Eq. 4.4.5-2

$$S_s = \frac{2 \text{ GW}}{\rho V^2 C_{DS} \sin \phi} \left(\frac{R/D}{V} - \frac{1}{L/D} \right)$$

$$C_{DS} = 1 \text{ (Ref. 73, Ch. 13, p. 11)}$$

$$V = 640 \text{ ft/sec, L/D} = 16.24 \text{ (From A.4.1.11)}$$

$\phi = 60^\circ$ (Figure 4.4.5-1)

$\rho = 0.000890$ (30,000 ft)

therefore: $S_s = 3321$ sq ft of speed brakes

A.4.1.13 LANDING PERFORMANCE (SECTION 4.4.6):

By Eq. 4.4.6-1:

$$d_{50} = L/D \left(\frac{V_{50}^2 - V_{TD}^2}{2g} + 50 \right)$$

By Section A.4.1.6 with $C_{LMAX} = 2$: $L/D = 10.50$

By Eq. 4.4.1-1: $V_{SO} = [2 GW/(\rho S_T C_{LMAX})]^{1/2}$

$V_{SO} = 166$ ft/sec = 98 kts at 3000 ft field elevation

$V_{50} = 1.3 V$; $V_{TD} = 1.15 V$

$V_{50} = 216$ ft/sec = 130 kts; $V_{TD} = 191$ ft/sec = 113 kts

therefore: $d_{50} = 2184$ ft

By Eq. 4.4.6-2:

Ground deceleration distance, $d_G = V_{TD}^2/2a$

$a = 6$ ft/sec² (Ref. 33, Ch. 2, p. 14)

$d_G = 4378$ ft

By Eq. 4.4.6-3: Landing field required = $(d_{50} + d_G)1.67$

Landing field required = 10,960 ft

By Eq. 4.4.6-4: R/D at Touch down = $V_{TD}(50/d_{50})$

therefore R/D at Touch down = 4.4 ft/sec = 262 fpm

A.4.1.14 AIRCRAFT TIRES (SECTION 4.3.7.1):

Minimum footprint = $GW/250$ psi = 8000 sq in

With 56 x 16 tires with a 241 sq in footprint/tire

$$\text{Number of tires} = \frac{\text{minimum footprint}}{\text{footprint/tire}} = 33.2$$

therefore use 36 tires

therefore: aircraft footprint = 8700 sq in

and aircraft pressure print = 230 psi

A.4.1.15 LANDING GEAR STRUT (SECTION 4.3.7.2):

By Eq. 4.3.7-1: Energy = $\frac{1}{2} m V^2$

By Eq. 4.3.7-2: $m = (GW/g) = 62,112 \text{ lb sec}^2/\text{ft}$

$V = \text{Max R/D at Touch down} = 500 \text{ fpm (Aircraft limitation)}$

therefore: Energy = 2,156,600 ft-lbs

with four main gear: Energy/Gear = 539,165 ft-lbs

with Aluminum 7075 struts with 3 in. thick walls the allowable pressure =
1,800,000 lbs/sq ft = 12,500 psi

By Eq. 4.3.7-3: Energy absorbed = Strut pressure change x strut volume change

or: Energy/Allowable pressure = Volume change

therefore: Volume change = 0.30 cu ft with a strut deflection of 2 ft, internal strut area

is 0.15 sq ft

with a triple oleo strut:

internal oleo diameter = 5.25 in.

outside oleo diameter = 11.25 in.

A.4.1.16 AIRCRAFT COMPONENT SIZE AND WEIGHT: An initial GC was located at 260 ft from the canard aircraft nose with the use of structural component weight as a percent of total structural weight as shown in Table A.4.1

TABLE A.4.1 COMPONENT WEIGHTS (REF. 33, CH.4, P. 41)

COMPONENT	% OF STRUCTURE WEIGHT	LOCATION OF CG
WING	40.0	25% M. A. C.
FUSELAGE	30.6	40% OF FUSELAGE
TAIL	7.8	25% TAIL M. A. C.
NACELLE	5.6	40% OF NACELLE
LANDING GEAR	16.0	AT AIRCRAFT CG

Wing/Canard area:

$$\text{By Eq. 4.3.1-1: } S_C = \frac{S_W C_{LW} dW}{C_{LC} dC}$$

where: C_{LW} = wing lift coef.

$$C_{LC} = \text{canard lift coef.} = C_{LW}$$

dW = distance from wing quarter chord to CG

dC = distance from canard quarter chord to CG

$$\text{therefore: } S_C = 6683 \text{ sq ft}$$

Both wing and canard have lift and total lift area required is 33,333 sq ft. Total available lift area is $S_W + S_C$.

$$\text{therefore: reduce } S_W \text{ to: } \left(\frac{S_W^2}{S_W + S_C} \right)$$

$$\text{and } S_C \text{ to: } \left(\frac{S_C S_W}{S_W + S_C} \right)$$

$$\text{therefore: } S_W = 27,800 \text{ sq ft; } S_C = 5600 \text{ sq ft}$$

Vertical tail area:

$$\text{By Eq. 4.3.1-2 } S_{VT} = \frac{0.5 DF C_{DF} (dF^2 - dA^2)}{C_{DVT} dVT}$$

where: S_{VT} = vertical tail area
 DF = fuselage diameter = 40 ft
 C_{DF} = fuselage drag coefficient = 0.5
 dF = distance fwd of CG
 dA = distance aft of CG
 C_{DVT} = vertical tail drag coef. = 0.91
 dVT = distance from CG to vertical tail quarter cord

therefore: $S_{VT} = 4,300$ sq ft

Wing/canard planform:

By Eq. 4.3.4-2: Span, $b_W = (AR S_W)^{1/2}$

By Eq. 4.3.4-3

$$\text{Root chord, } C_R = \left(\frac{2}{1 + \lambda} \right) \left(\frac{S_W}{AR} \right)^{1/2}$$

By Eq. 4.3.4-4: Tip chord, $C_T = \lambda C_R$

By Eq. 4.3.4-5:

$$MAC = 2/3 C_R \left(\frac{1 + \lambda + \lambda^2}{1 + \lambda} \right)$$

therefore;	Wing	Canard
b_W (ft)	500	225
C_R (ft)	79	35.6
C_T (ft)	31.6	14.2
MAC (ft)	58.7	26.5

Component weights: (Section 4.3.2)

By Eq. 4.3.2-6 Wing weight = $1624 \left(\frac{W/S S_W LF b_W S_W}{\text{wing root thickness} \times 10^9} \right)^{0.584}$

Wing weight = 210,200 lbs

$$\text{By Eq. 4.3.2-7: Canard weight} = 1624 \left(\frac{W/S S_C LF b_C S_C}{\text{canard root thickness} \times 10^9} \right)^{0.584}$$

Canard weight = 31,200 lbs

$$\text{By Eq. 4.3.2-3 Vertical tail weight} = 1.197 (S_{VT})^{1.24}$$

Vertical tail weight = 38,000 lbs

By Eq. 4.3.2-4: Fuselage weight =

$$0.273 \left[\left(\frac{\text{length} \times LF}{\text{height}} \right)^{0.15} (Q_{\max})^{0.16} (\text{wetted area})^{1.05} \right]^{0.88}$$

where: $Q_{\max} = \frac{1}{2} \rho V^2$ and $V = 524$ ft/sec at sea level

$$Q_{\max} = 326 \text{ lb/sq ft}$$

thus: Fuselage weight = 188,000 lbs

$$\text{By Eq. 4.3.2-5 Landing gear weight} = 0.00916 (GW)^{1.124}$$

Landing gear weight = 111,000 lbs

A.4.1.17 AIRCRAFT WEIGHT AND BALANCE (SECTION 4.3.8.1): No chemical fuel will be used in this example. The fuel may be used to shift the CG position if necessary. The components weight moments are summed about the aircraft nose so that:

$$\text{CG moment arm} = \frac{\text{Sum of (component weights} \times \text{moment arms)}}{\text{total weight}}$$

therefore:

ITEM	WEIGHT (lbs)	LOCATION (ft)	MOMENT ft-lbs x 10 ⁶
Wing	210,200	300	63.06
Canard	31,200	60	1.87
Vert. Tail	38,000	360	13.68
Fuselage	188,000	172	32.34
Landing Gear	111,000	300	33.30
Chemical Engines	50,000	300	15.00
Fixed Equipment	200,000	75	15.00
Nuclear Reactor	603,000	300	180.90
Payload	372,000	200	74.40
Total	1,803,400		429.21

Thus: CG at 238 ft from aircraft nose with no chemical fuel. Up to 196,600 lbs of chemical fuel may be carried by the aircraft. This results in a tradeoff between the payload and chemical fuel weights and iteration of the aircraft design.

A.4.1.18 WING SECTION PROPERTIES (SECTION 4.3.4.5): Section property calculations are made at the wing station for the mean aerodynamic chord. The beam section area moment of inertia is calculated from Eq. 4.3.4-8.

$$I = \frac{(LF) M h_1}{2 \tau_a} = \frac{(2.5) (21,800,000) (8.06)}{(2) (40,000) (144)}$$

$$= 38.12 \text{ ft}^4$$

From Eq. 4.3.4-9

$$h_2 = \sqrt[3]{h_1^3 - \frac{12 I}{l_1}} = \sqrt[3]{8.06^3 - \frac{12 (38.12)}{34.15}}$$

$$= 7.99 \text{ ft}$$

The beam cap thickness is calculated from Eq. 4.3.4-10

$$t_c = \frac{1}{2} (h_1 - h_2) = \frac{8.06 - 7.99}{2} = 0.035 \text{ ft} = 0.42 \text{ in.}$$

The beam shear web thickness is calculated from Eq. 4.3.4-12

$$t_w = \frac{(LF) P}{2 h_2 \tau_3} = \frac{(2.5) (355,100)}{(2) (7.99) (40,000) (144)}$$

$$= 0.0096 \text{ ft} = 0.115 \text{ in.}$$

So set $t_w = 0.125 \text{ in.}$

A.4.1.19 RIB SPACING CALCULATION (SECTION 4.3.4-6): The stiffener spacing, b , is found from Eq. 4.3.4-13

$$b = \left(\frac{KE_c t_c^2}{\tau_{CCR}} \right)^{1/2} = \left[\frac{(6.35) (10.7 \times 10^6) (0.42)^2}{40,000} \right]^{1/2} = 17.15 \text{ in.}$$

The rib spacing, a , is equal to the a/b ratio times b .

$$a = 4b = (4) (17.15) = 68.6 \text{ in.}$$

The number of ribs in the wing is found by dividing the wing span by the rib spacing.

$$\# \text{ ribs} = \frac{b_w}{a} = \frac{499.9 \times 12}{68.6} = 87.4 \approx 87$$

A.4.1.20 DIVERGENCE SPEED: Divergence speed is found from Eq. 4.3.4-14. The matrices $[c]$, $[\int_J^1 dy]$, $[e]$ and $[W]$ are presented along with their matrix product. Elements of each matrix are calculated at the six wing stations given as distances in ft from the aircraft centerline:

$$\begin{aligned} y_1 &= 241.43 \\ y_2 &= 216.46 \\ y_3 &= 176.74 \\ y_4 &= 124.98 \\ y_5 &= 64.69 \\ y_6 &= 0 \end{aligned}$$

$$[c] = \begin{bmatrix} 33.36 & 0 & 0 & 0 & 0 & 0 \\ 0 & 3812 & 0 & 0 & 0 & 0 \\ 0 & 0 & 45.68 & 0 & 0 & 0 \\ 0 & 0 & 0 & 55.54 & 0 & 0 \\ 0 & 0 & 0 & 0 & 67.03 & 0 \\ 0 & 0 & 0 & 0 & 0 & 79.35 \end{bmatrix} \text{ ft}$$

$$[\int_J^1 dy] = \begin{bmatrix} 11.52 & 11.52 & 11.52 & 11.52 & 11.52 & 0 \\ 11.52 & 6.35 & 6.35 & 6.35 & 6.35 & 0 \\ 11.52 & 6.35 & 2.36 & 2.36 & 2.36 & 0 \\ 11.52 & 6.35 & 2.36 & .85 & .85 & 0 \\ 11.52 & 6.35 & 2.36 & .85 & .26 & 0 \\ 0 & 0 & 0 & 0 & 0 & 0 \end{bmatrix} \frac{1}{\text{ft}^3}$$

$$[e] = \begin{bmatrix} 5.18 & 0 & 0 & 0 & 0 & 0 \\ 0 & 5.48 & 0 & 0 & 0 & 0 \\ 0 & 0 & 5.96 & 0 & 0 & 0 \\ 0 & 0 & 0 & 6.59 & 0 & 0 \\ 0 & 0 & 0 & 0 & 7.31 & 0 \\ 0 & 0 & 0 & 0 & 0 & 8.09 \end{bmatrix} \text{ ft}$$

$$[W] = \begin{bmatrix} 16.94 & 0 & 0 & 0 & 0 & 0 \\ 0 & 32.72 & 0 & 0 & 0 & 0 \\ 0 & 0 & 46.27 & 0 & 0 & 0 \\ 0 & 0 & 0 & 56.67 & 0 & 0 \\ 0 & 0 & 0 & 0 & 63.21 & 0 \\ 0 & 0 & 0 & 0 & 0 & 32.72 \end{bmatrix} \text{ ft}$$

$$[c] \left[\int \frac{1}{y} dy \right] [e][W] = \begin{bmatrix} .0337 & .0689 & .1060 & .1435 & .1777 & 0 \\ .0385 & .0434 & .0667 & .0903 & .1118 & 0 \\ .0462 & .0520 & .0297 & .0403 & .0498 & 0 \\ .0562 & .0632 & .0362 & .0175 & .0217 & 0 \\ .0678 & .0763 & .0436 & .0212 & .0081 & 0 \\ 0 & 0 & 0 & 0 & 0 & 0 \end{bmatrix} \times 10^6$$

The eigenvalue, r , of the matrix product is 0.2934×10^6 . The divergence speed is found from Eq. 4.3.4-17.

$$v_D = \sqrt{\frac{2G}{\rho r \left(\frac{\partial C_L}{\partial \alpha} \right)}} = \sqrt{\frac{(2)(4 \times 10^6)(144)}{(0.002378)(0.2934 \times 10^6)(4.94)}}$$

$$\begin{aligned} &= 578 \text{ ft/sec at sea level} \\ &= 343 \text{ kts} \end{aligned}$$

A.4.1.21 REACTOR MOUNTING STRUCTURE: (SECTION 4.3.6): The design algorithm for the largest column is given here. It has an axial g-loading of 10.61, so the compressive load is $(10.61)(800,000) = 8.488 \times 10^6$ lbs and is 150 in. long. From equation 4.3.6-1 the cross sectional area of the tube is

$$A = F/\tau_{cy} = 8.488 \times 10^6 / 1.79 \times 10^5 = 47.42 \text{ sq in.}$$

The radius is given by Eq. 4.3.6-2

$$r = \left(\frac{2\pi}{25} A \right)^{1/2} = \sqrt{\frac{2\pi}{25} 47.42} = 13.74 \text{ in.}$$

The moment of inertia of the section is given by Eq. 4.3.6-3.

$$I = \frac{\pi}{25} r^4 = \frac{\pi}{25} (13.74)^4 = 4773 \text{ in.}^4$$

The radius of gyration is given by Eq. 4.3.6-4

$$\rho = \sqrt{I/A} = \sqrt{4773/47.42} = 9.71 \text{ in.}$$

The effective length of the column is given by Eq. 4.3.6-6

$$l' = K l = (0.7) (150) = 105 \text{ in.}$$

The critical buckling stress is given by Eq. 4.3.6-5

$$\begin{aligned} \tau_{CR} &= 179,000 - 27.95 (l'/\rho)^2 \\ &= 179,000 - 27.95 (105/9.71)^2 \\ &\approx 175,000 \text{ psi} \end{aligned}$$

The critical cross sectional area is 48.50 sq in.

The thickness of the tube is 0.562 in.

The design algorithm for the vertical stiffened plate structure follows. The plate is 120 x 120 in. and carries 4×10^6 lbs in compression and 8×10^6 lbs in shear. The plate thickness required to carry the shear load is

$$t_s = \frac{F_s}{120 \tau_{sy}} = \frac{8 \times 10^6}{(120) (73 \times 10^3)} = 0.913 \text{ in.}$$

The plate thickness required to carry the compressive load is

$$t_c = \frac{F_c}{120 \tau_{cy}} = \frac{4 \times 10^6}{(120) (179 \times 10^3)} = 0.186 \text{ in.}$$

The actual plate thickness required to carry the combined load is between 0.913 inches and $0.913 + 0.186 = 1.099$ in. and is found by trial and error by selecting a thickness and then checking to see if it satisfies the interaction Eq. 4.3.6-8

Let $t = 1.05$ in.

The working compressive stress is

$$f_c = \frac{F_c}{120 t} = \frac{4 \times 10^6}{(120) (1.05)} = 31,750 \text{ psi}$$

The working shear stress is

$$f_s = \frac{F_s}{120 t} = \frac{8 \times 10^6}{(120) (1.05)} = 63,500 \text{ psi}$$

The critical buckling stresses are calculated using Eq. 4.3.6-10

$$\tau_{CR} = K E (t/b)^2$$

$$\tau_{CCR} = (6.35) (29.0 \times 10^6) (1.05/24)^2 = 352,000 \text{ psi}$$

$$\text{so set } \tau_{CCR} = 179,000 \text{ psi}$$

$$\tau_{SCR} = (8.00) (29.0 \times 10^6) (1.05/24)^2 = 444,100 \text{ psi}$$

$$\text{so set } \tau_{SCR} = 73,000 \text{ psi}$$

The interaction Eq. 4.3.6-8 is

$$R_S^{1.5} + R_C \leq 1$$

$$(f_S/\tau_{SCR})^{1.5} + (f_C/\tau_{CCR}) \leq 1$$

$$\left(\frac{63,500}{73,000} \right)^{1.5} + \left(\frac{31,750}{179,000} \right) = 0.989 < 1$$

Therefore, a plate thickness of 1.05 in. will satisfactorily carry the combined load.

A.4.2 COMPUTER PROGRAM LOGIC CHARTS

A.4.2.1 AIRCRAFT PARAMETER LOGIC: The computer program inputs mission requirements and wing planform, iterates through the design method contained in Section 4, and outputs resultant aircraft parameters. The program variables are shown in Figure A.4.2.1-1. The program logic is shown in Figure A.4.2.1-2. The following symbols are used in the logic diagram:

ALT	Altitude (ft)
AR	Aspect ratio
C_{LMAX}	Maximum lift coefficient
d_{TO}	Takeoff distance (ft)
GW	Aircraft gross weight (lbs)
K	1000
L/D	Lift to drag ratio
OUT	Output
R/C	Rate of climb (fpm)
t/c	Thickness ratio
V	Velocity (ft/sec)
W/S	Wing loading (lbs/sq ft)
WT	Weight (lbs)
λ	Taper ratio

INPUT	VARY	OUTPUT
CRUISE SPEED CRUISE ALTITUDE ASPECT RATIO TAPER RATIO THICKNESS RATIO TAKEOFF DISTANCE FUSELAGE AREA MAX LIFT COEFFICIENT	GROSS WEIGHT: 800,000 - 2,400,000 LBS WING LOADING: 20 - 160 LB/SQ FT ENGINE NUMBER: 2 - 10 REACTOR TYPE: GAS or LIQ METAL REACTOR NUMBER: 1 or 2 TAKEOFF: JP-4 or NUCLEAR SPEED ALTITUDE	PAYLOAD STRUCTURE WEIGHT ENGINE WEIGHT CREW & MISC. WEIGHT TAKEOFF THRUST CRUISE POWER REACTOR WEIGHT OPTIMUM WING LOADING WING AREA L/D

Figure A.4.2.1-1 Aircraft Design Parameters

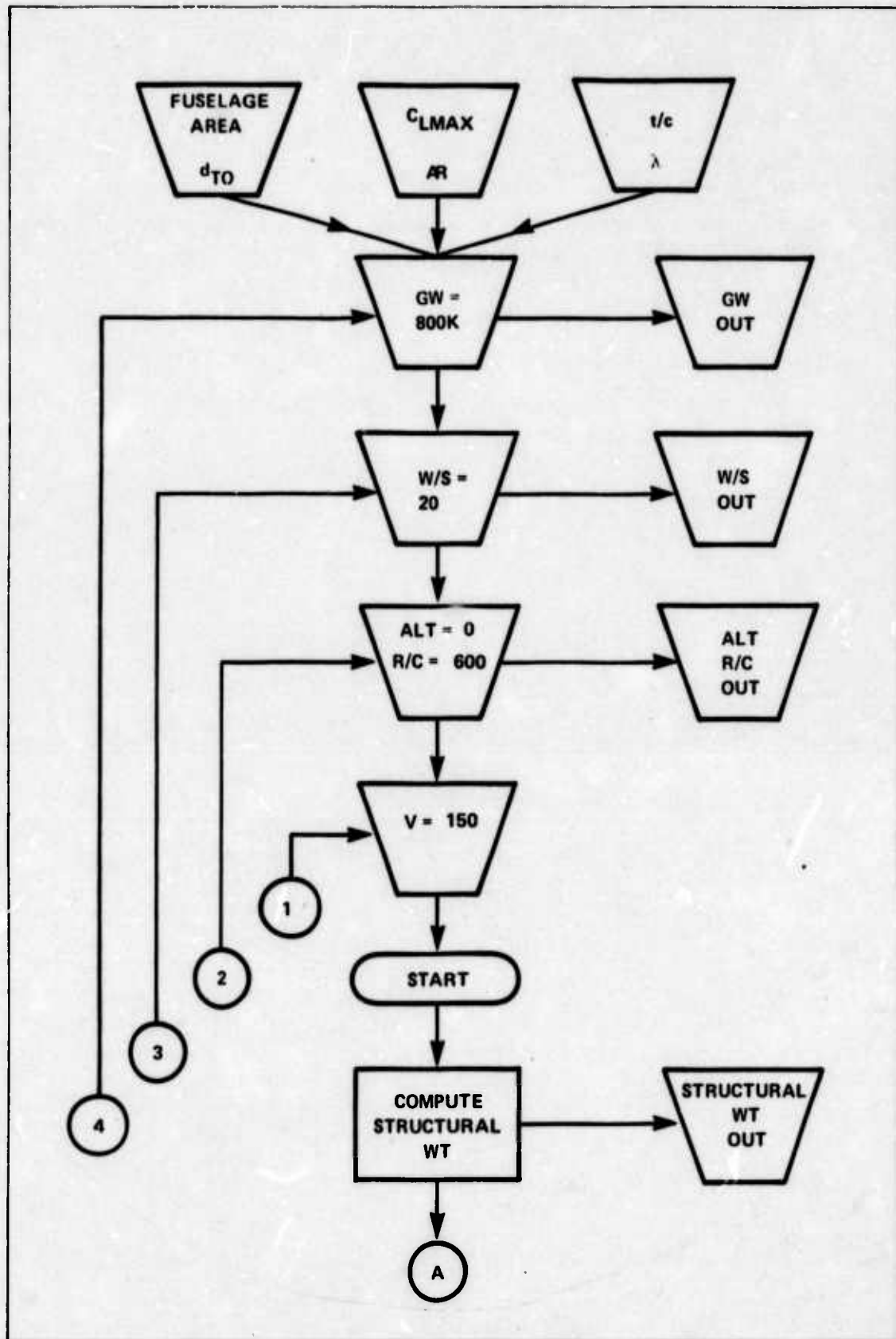


Figure A.4.2.1-2. Aircraft Parameter Logic
(Page 1 of 5)

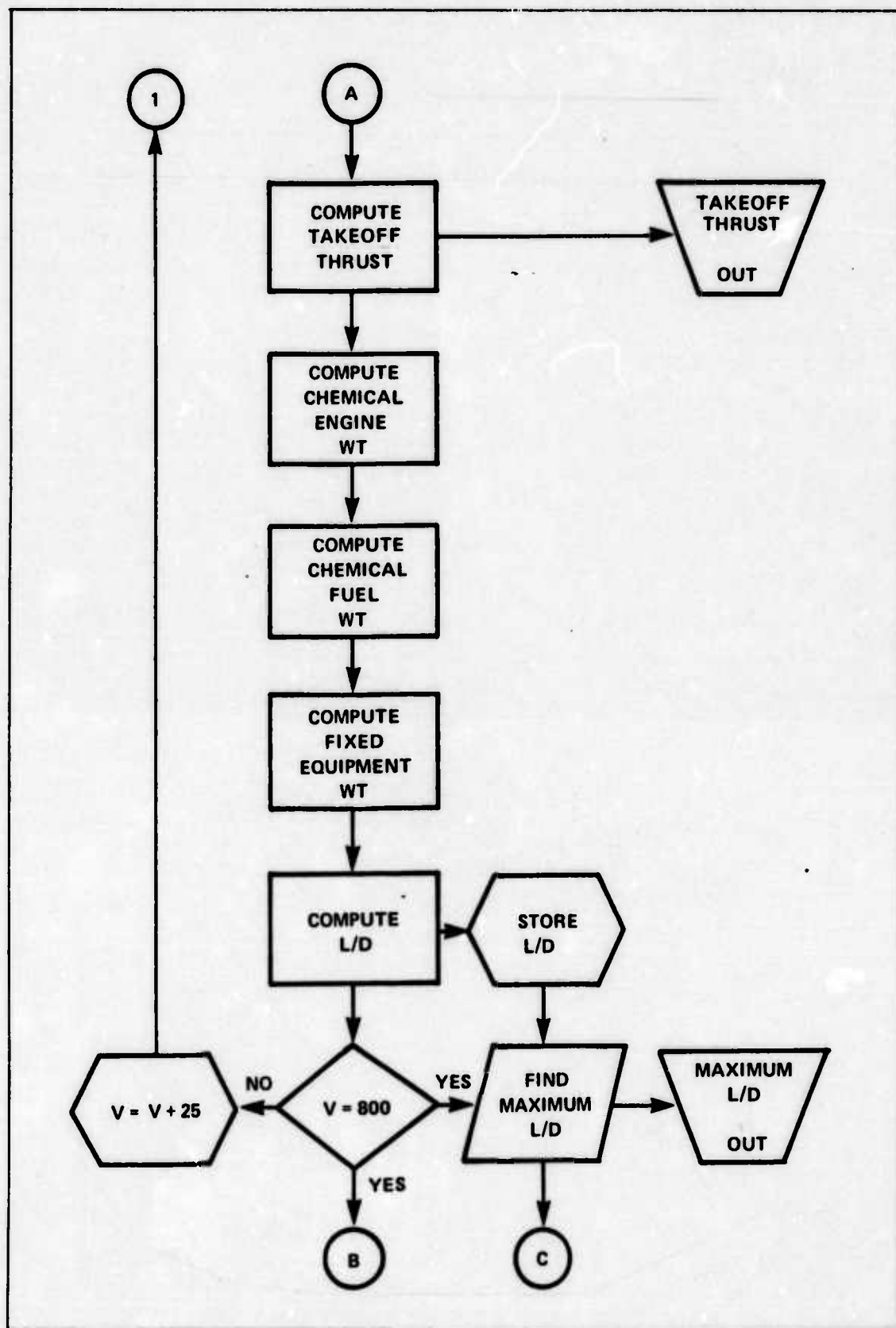


Figure A.4.2.1-2. Aircraft Parameter Logic
(Page 2 of 5)

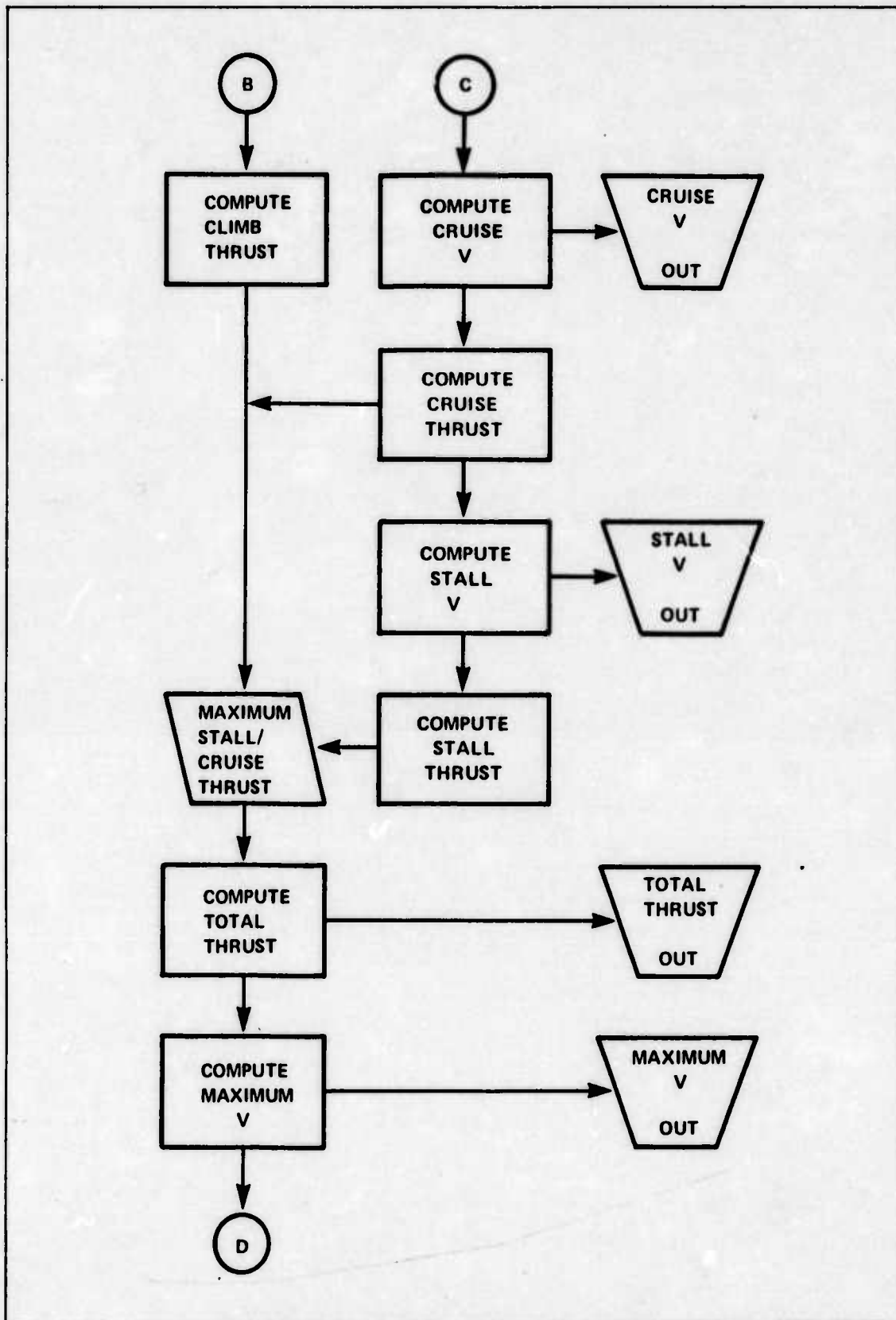


Figure A.4.2.1-2. Aircraft Parameter Logic
(Page 3 of 5)

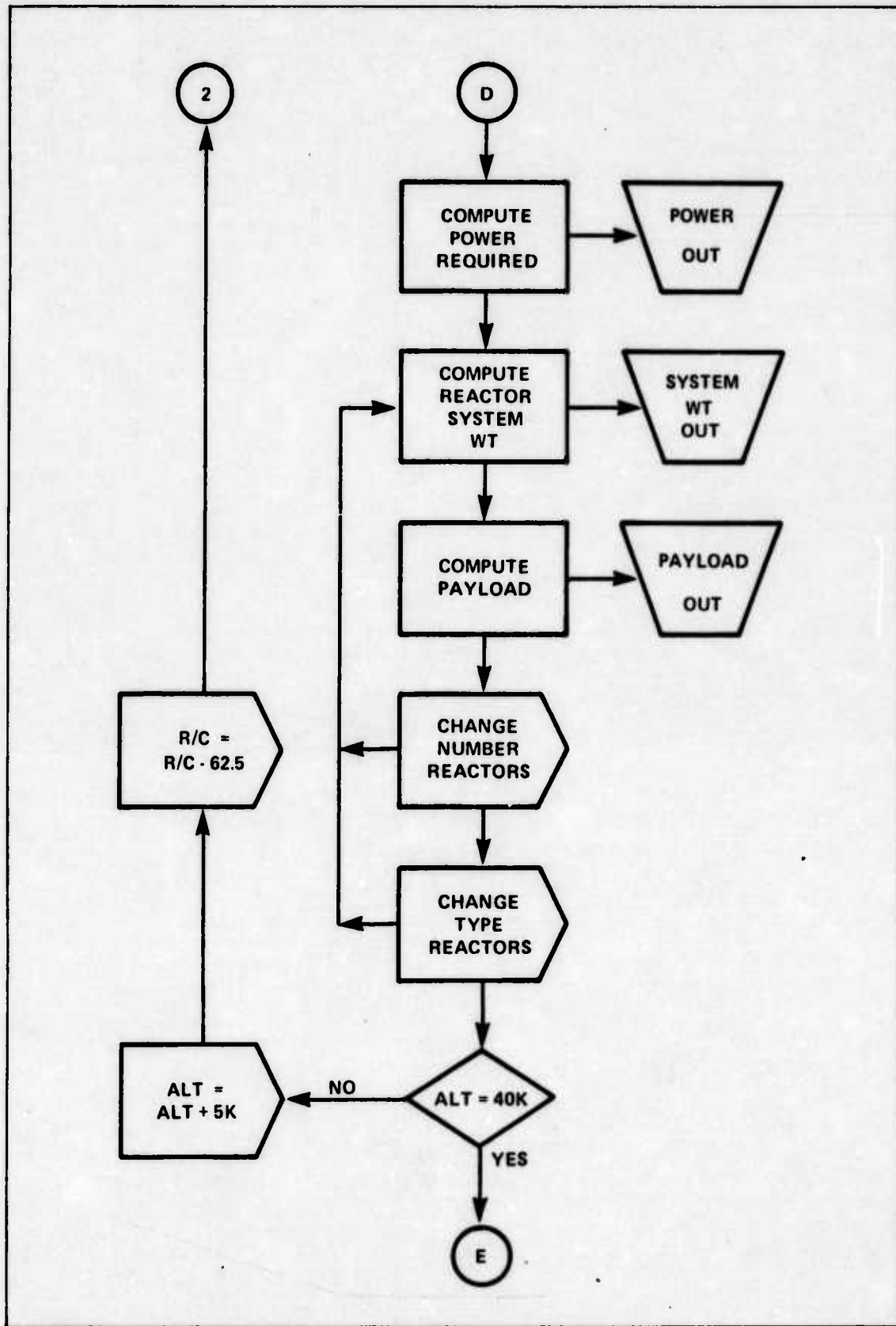


Figure A.4.2.1-2. Aircraft Parameter Logic
(Page 4 of 5)

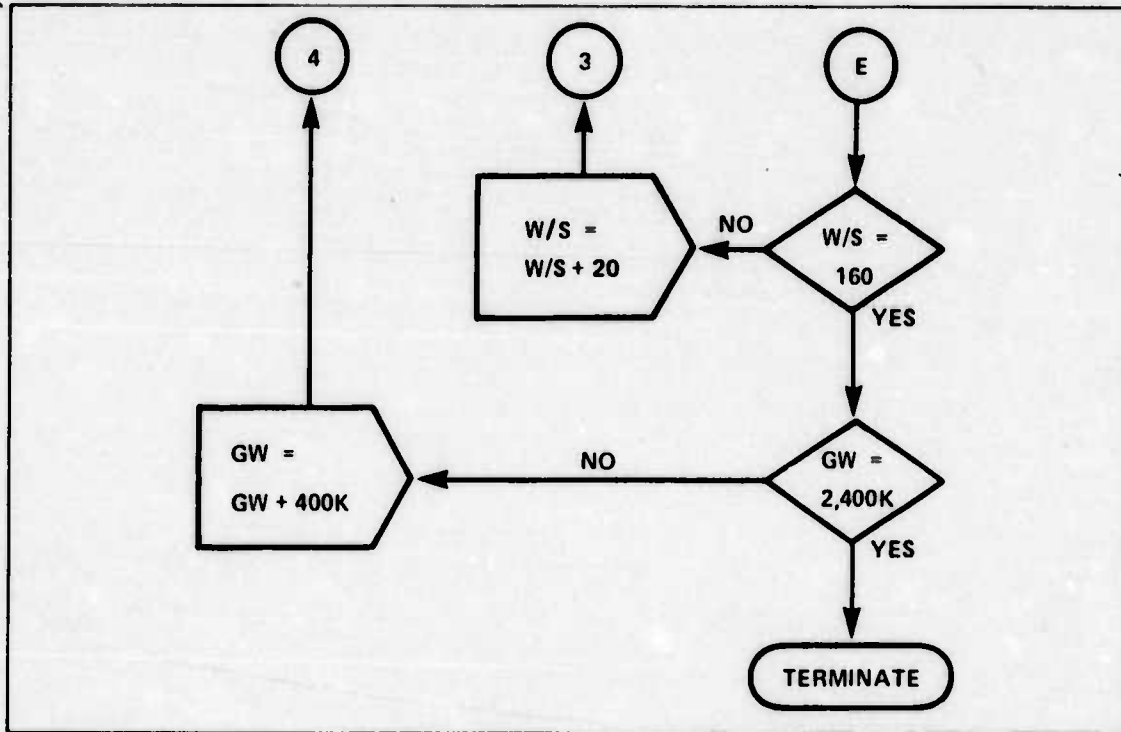


Figure A.4.2.1-2. Aircraft Parameter Logic
(Page 5 of 5)

A.4.2.2 WING ANALYSIS LOGIC: The computer program performs most of the analysis of Section 4.3.4. It takes the wing design criteria and calculates wing loads and section properties at several wing stations. The program variables are shown in Figure A.4.2.2-1. The program logic is shown in Figure A.4.2.2-2.

INPUTS	OUTPUTS
LIFT OF THE WING, L WING LOADING, W/S ASPECT RATIO, A/R TAPER RATIO, λ WING STATION SPACING, Δy WING WEIGHT ESTIMATE, W_1 LOAD FACTOR, LF ALLOWABLE STRESS, τ MINIMUM MATERIAL GAUGE, t_{MIN}	AT EACH WING STATION: WING STATION, y_i WING BEAM LOADING, W_i SHEAR FORCE, P_i BENDING MOMENT, M_i HEIGHT OF BEAM ENVELOPE, h_{1i} CHORDWISE LENGTH OF BEAM ENVELOPE, l_{1i} AREA MOMENT OF INERTIA, I_i BEAM CAP THICKNESS, t_{ci} BEAM WEB THICKNESS, t_{wi} LOCAL CHORD, C_i LOCAL TORQUE ARM, e_i TORSIONAL STIFFNESS, J_i INFLUENCE COEFFICIENT, $\int dy_i$ BEAM CAP WEIGHT, W_1 BEAM WEB WEIGHT, W_2 WING SKIN WEIGHT, W_3 FLAP WEIGHT, W_4 TOTAL WING WEIGHT, W_W WING AREA, S_W WING SPAN, b_W TIP CHORD, C_T ROOT CHORD, C_R

Figure A.4.2.2-1 Wing Design Variables

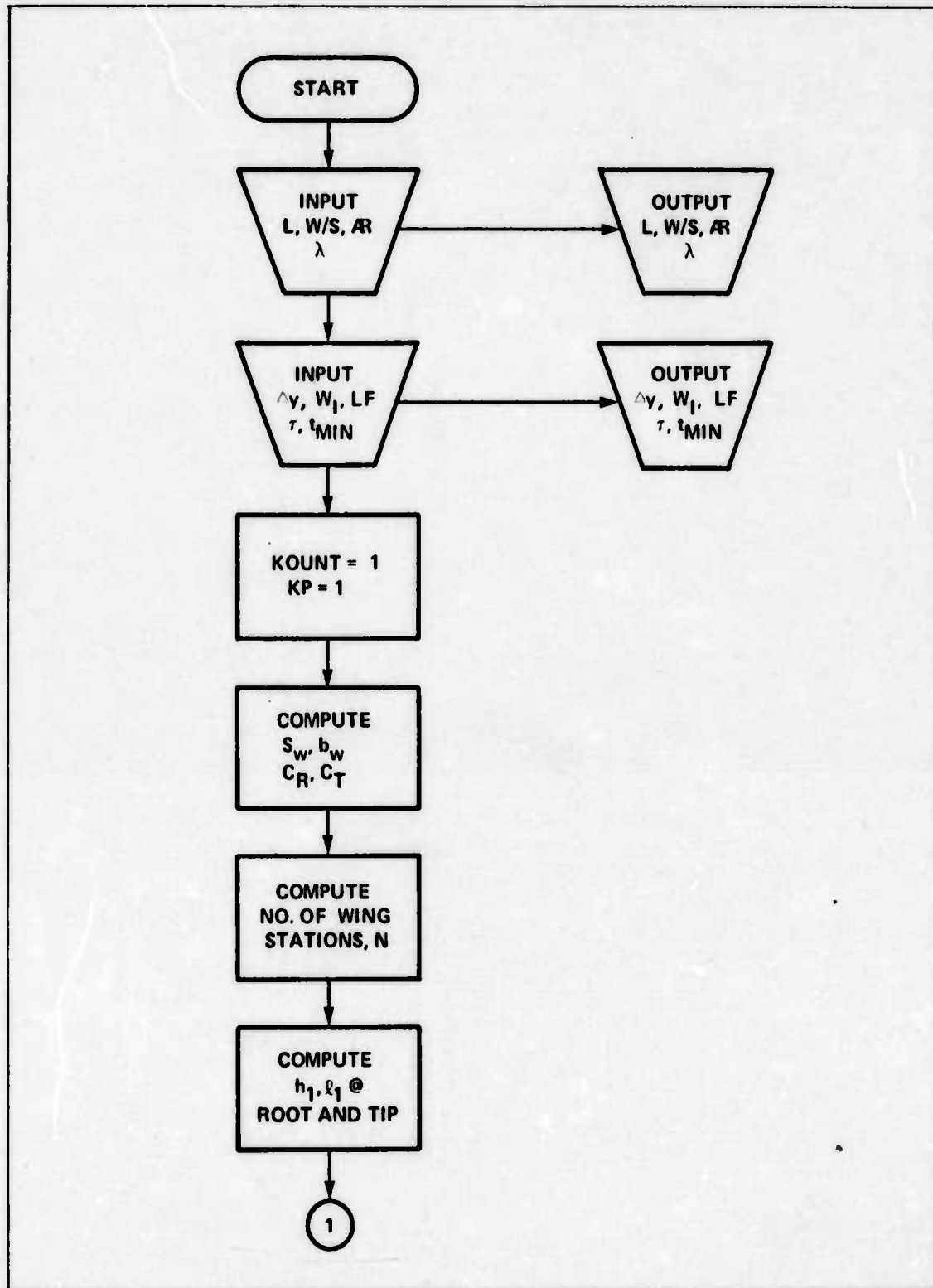


Figure A.4.2.2-2. Wing Analysis Logic
(Page 1 of 4)

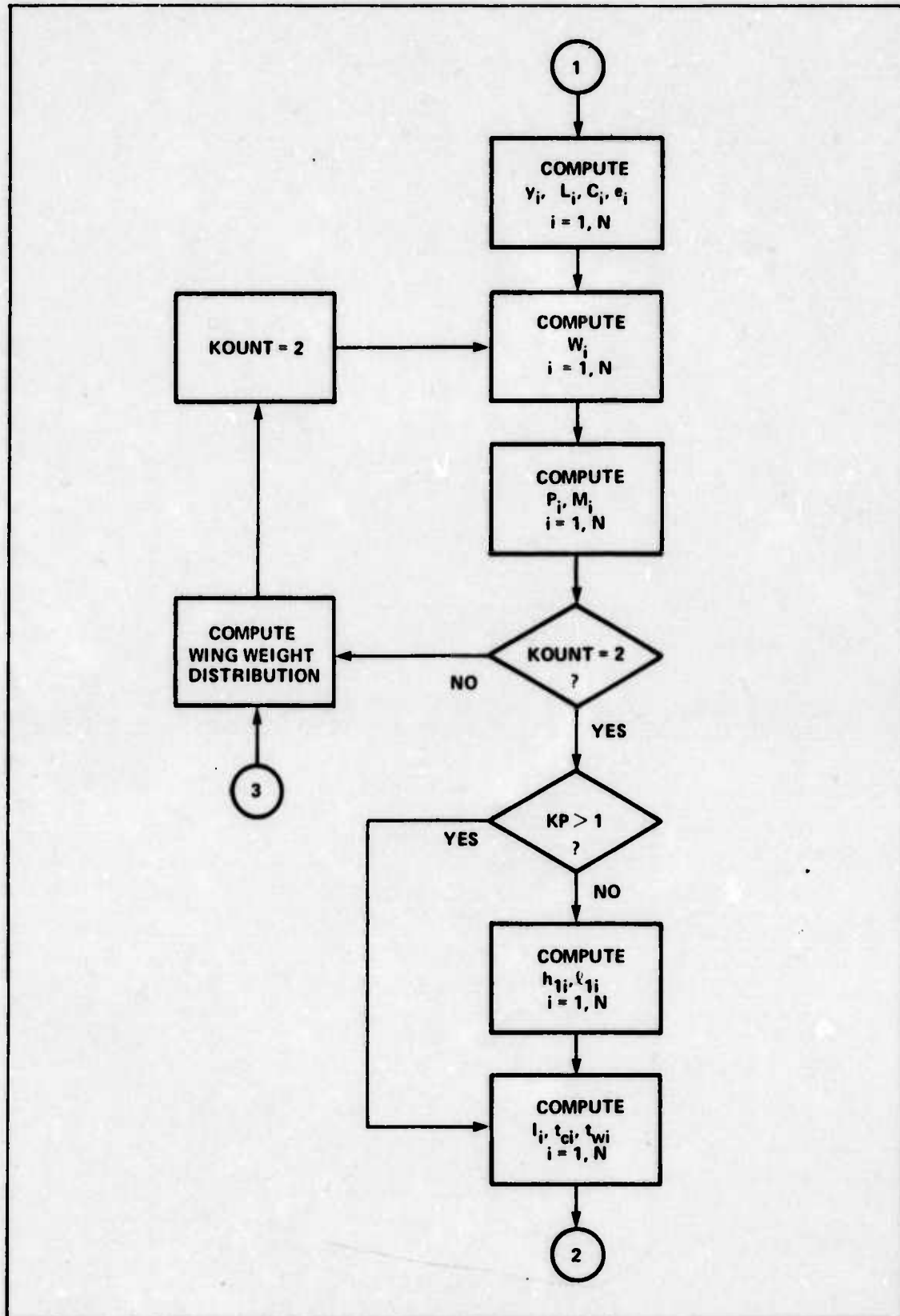


Figure A.4.2.2-2. Wing Analysis Logic
(Page 2 of 4)

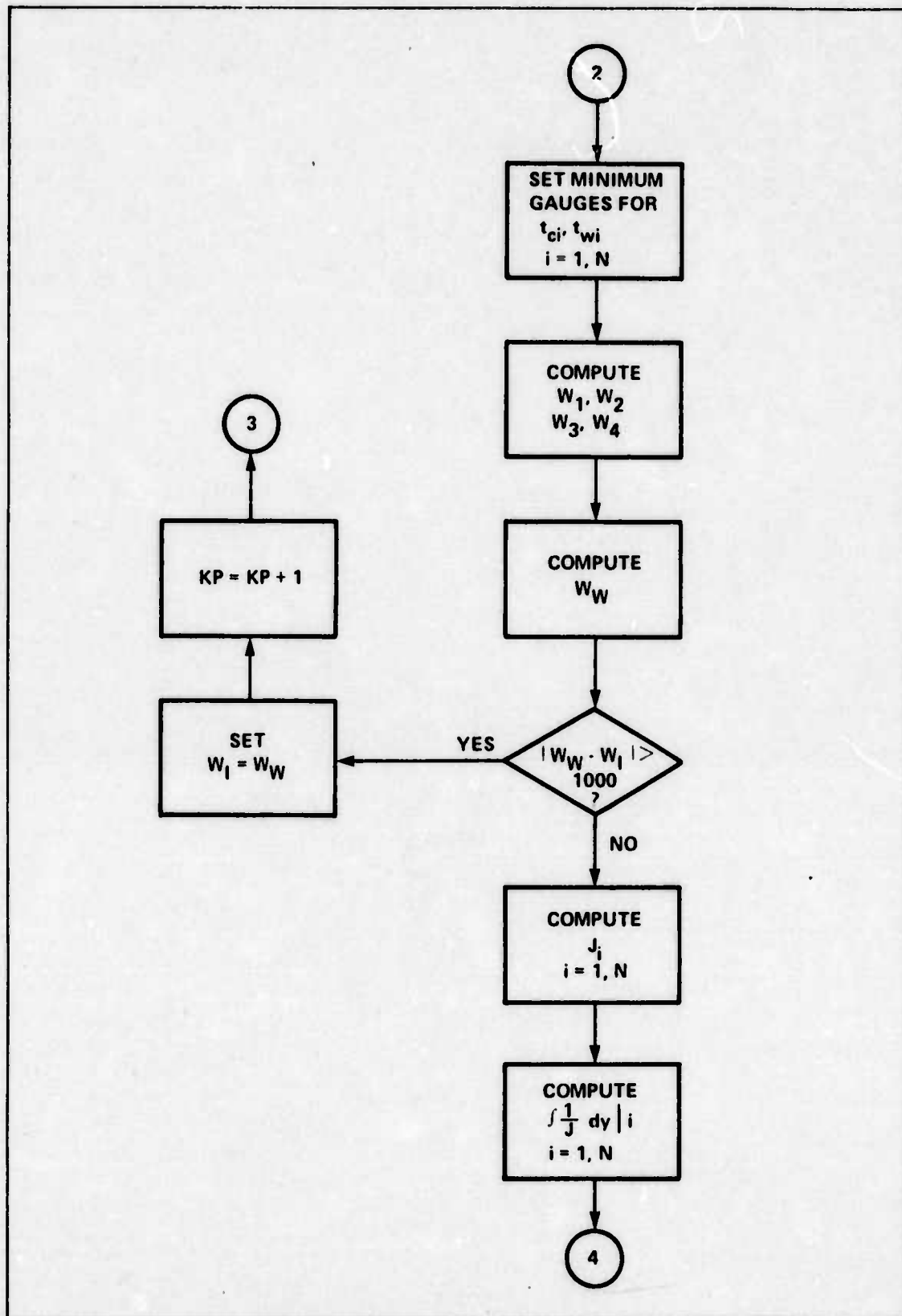


Figure A.4.2.2-2. Wing Analysis Logic.
(Page 3 of 4)

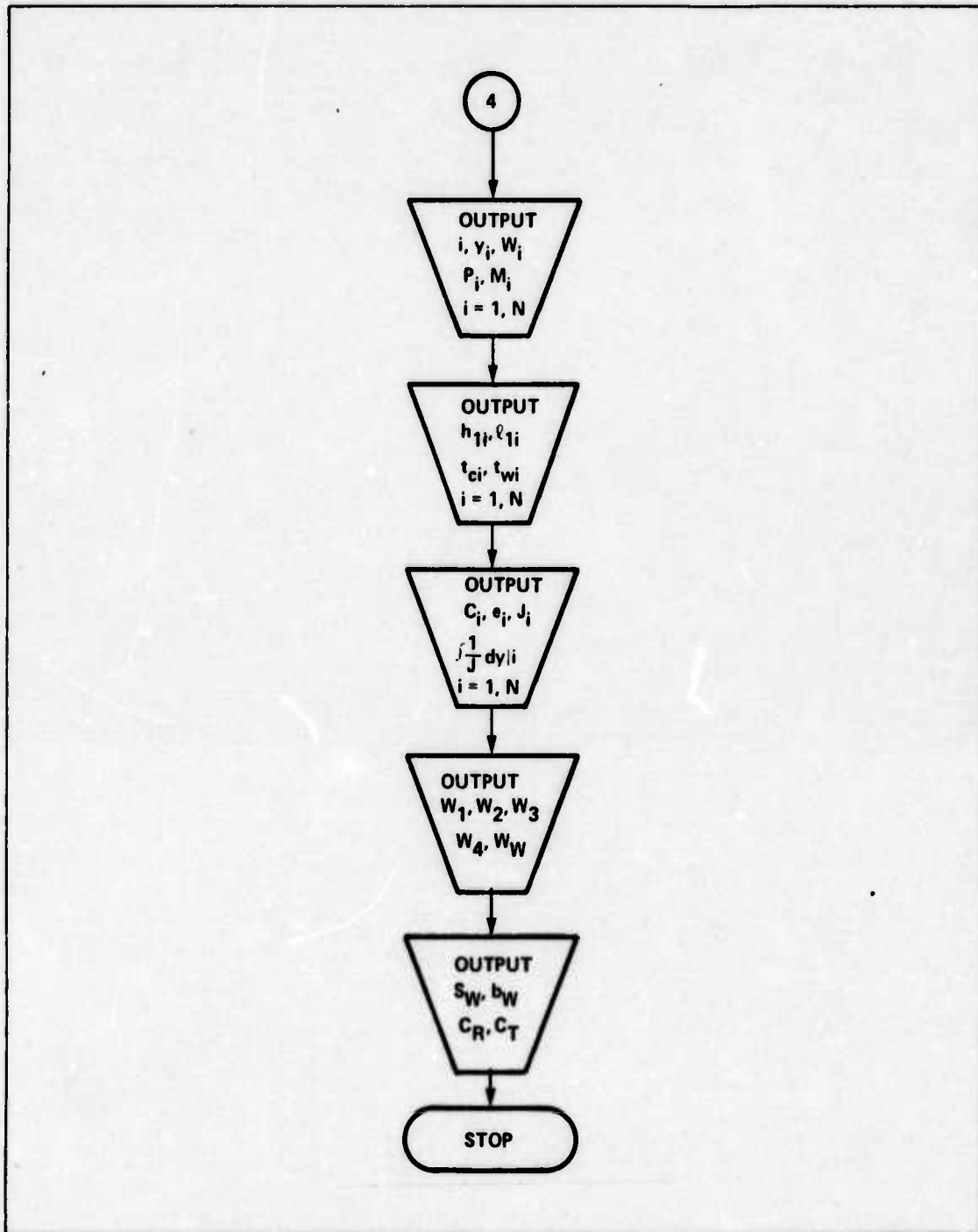


Figure A.4.2.2-2. Wing Analysis Logic
(Page 4 of 4)

A.4.3 AIRFOIL CHARACTERISTICS:

Selection of the airfoils was discussed in Section 4.3.4. The NACA 65₃-618 airfoil was selected as the root section. The NACA 65-410 airfoil was selected as the tip section. This appendix is included to present the detailed coordinate definitions of the airfoil shapes and the aerodynamic characteristics of the airfoils. Figure A.4.3-1 lists the airfoil shape coordinates for both airfoils. Figure A.4.3-2 shows the aerodynamic characteristics of the root section and Figure A.4.3-3 shows the aerodynamic characteristics of the tip section. For the root section, the slope of the lift coefficient curve, a_0 , is 6.60 per radian. For the tip section, a_0 is 6.17 per radian. Although a_0 varies uniformly along the wing from the root to the tip, the root section value was used in the divergence speed calculations because it yields a slightly conservative value of the divergence speed. The data presented in this appendix were taken from *Theory of Wing Sections* (Ref. 1, p. 434, 439, 614-615, 640-641).

NACA 65 ₃ -618 (STATIONS AND ORDINATES GIVEN IN PER CENT OF AIRFOIL CHORD)				NACA 65-410 (STATIONS AND ORDINATES GIVEN IN PER CENT OF AIRFOIL CHORD)			
UPPER SURFACE		LOWER SURFACE		UPPER SURFACE		LOWER SURFACE	
STATION	ORDINATE	STATION	ORDINATE	STATION	ORDINATE	STATION	ORDINATE
0	0	0	0	0	0	0	0
0.172	1.446	0.828	-1.146	0.372	0.861	0.628	-0.661
0.385	1.776	1.115	-1.356	0.607	1.061	0.893	-0.781
0.839	2.293	1.661	-1.651	1.089	1.372	1.411	-0.944
2.026	3.268	2.974	-2.152	2.318	1.935	2.682	-1.191
4.462	4.776	5.538	-2.880	4.797	2.800	5.203	-1.536
6.936	5.971	8.064	-3.427	7.289	3.487	7.711	-1.791
9.431	6.978	10.569	-3.876	9.788	4.067	10.212	-1.999
14.455	8.602	15.545	-4.564	14.798	5.006	15.202	-2.314
19.506	9.848	20.494	-5.072	19.817	5.731	20.183	-2.547
24.574	10.803	25.426	-5.433	24.843	6.290	25.157	-2.710
29.652	11.504	30.348	-5.672	29.872	6.702	30.128	-2.814
34.738	11.972	35.262	-5.792	34.903	6.983	35.097	-2.863
39.826	12.210	40.174	-5.784	39.936	7.138	40.064	-2.854
44.915	12.186	45.085	-5.616	44.968	7.153	45.032	-2.773
50.000	11.877	50.000	-5.259	50.000	7.018	50.000	-2.606
55.077	11.293	54.923	-4.723	55.029	6.720	54.971	-2.340
60.141	10.479	59.859	-4.053	60.053	6.288	59.947	-2.004
65.189	9.482	64.811	-3.302	65.073	5.741	64.927	-1.621
70.219	8.338	69.781	-2.506	70.085	5.099	69.915	-1.211
75.230	7.075	74.770	-1.705	75.090	4.372	74.910	-0.792
80.220	5.719	79.780	-0.943	80.088	3.577	79.912	-0.393
85.189	4.306	84.811	-0.268	85.076	2.729	84.924	-0.037
90.138	2.863	89.862	0.239	90.057	1.842	89.943	0.226
95.068	1.433	94.932	0.463	95.029	0.937	94.971	0.327
100.000	0	100.000	0	100.000	0	100.000	0
L.E. RADIUS: 1.96 SLOPE OF RADIUS THROUGH L.E.: 0.253				L.E. RADIUS: 0.687 SLOPE OF RADIUS THROUGH L.E.: 0.168			

Figure A.4.3-1 Airfoil Shape Coordinates

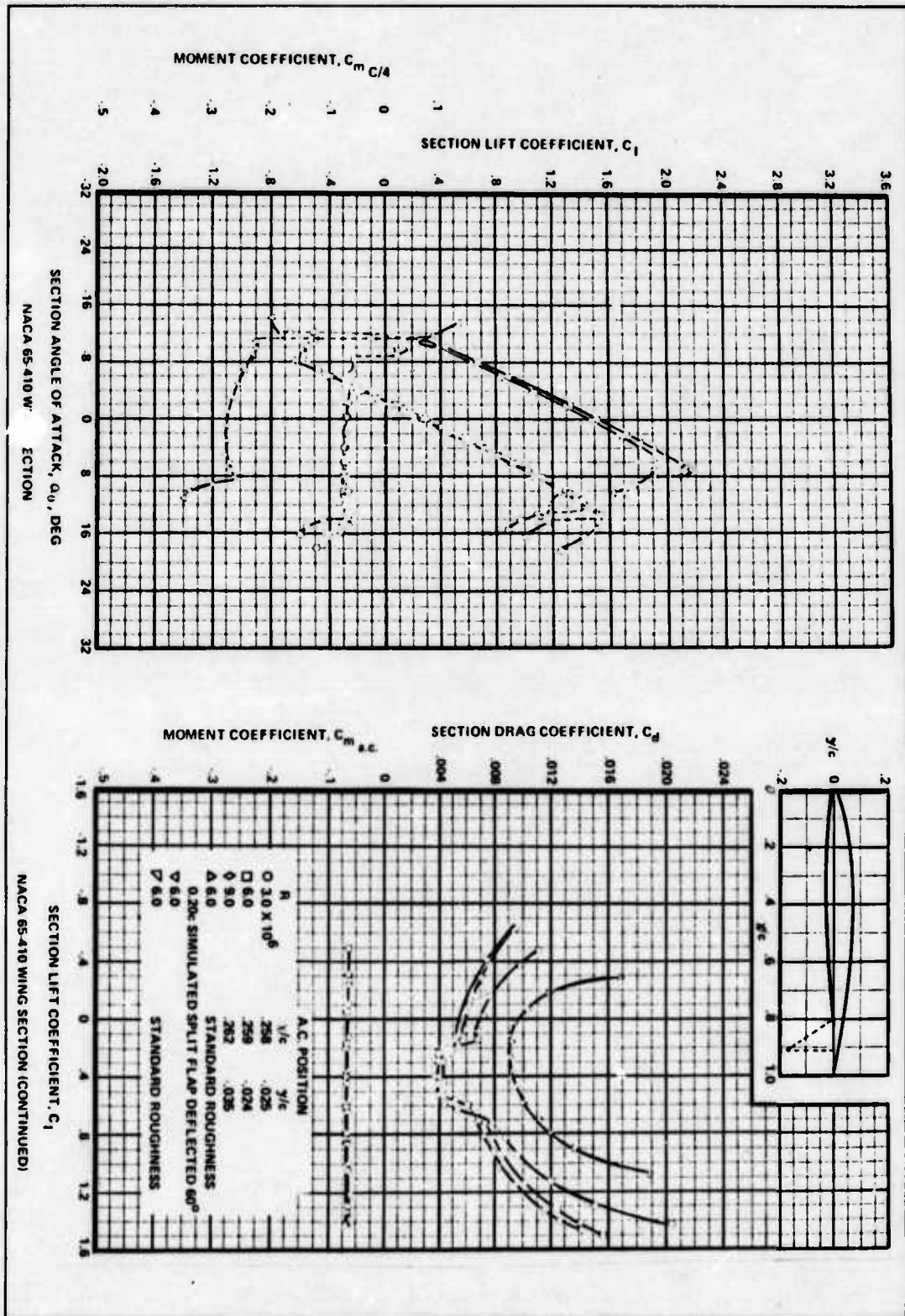


Figure A.4.3-3. Tip Section Characteristics

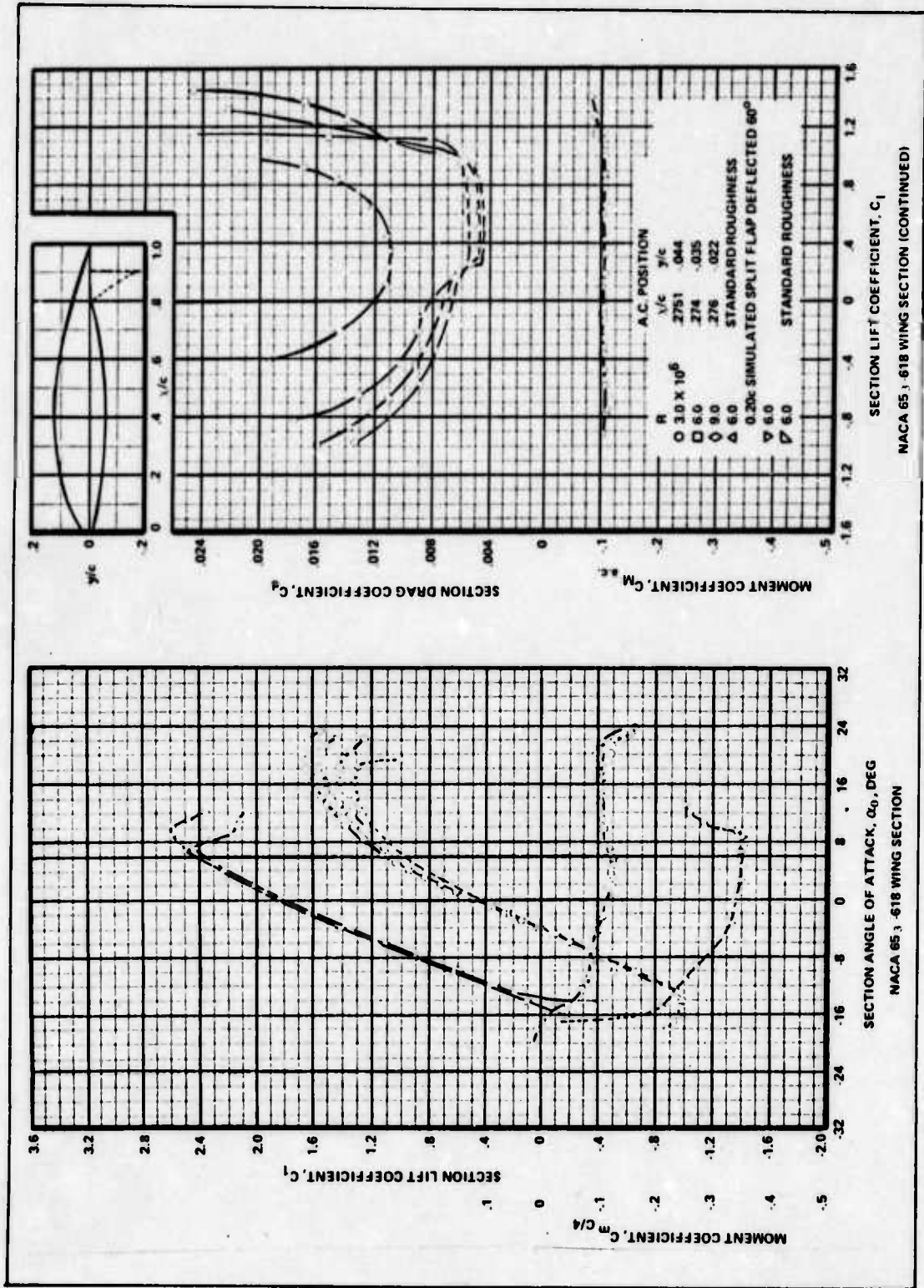


Figure A.4.3-2. Root Section Characteristics

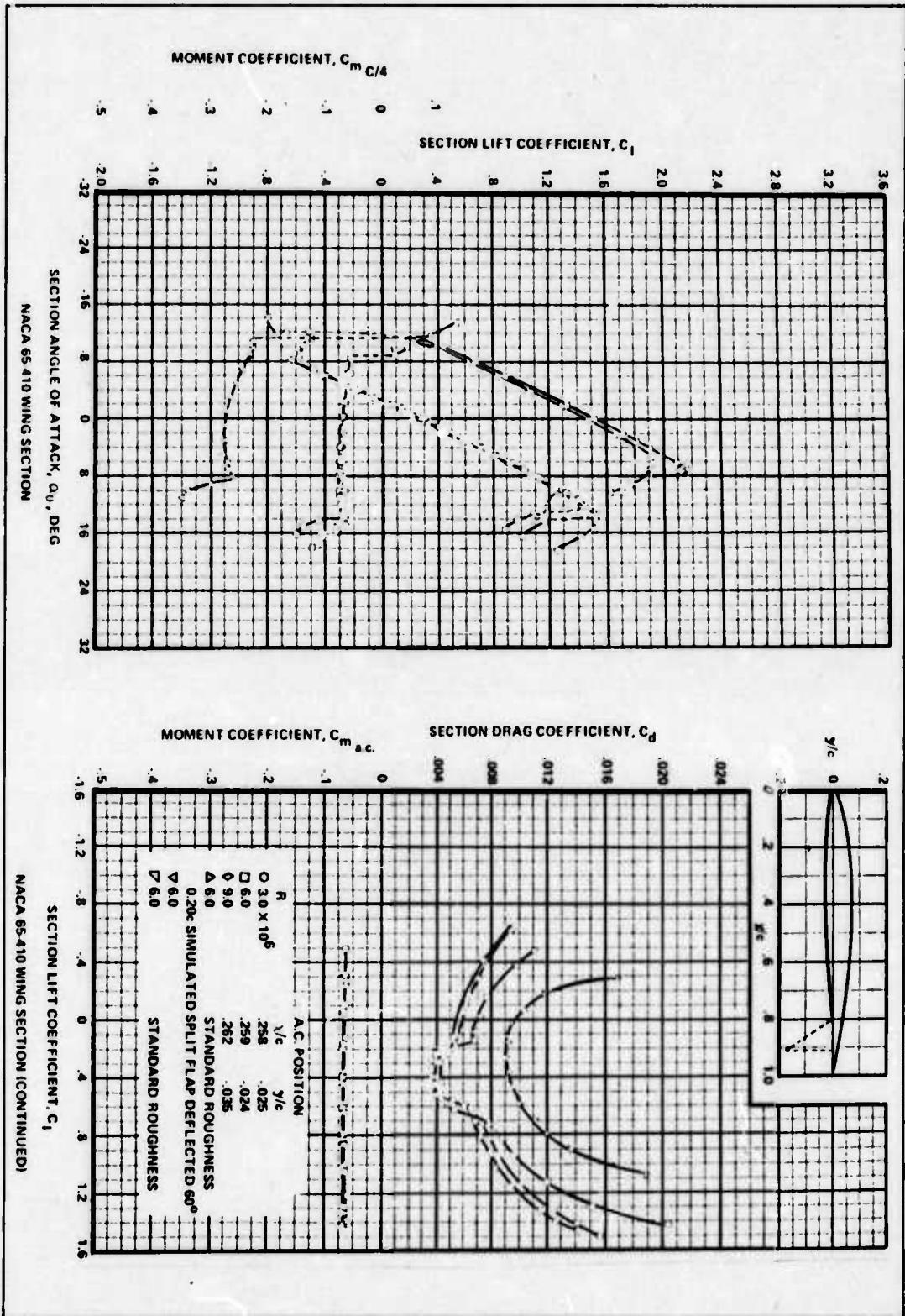


Figure A.4.3-3. Tip Section Characteristics

APPENDIX A.6 ENGINES

A.6.1 RELIABILITY

In evaluating the probability of system failure where the systems are JP-4 engines, dedicated nuclear engines, dual mode nuclear engines, or a combination of JP-4 and dedicated nuclear engines, the assumptions are:

- 1) The probability of failure of the engine to deliver fuel $P(1)$ is ≤ 0.1
- 2) Probability of engine failure due to some reason other than not getting the fuel $P(2) \leq 0.1$
- 3) Probability of the nuclear heat exchanger becoming inoperative for some reason $P(3) \leq 0.1$

These assumptions imply that the product of the probabilities is much smaller than the sum. Thus, from Figure A.6.1-1, the probability of failure of a JP-4 engine is

$$P_1 = P(1) + P(2) - P(1)P(2)$$

but $P(1)P(2) \leq \min [P(1), P(2)]$

thus

$$P_1 = P(1) + P(2)$$

The figure presents the system in terms of increasing reliability so that the last one presented, i.e., the combination of JP-4 and dedicated nuclear engines, offers the greatest reliability. In other words, this combination has the least probability of total system failure.

The validity of the assumption that $P(1)$ and $P(2)$ are less than 0.1 derives from the relationship that the total engine failure probability is equal to $P(1) + P(2)$. Data for the General Electric CF6 engine (Sections 8.1.4.4 and Appendix A.8.1.2.2) give a total engine failure probability of approximately 0.03; therefore, both $P(1)$ and $P(2)$ must be less than 0.1.

The assumption that $P(3)$ is less than 0.1 is based on a liquid metal heat exchanger failure rate taken from a nuclear systems failure data handbook (Ref. 52, p. 211). That failure rate of 3.2×10^{-5} failure per hour was used with a negative exponential failure probability distribution with time equal to mission time of 330 hours to yield a failure probability of 0.01. Since this point calculation was one order of magnitude less than 0.1, the assumption that $P(3)$ would be less than 0.1 was felt to be reasonable.

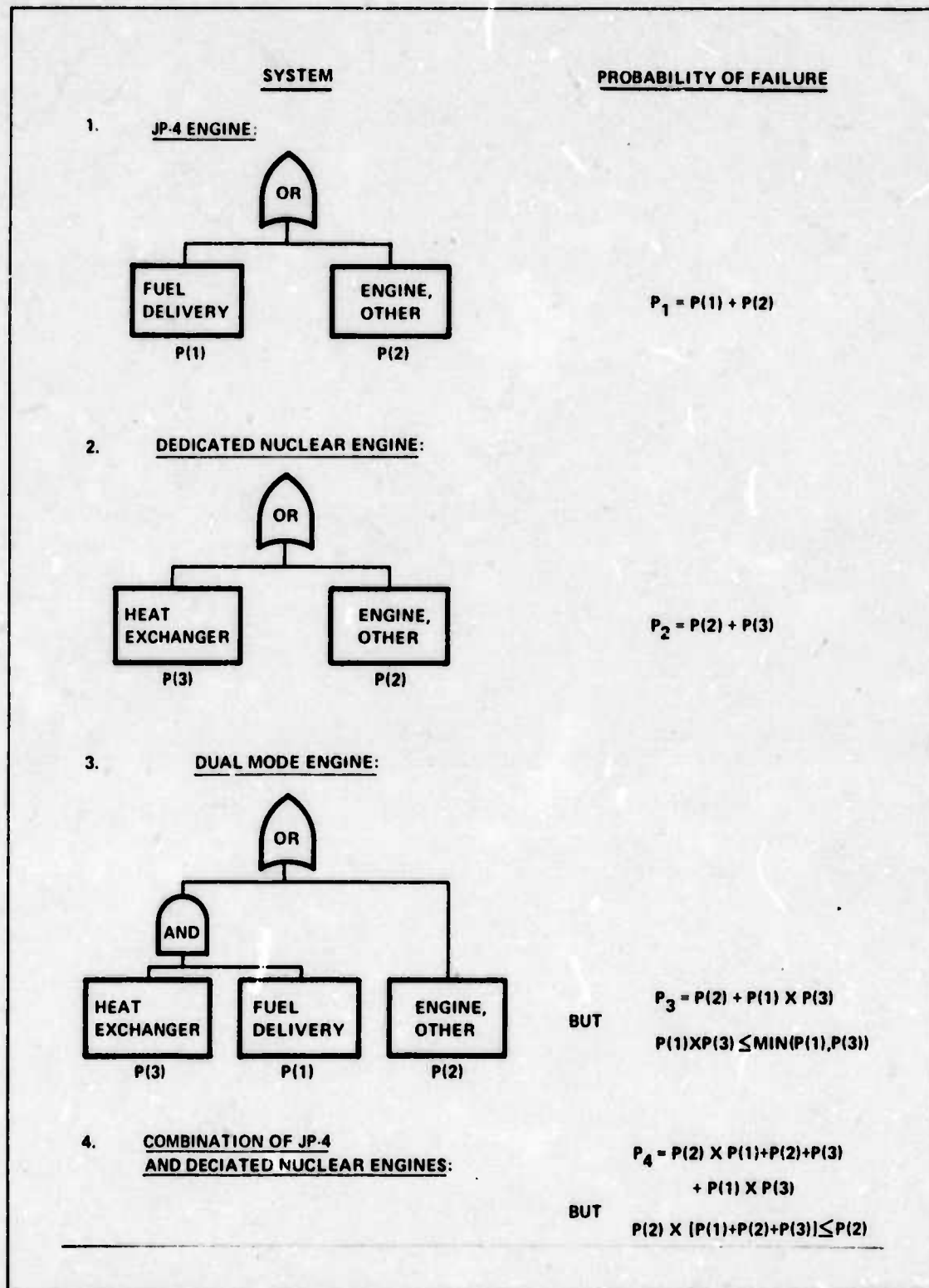


Figure A.6.1-1. Reliability of Engine System Concepts and Combinations

A.6.2 DERIVATION OF OPTIMUM EQUATIONS FOR THE BRAYTON CYCLE

The net work obtained per lb of working fluid is the difference between the work output of the turbine and the work required by the compressor. Assuming constant specific heats:

$$W_n = W_t - W_c = c_p \eta_t (T_{t3} - T_{t4}') - \frac{c_p}{\eta_c} (T_{t2}' - T_{t1})$$

$$W_n = c_p T_{t3} \eta_t \left[1 - \frac{1}{X_t} \right] - \frac{c_p T_{t1}}{\eta_c} [X_c - 1] \quad (\text{A.6.2-1})$$

where:

$$X_t = (P_{t3}/P_{t4})$$

$$X_c = (P_{t2}/P_{t1}) \quad k = \frac{\gamma - 1}{\gamma}$$

Assuming pressure losses are negligible, which implies that $X_t = X_c = X$, then the pressure ratio corresponding to maximum net work may be found by differentiating Eq. A.6.2-1 with respect to X (Ref. 77, p. 51).

$$\frac{dW_n}{dX} = \frac{c_p T_{t3} \eta_t}{X^2} - \frac{c_p T_{t1}}{\eta_c} = 0$$

$$X^2 = \frac{\eta_c \eta_t T_{t3}}{T_{t1}}$$

$$X = \sqrt{Z \eta_c \eta_t}$$

where:

$$Z = T_{t3}/T_{t1}$$

therefore: $r_p = [Z \eta_c \eta_t]^{1/2k} \quad (\text{A.6.2-2})$

An alternative method for obtaining the pressure ratio for max net work is discussed in Reference 45, p. 194, where an ideal process is assumed and $X_t = X_c = X$. For an ideal (isentropic process)

$$(P_{t3}/P_{t4})^k = T_{t3}/T_{t4} \quad (P_{t2}/P_{t1})^k = T_{t2}/T_{t1}$$

also

$$P_{t2} = P_{t3} \text{ and } P_{t1} = P_{t4}$$

$$T_{t4} = \frac{T_{t3}}{X} = \frac{T_{t3} T_{t1}}{T_{t2}}$$

Substituting this into Eq. A.6.2-1

$$W_n = c_p \left\{ T_{t3} - \frac{T_{t1} T_{t3}}{T_{t2}} + T_{t1} - T_{t2} \right\}$$

and assuming T_{t_1} to be constant and differentiating W_n with respect to T_{t_2} , i.e. compressor outlet temperature:

$$\frac{d W_n}{d T_{t_2}} = \frac{T_{t_1} T_{t_3}}{T_{t_2}^2} - 1 = 0$$

which gives

$$T_{t_2} = \sqrt{T_{t_1} T_{t_3}} \quad (\text{A.6.2-3})$$

Once this temperature is determined, the ideal pressure ratio may be found from the isentropic relationships presented on the previous page.

Besides optimizing a cycle for net work, a cycle can be optimized for maximum thermal efficiency, as shown by Dusiherre (Ref. 45, p. 31) and Hosney (Ref. 77, p. 42). Starting with Eq. A.6.2-1 and noting that the thermal efficiency of a cycle is given by

$$\eta_{th} = \frac{W_n}{q}$$

Then for constant specific heats:

$$\eta_{th} = \frac{\eta_t T_{t_3} \left[1 - \frac{1}{X} \right] - \frac{T_{t_1}}{\eta_c} (X - 1)}{T_{t_3} - T_{t_1} \left[\frac{X-1}{\eta_c} + 1 \right]}$$

Rearranging terms:

$$\eta_{th} = \frac{\eta_t Z \left(1 - \frac{1}{X} \right) - \frac{1}{\eta_c} (X - 1)}{Z - \left[\frac{X-1}{\eta_c} + 1 \right]} \quad (\text{A.6.2-4})$$

To find optimum pressure ratio corresponding to maximum efficiency, differentiate with respect to X and set equal to 0.

$$\frac{d \eta_{th}}{d X} = u \frac{dv}{dx} - v \frac{du}{dX} = 0$$

where:

$$u = \eta_t Z \left(1 - \frac{1}{X} \right) - \frac{1}{\eta_c} (X - 1)$$

$$v = Z - \left(\frac{X-1}{\eta_c} + 1 \right)$$

then:

$$\frac{dv}{dX} = \frac{1}{\eta_c} \quad \text{and} \quad \frac{du}{dX} = \frac{\eta_t Z}{X^2} - \frac{1}{\eta_c}$$

and:

$$\left(Z - \frac{X}{\eta_c} + \frac{1}{\eta_c} - 1 \right) \left(\frac{\eta_t Z}{X^2} - \frac{1}{\eta_c} \right) - \left\{ \left[\eta_t Z - \frac{\eta_t Z}{X} - \frac{X}{\eta_c} + \frac{1}{\eta_c} \right] \left(-\frac{1}{\eta_c} \right) \right\} = 0$$

$$\frac{Z^2 \eta_t}{X^2} - \frac{\eta_t Z}{\eta_c X} + \frac{\eta_t Z}{\eta_c X^2} - \frac{Z}{\eta_c} - \frac{\eta_t^2}{X^2} - \frac{X}{\eta_c^2} - \frac{1}{\eta_c^2} + \frac{1}{\eta_c}$$

$$- \left\{ -\frac{\eta_t Z}{\eta_c} + \frac{\eta_t Z}{\eta_c X} + \frac{X}{\eta_c^2} - \frac{1}{\eta_c^2} \right\} = 0$$

multiply through by $X^2 \eta_c$ to obtain

$$\eta_c \eta_t Z^2 - \eta_t Z X - \eta_t \eta_c Z + \eta_t Z - Z X^2 + X^2 + \eta_t Z X^2 - \eta_t Z X = 0$$

collecting terms

$$[(\eta_t - 1) Z + 1] X^2 - 2 \eta_t Z X + [(1 - \eta_c) \eta_t + \eta_c \eta_t Z] Z = 0$$

solving the quadratic for the pressure ratio which is defined by

$$r_p = X^{\frac{1}{k}}$$

thus:

$$r_p \eta_{\max} = \left[\frac{b - \sqrt{b^2 - 4ac}}{2a} \right]^{\frac{1}{k}} \quad (\text{A.6.2-5})$$

where:

$$a = (\eta_t - 1) Z + 1$$

$$b = 2 \eta_t Z$$

$$c = [(1 - \eta_c) \eta_t + \eta_c \eta_t Z] Z$$

A.6.3 METHODOLOGY USED IN INDIRECT CYCLE HEAT EXCHANGER ENGINE ANALYSIS

Program CARPET, written by Capt. R. E. Witherell (Ref. 192), a design point program, was used to find an optimum design at 30,000 ft. The input conditions were:

- 1) turbine inlet temperature $T_{t4} = 1960^\circ\text{R}$
- 2) overall pressure ratio $R_p = 16.8$
- 3) mass flow of air through the engine core $M_c = 200 \text{ lb/sec}$
- 4) pressure loss in engine $\Delta P = 6 \text{ to } 16\%$

The methodology followed a format as that shown in Figure A.6.3-1. A simplified diagram for CARPET is presented in Figure A.6.3-2 which gives an idea of the program's format.

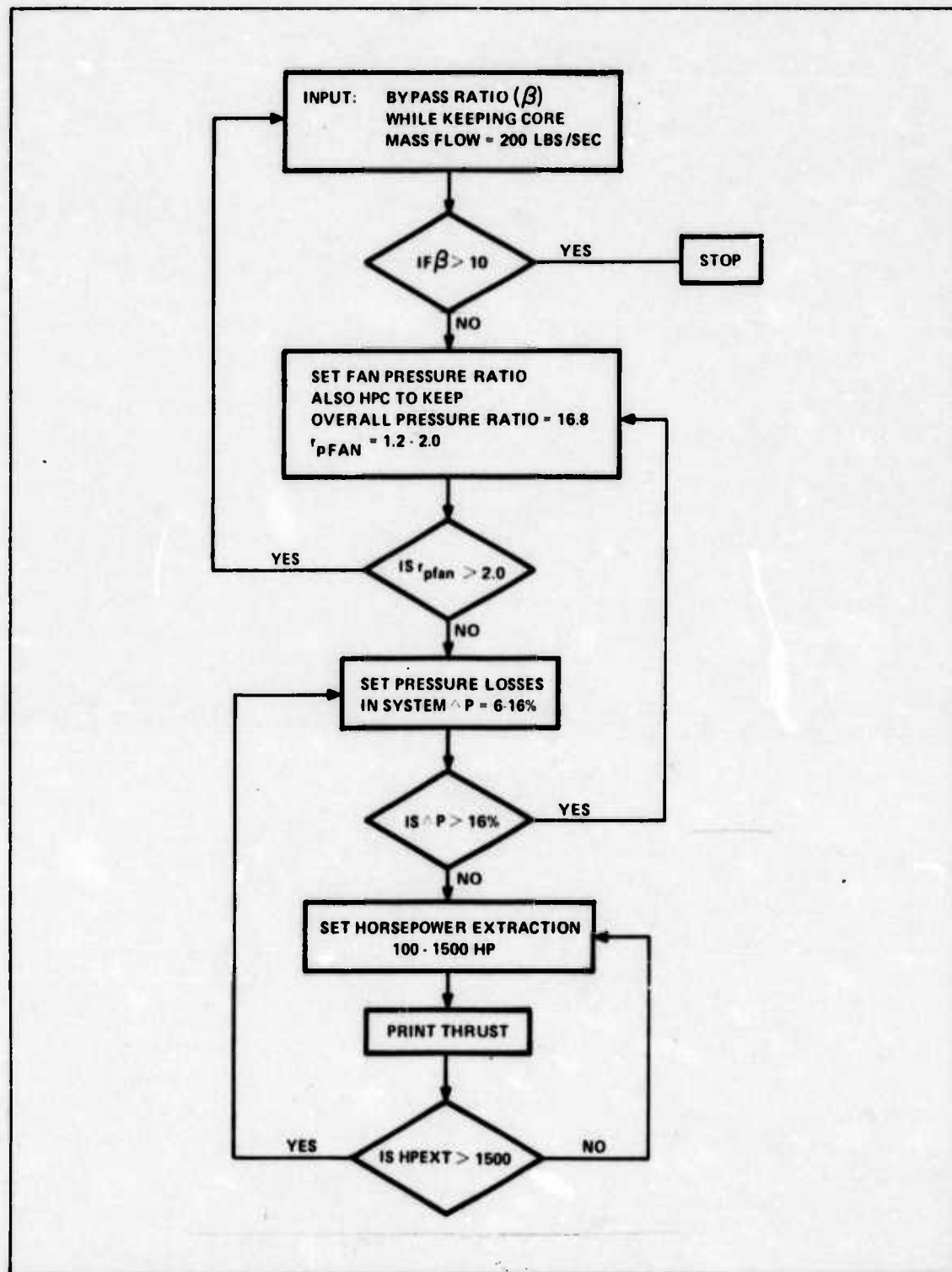


Figure A.6.3-1. Computer Logic for CARPET

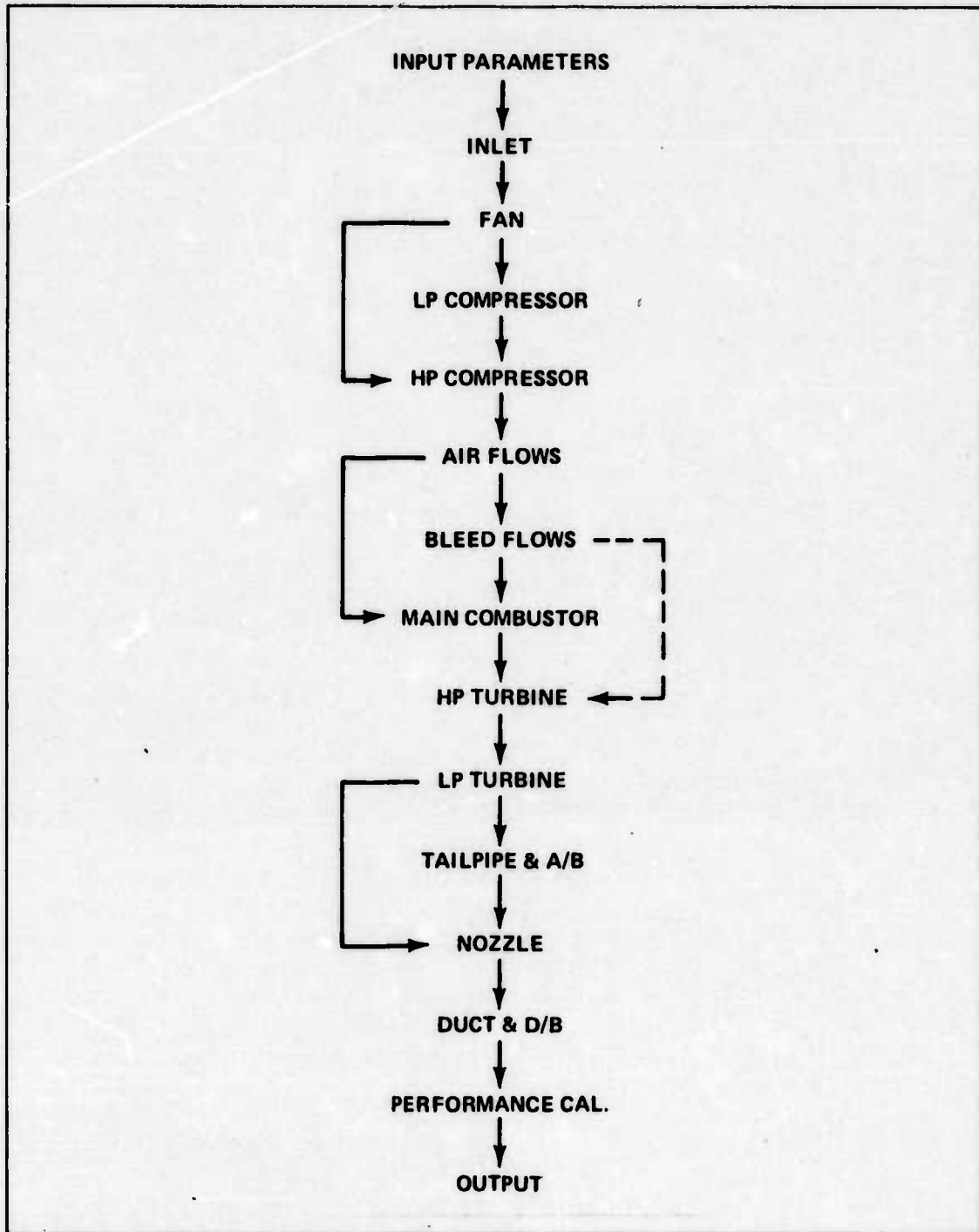


Figure A.6.3-2. Simplified Flow Diagram for CARPET

A.6.4 SAMPLE CALCULATION OF THE HEAT EXCHANGER TURBOFAN ENGINE

The example problem will be for an engine having the following specifications:

- 1) bypass ratio $\beta = 4.0$

- 2) compressor efficiency $\eta_C = 0.88$
- 3) fan efficiency $\eta_F = 0.88$
- 4) turbine efficiency $\eta_t = 0.9$
- 5) flight speed Mach = 0.6, $V_O = 596$ ft/sec
- 6) altitude = 30,000 ft
- 7) fan pressure ratio $R_{pf} = 1.4$
- 8) overall engine pressure ratio $R_p = 16.8$
- 9) ram recovery factor $\eta_{ram} = 0.9$
- 10) ambient pressure $P_O = 627$ lbs/sq ft
- 11) ambient temperature $T_O = 412^\circ R$

The stations are identified in Figure A.6.4-1.

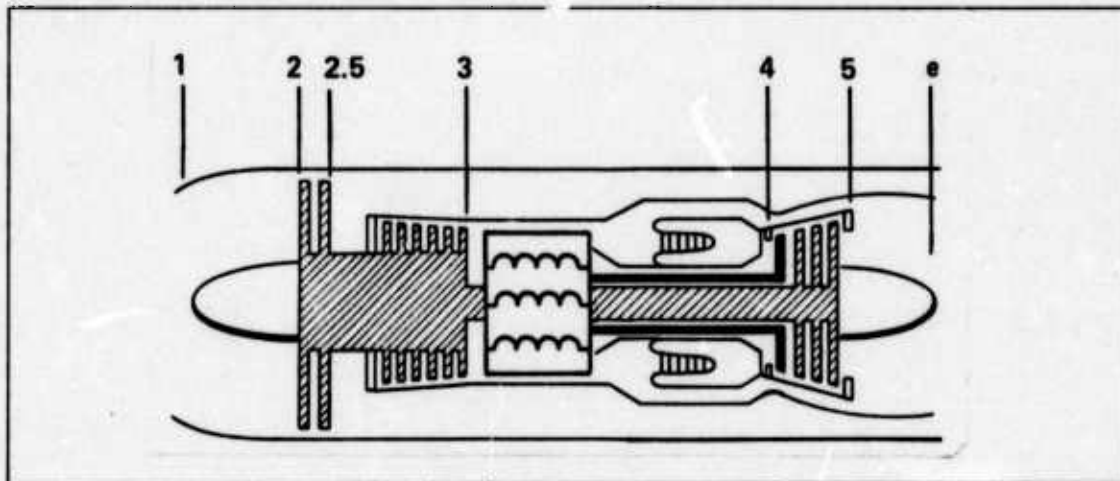


Figure A.6.4-1. Stations in Nuclear Engine

SOLUTION:

A. DIFFUSER: From Figure 5.3 on page 103 of Hesse (Ref. 69)

$$\frac{P_{t2}}{P_O} = 1.148$$

$$\frac{T_{t2}}{T_O} = 1.072$$

thus, the conditions at the face of the fan are:

$$P_{t2} = (1.148) (627 \text{ lb/ft}^2) = 720 \text{ lb/ft}^2$$

$$T_{t2} = (1.072) (412^\circ R) = 442^\circ R$$

B. FAN: for a fan pressure ratio of 1.4

$$P_{t2.5} = (1.4) (720 \text{ lb/ft}^2)$$

$$P_{t2.5} = 1008 \text{ lb/ft}^2$$

The fan work/lb air is given by

$$W_f = \frac{c_p T_{t2} X_f}{\eta_f} = \frac{(0.24) (0.442) (0.1004)}{0.88}$$

$$W_f = 12.1 \text{ BTU/lb}$$

where $X_f = r_p^k - 1$ and is in table form in (Ref. 69)

The fan horsepower is

$$\text{HP} = \frac{\dot{m}_f W_f}{0.707} = \frac{(1000) (12.1)}{0.707} = 17118$$

The temperature at the fan outlet is given by

$$T_{t2.5} = T_{t2} + \frac{W_f}{c_p}$$

$$T_{t2.5} = 442^\circ\text{R} + 50.42^\circ\text{R}$$

$$T_{t2.5} = 492.4^\circ\text{R}$$

C. COMPRESSOR: Because the overall engine pressure ratio must be 16.8, the high pressure compressor (HPC) pressure ratio is 12.0. Thus

$$P_{t3} = (12) P_{t2.5} = 12096 \text{ lb/ft}^2$$

and the compressor work is found from

$$W_c = \frac{0.24 T_{t2.5} X_c}{\eta_c} = \frac{(0.24) (492.4) (1.34)}{0.88}$$

$$W_c = 139.95 \text{ BTU/lb}$$

The horsepower required to drive the compressor is

$$\text{HP}_c = \frac{\dot{m}_c W_c}{0.707} = \frac{(200) (139.95)}{0.707} = 39,109$$

Temperature at the compressor outlet is

$$T_{t3} = T_{t2.5} + \frac{T_{t2.5}}{\eta_c} [r_p^k - 1]$$

$$T_{t3} = 492.4 + \frac{492.4}{0.88} [(12)^{0.285} - 1]$$

$$T_{t3} = 1069^\circ\text{R}$$

D. TURBINE: To find the turbine exit pressure:

$$P_{t5} = r \eta_r P_o \left[\left(1 + \frac{\gamma-1}{2} M_o^2 \right) \left(1 - \frac{x_c}{\eta_t \alpha \eta_c} - \beta \frac{x_f}{\eta_t \alpha \eta_f} \right) \right]^{\frac{1}{k}}$$

which is an equation presented by Hesse (Ref. 69, p. 272) where

r = total engine pressure ratio

α = total cycle temperature ratio T_{t4}/T_{t2}

thus

$$P_{t5} = (16.8) (0.9) (629) \left[\left(1 + 0.4 (0.36) \right) \left(1 - \frac{1.03}{(0.9) (4.43) 0.88} - 4 \frac{0.1}{(0.9) (4.43) 0.88} \right) \right]^{3.5}$$

$$P_{t5} = 1522 \text{ lb/ft}^2$$

Checking to see if the nozzle is operating supercritically:

$$\frac{P_o}{P_{t5}} = 0.4133$$

which is less than the 0.495 required for supercritical operation with a nozzle efficiency of 0.98; therefore, the nozzle is supercritical.

Total pressure entering the turbine. Accounting for the pressure drop across the heat exchanger and the combustor for a dual mode engine, the pressure less will be assumed to be 11% (Section 6.1.5). Then, P_{t4} may be found from

$$P_{t4} = (1 - 0.11) P_{t5} = 10765 \text{ lb/ft}^2$$

so the pressure ratio across the turbine is

$$\frac{P_{t4}}{P_{t5}} = 7.07$$

Turbine exit temperature may be found from

$$T_{t5} = T_{t4} - \eta_t T_{t4} \left[1 - \frac{1}{r_p^k} \right]$$

$$T_{t5} = 1205^\circ\text{R}$$

The turbine work must equal that required by the compressor and the fan, thus

$$W_t = W_c + \beta W_f$$

$$W_t = 139.95 + 4 (12.1)$$

$$W_t = 188.4 \text{ BTU/lb}$$

The horsepower delivered by the turbine is

$$HP_t = \frac{(200)(188.4)}{0.707} = 53,295$$

Because supercritical flow exists, the exit pressure is the critical pressure:

$$P_{ce} = P^* = (0.495)(1522) = 761 \text{ lb/ft}^2$$

similarly for the exit temperature

$$T_{ce} = T^* = \frac{T_{t5}}{1.165} = 1034^\circ\text{R}$$

E. EXIT: The exit velocity of the engine core is given by

$$V_e = \sqrt{2 \gamma R T^*}$$

$$V_e = 1576 \text{ ft/sec}$$

The area exit of the nozzle is found from the law of continuity:

$$\dot{m} = \rho A V$$

$$A = \frac{\dot{m}}{\rho V} = \frac{\dot{m} R T}{P V}$$

$$A = \frac{(200 \text{ lb/sec}) \left(53.3 \frac{\text{ft-lb}}{\text{lb-}^\circ\text{R}} \right) (1034^\circ\text{R})}{(761 \text{ lb/ft}^2)(1576 \text{ ft/sec})}$$

$$A_{ce} = 9.2 \text{ ft}^2$$

or a diameter of

$$D_{ce} = 3.42 \text{ ft}$$

Denoting the exit of the fan as Station 8, the conditions there are

$$P_{t8} = P_{t2.5} = 1008 \text{ lb/ft}^2$$

$$T_{t8} = T_{t2.5} = 492.4^\circ\text{R}$$

The exit velocity of the bypass air is given by Eq. 5.33 of Hesse (Ref. 69, p. 128)

$$V_8 = \left\{ \frac{2g \gamma R}{\gamma - 1} T_{t8} \left[1 - \left(\frac{P_0}{P_{t8}} \right)^k \right] \right\}^{1/2}$$

which gives:

$$V_8 = 862 \text{ ft/sec}$$

The exit area of the fan nozzle may be found as follows:

$$A_2 = \pi r_2^2 - \pi r_1^2$$

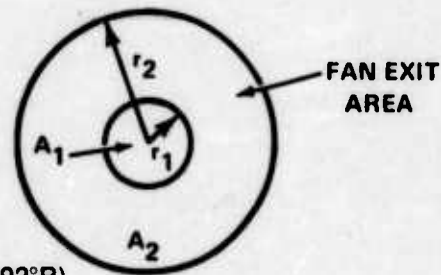
$$r_2 = \left[\frac{A_2}{\pi} + r_1^2 \right]^{1/2}$$

$$A_2 = \frac{\dot{m} R T}{P V} = \frac{(800) \left(53.3 \frac{\text{ft-lb}}{\text{lb-}^\circ\text{R}} \right) (492^\circ\text{R})}{(1008 \text{ lb/ft}^2) (862 \text{ ft/sec})}$$

$$A_2 = 24.14 \text{ ft}^2$$

$$\therefore r_2 = 3.26 \text{ ft}$$

$$D_{ef} = 6.51 \text{ ft}$$



F. THRUST: The net thrust of a turbofan engine is equal to the gross thrust of the core and bypass minus the ram drag:

$$F_n = \frac{\dot{m}_b}{g} (V_{ef} - V_o) + \frac{\dot{m}_c}{g} (V_{ce} - V_o) + (P_{ef} - P_o) A_{ef} + (P_{ce} - P_o) A_{ce}$$

However, $P_{ef} = P_o$, i.e., the exit pressure of the bypass air is equal to the ambient air pressure because it is expanded to atmospheric pressure.

Thus:

$$F_n = \frac{800}{32.2} (862 - 596) + \frac{200}{32.2} (1576 - 596) + (761 - 629) 9.2$$

$$F_n = 6608 + 6087 + 1214$$

$$F_n = 13910 \text{ lb}$$

A.6.5 ADDITIONAL GRAPHS FOR THE HEAT EXCHANGER TURBOFAN ENGINE

Several graphs for the heat exchanger turbofan engine with bypass ratios of 6.5 and 8.0 showing the affects of overall engine pressure ratio and horsepower extraction on the net thrust are presented in Figures A.6.5-1 through A.6.5-4.

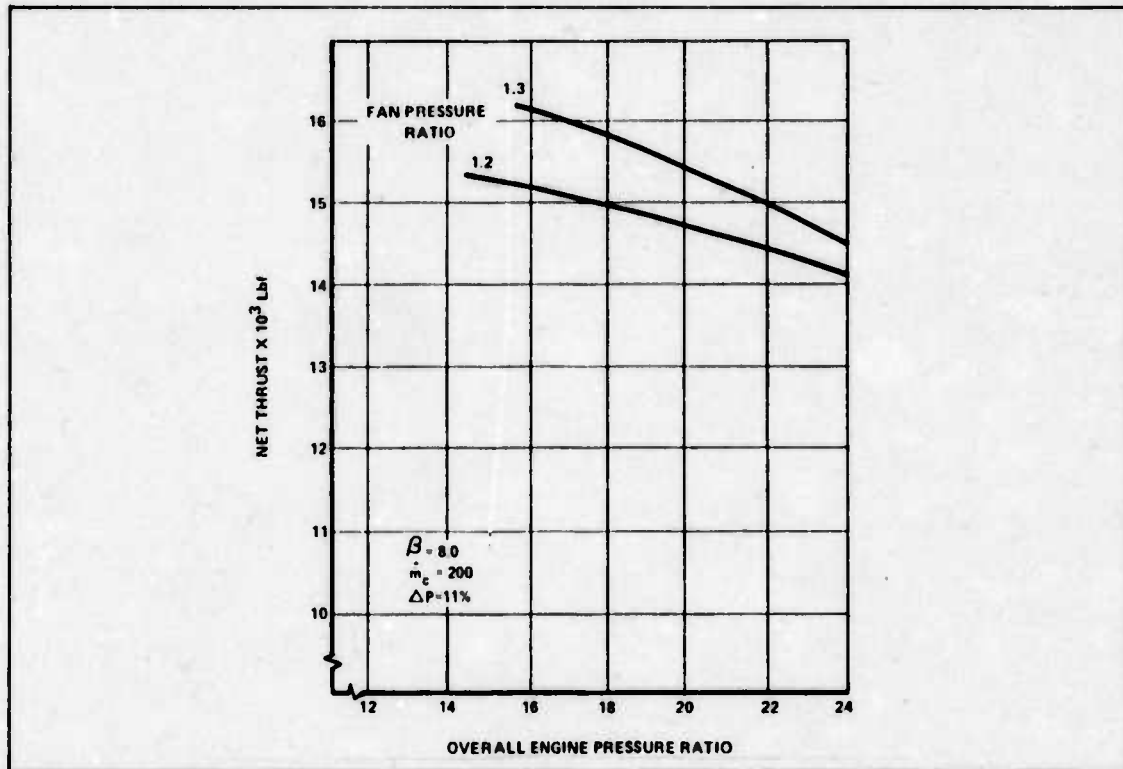


Figure A.6.5-1. Overall Engine Pressure Ratio vs Net Thrust

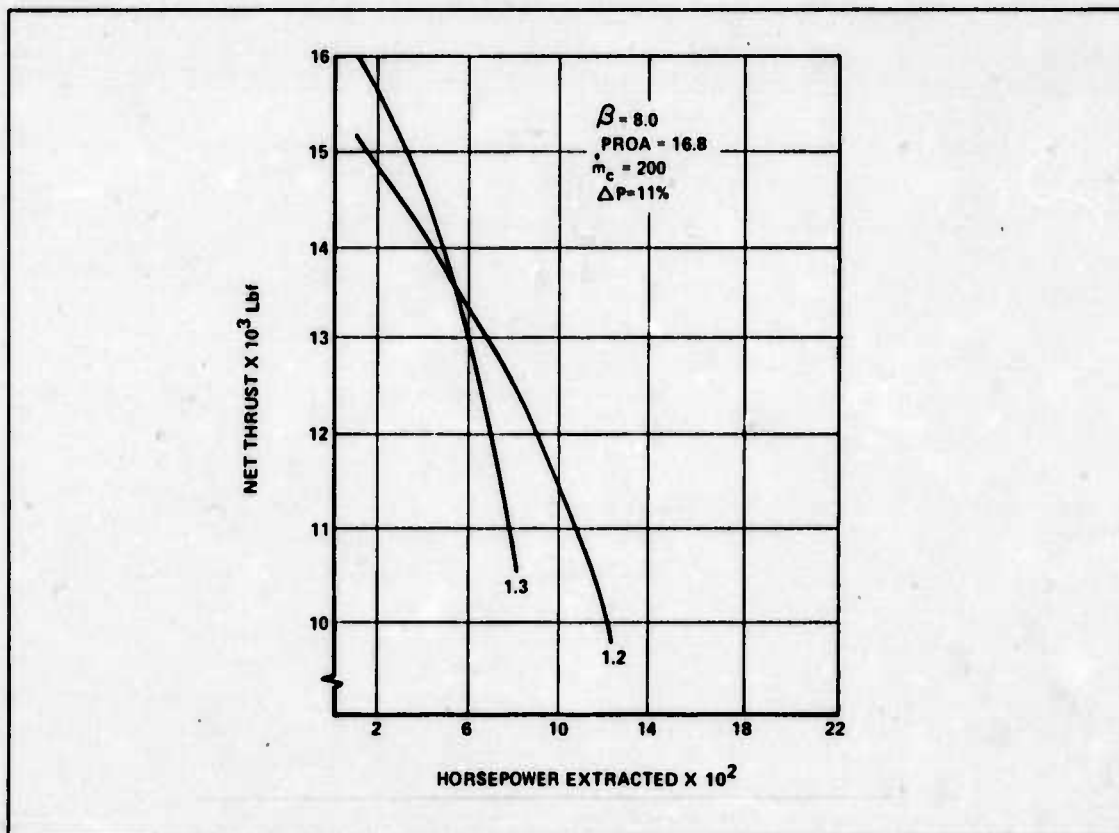


Figure A.6.5-2. Horsepower Extracted vs Net Thrust

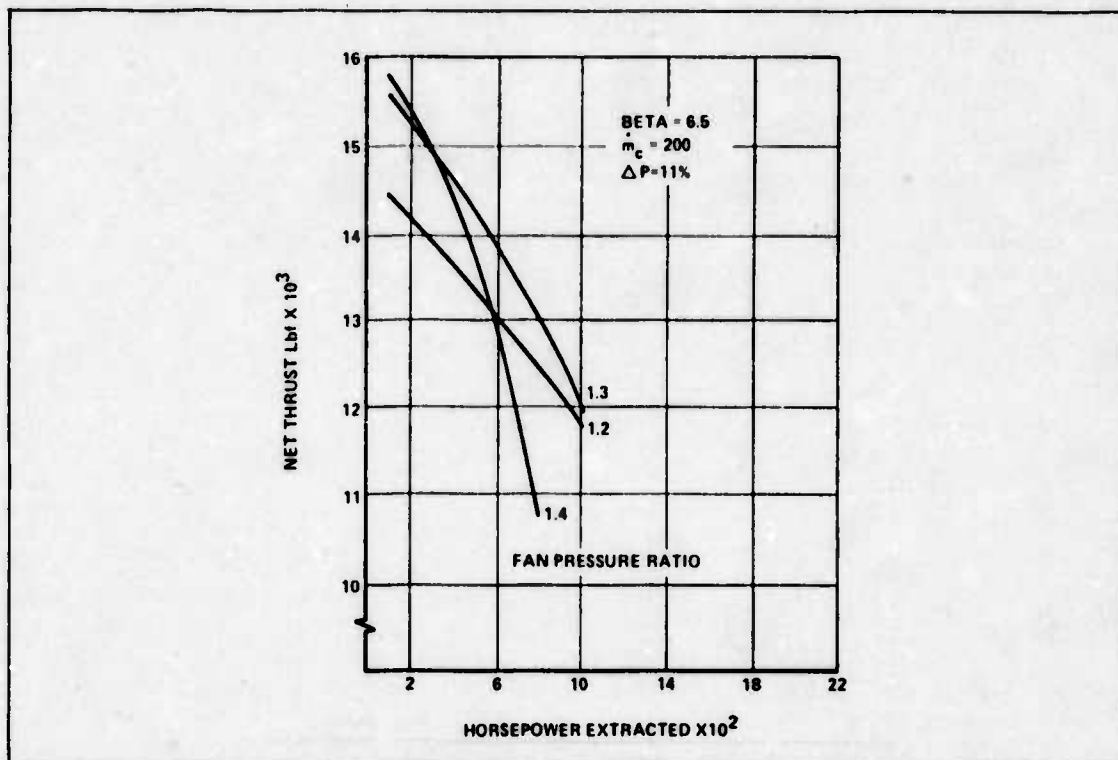


Figure A.6.5-3. Horsepower Extracted vs Net Thrust

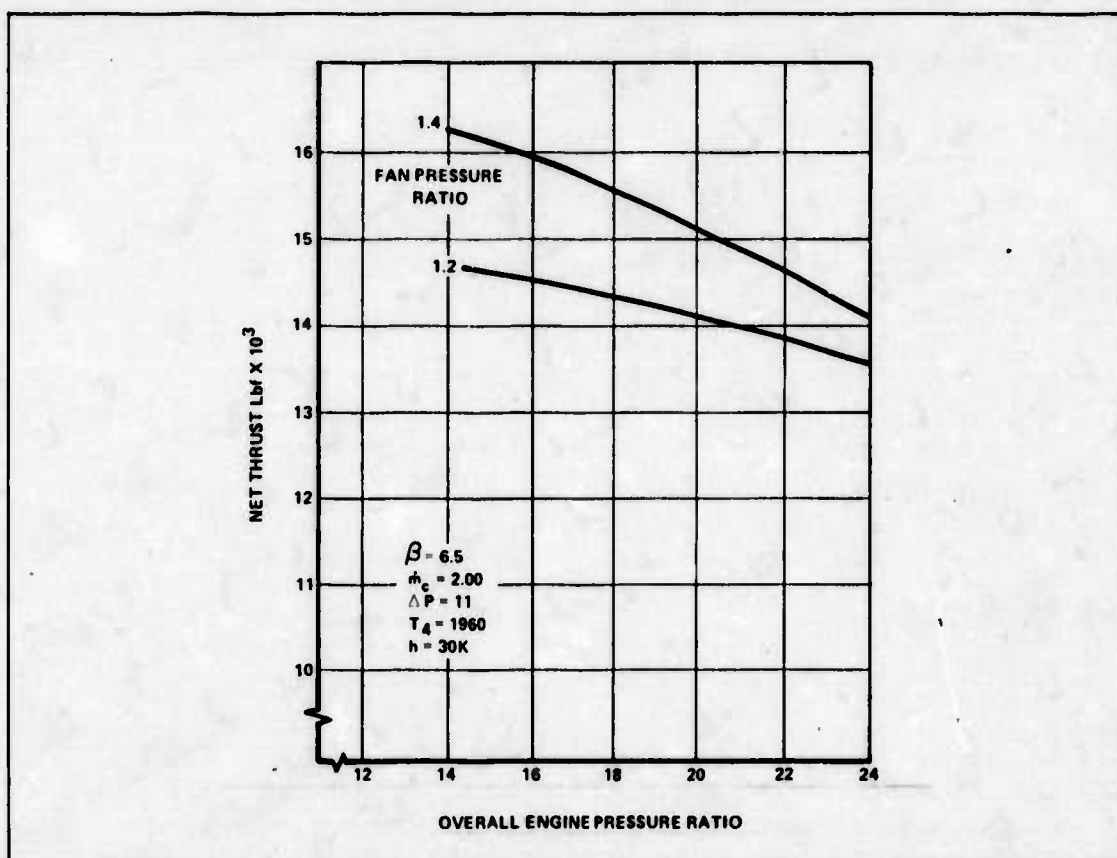


Figure A.6.5-4. Overall Engine Pressure Ratio vs Net Thrust

A.6.6 FLOW DIAGRAM OF COMPUTER PROGRAM USED FOR THE DIRECT CYCLE

A computer program was written in order to study the direct cycle ducted fan engine concept. Input parameters for the program were:

- 1) flight speed
- 2) efficiencies of the compressor, turbine, and fan
- 3) pressure losses
- 4) altitude conditions
- 5) temperature and pressures for the compressor and turbine.

The program was designed to calculate the net thrust for various:

- 1) mass flow of helium (the working medium in the gas turbine generator)
- 2) fan pressure ratios

Also, it calculated the thrust for a fully expanded nozzle as well as a choked nozzle when the pressure ratio across the exit nozzle met critical conditions.

Figure A.6.6-1 presents a flow diagram of the computer program.

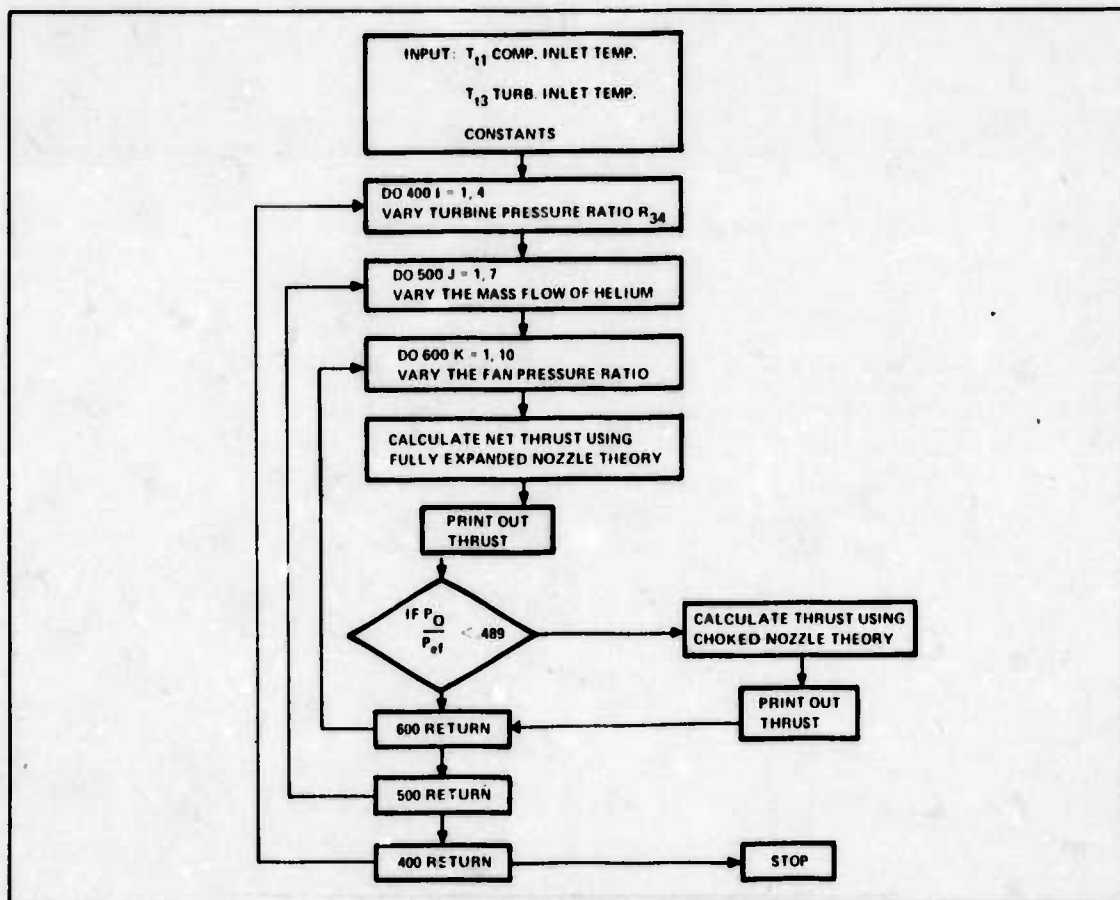


Figure A.6.6-1. Computer Logic for Direct Cycle Engine

A.6.7 SAMPLE CALCULATION FOR THE DIRECT CYCLE

The following example will show the equations used in the computer program discussed in Appendix A.6.6 and how they were used.

GIVEN:

$$P_0 = 629 \text{ lb/ft}^2$$

$$T_{t0} = 412^\circ\text{R}$$

$$r_{\text{helium}} = 1.67$$

$$V_0 = 596 \text{ ft/sec}$$

$$T_{t3} = 2060^\circ\text{R}$$

$$c_{p \text{ helium}} = 1.242 \frac{\text{BTU}}{\text{lb}^\circ\text{R}}$$

$$R_{pc} = 2.7 = P_{t2}/P_{t1}$$

$$\eta_t = 0.9, \eta_c = 0.88, \eta_f = 0.85$$

$$c_{p \text{ air}} = 0.24 \frac{\text{BTU}}{\text{lb}^\circ\text{R}}$$

SOLUTION:

1. TURBINE WORK (per lb)

$$W_t = c_p \eta_t T_{t3} \left[1 - \frac{1}{X_t} \right]$$

where

$$X_t = (P_{t3}/P_{t4})^k = 0.98 (P_{t2}/P_{t1})$$

thus

$$W_t = (1.242) (0.9) (2060) \left[1 - \frac{1}{1.48} \right]$$

$$W_t = 742.4 \text{ BTU/lb}$$

2. COMPRESSOR WORK (per lb)

$$W_c = \frac{c_p T_{t1}}{\eta_c} [X_c - 1]$$

$$W_c = \frac{\left(1.242 \frac{\text{BTU}}{\text{lb}^\circ\text{R}} \right) (650^\circ\text{R}) [1.49 - 1]}{0.88}$$

$$W_c = 449.5 \text{ BTU/lb}$$

3. NET WORK (per lb): This work may be used to drive the fan or the circulator needed to pump the helium gas in the primary and secondary coolant loops.

$$W_n = W_t - W_c$$

$$W_n = 742.4 - 449.5$$

$$W_n = 294.9 \text{ BTU/lb}$$

4. FAN WORK: Accounting now for the mass flow of helium and air, the fan work in terms of BTU/sec is given by

$$W_f = W_n \dot{m}_{\text{helium}} = (295 \text{ BTU/lb}) (70 \text{ lb/sec})$$

$$W_f = 20650 \text{ BTU/sec}$$

also

$$W_f = \frac{\dot{m}_{\text{air}} c_{\text{pair}} T_{t5}}{\eta_f} (X_f - 1)$$

and T_{t5} is equal to 442°R (See Appendix 6.4). Thus a tradeoff between fan pressure ratio and mass flow of air in the bypass (ducting) is presented. Selecting the fan pressure ratio as 1.6, then

$$\dot{m}_{\text{air}} = \frac{W_f \eta_f}{c_{\text{pair}} T_{t5} (X_f - 1)}$$

$$\dot{m}_{\text{air}} = 1154 \text{ lb air/sec}$$

Checking the pressure ratio across the exit nozzle of the bypass

$$P_{te} = P_{t6} = r_{pf} P_{t5} = 1155.2$$

and

$$\frac{P_o}{P_{te}} = 0.54$$

5. EXIT CONDITIONS: This engine has no core exhaust but rather just the air passing through the ducting. The temperature and pressure are calculated based on expansion nozzle theory as subcritical flow exits for this particular engine.

$$P_{ef} = 629.7 \text{ psf (static pressure)}$$

$$T_{tef} = T_{t6} = T_{t5} + \frac{c_p T_{t5}}{\eta_f} (X_f - 1) = 467^\circ\text{R}$$

$$P_{t6} = r_{pf} P_{t5} = 1155.2$$

The exit velocity may be found from

$$V_{ef} = \left\{ \frac{2g\gamma R}{\gamma-1} T_{ef} \left[1 - \left(\frac{P_{ef}}{P_{t6}} \right)^k \right] \right\}^{1/2}$$

$$V_{ef} = 985 \text{ ft/sec}$$

6. NET THRUST: Because it is an expanded nozzle, the pressure area term in the thrust equation becomes zero, leaving:

$$F_n = \frac{\dot{m}_{\text{air}}}{g} (V_{ef} - V_o)$$

thus

$$F_n = \frac{1154}{32.2} (389)$$

$$F_n = 13941 \text{ lb}$$

APPENDIX A.7 HEAT TRANSFER

A.7.1 PIPING CALCULATIONS

The calculations in this appendix are based on a single pipe as shown in Figure A.7.1-1

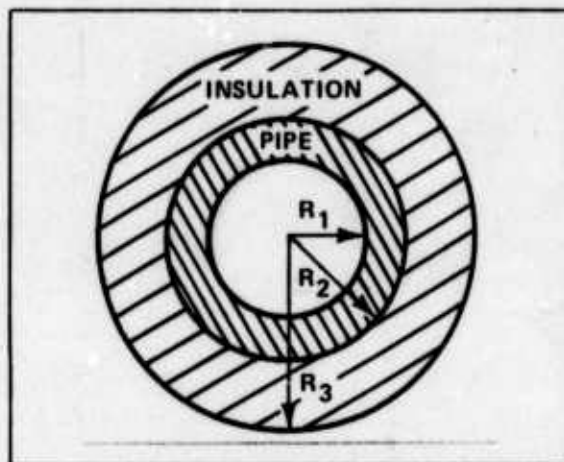


Figure A.7.1-1. Concentric Pipe Cross Section

The parameter values used in this development are those derived in Section 7.3.1 for the supply line of the two-loop helium indirect cycle. The mass flow rate of 70 lb/sec establishes the required flow area and radius R_1 :

$$R_1 = \sqrt{\frac{\dot{m}_s}{\pi \rho_{PI} v_{PI}}}$$

Substituting yields:

$$R_1 = .385 \text{ ft}$$

Use the thick-walled cylinder equation with the 10,000 hr creep rupture stress of Haynes 188 at 1600°F of 6000 psi, and the secondary loop operating pressure of 1800 psi to define R_2 .

$$R_2 = R_1 \sqrt{\frac{\text{stress} + \text{pressure}}{\text{stress} - \text{pressure}}}$$

Substituting yields:

$$R_2 = 0.525 \text{ ft}$$

This implies the pipe thickness is:

$$R_2 - R_1 = 0.525 - 0.385 = 0.140 \text{ ft} = 1.676 \text{ in.}$$

Using an initial assumed thickness of insulation around the pipe of 1 in., R_3 then equals 0.608 ft. Once the pipe and insulation dimensions are known, the thermal resistance of their combination can be calculated using

$$r = \frac{\ln (R_2/R_1)}{K_{PI}} + \frac{\ln (R_3/R_2)}{K_I} = 1.309 \text{ BTU/hr}\cdot\text{ft}^2\cdot^\circ\text{F} \quad (\text{Ref. 74, p. 22})$$

where K_{PI} and K_I are the thermal conductivity coefficients of the pipe and insulation, respectively. The next step is to define the thermal resistance of the heat transfer fluid, helium, on the inside of the pipe, and the thermal resistance of the stagnant, trapped air surrounding the outside of the pipe. The temperature of this trapped air is assumed to be -70°F for the reason explained in Section 7.1.1.1. To calculate these resistances, it is first necessary to define the absolute viscosity of the flowing helium. This is done by

$$\mu = \rho \nu = 3.1 \times 10^{-5} \text{ lb/ft}\cdot\text{sec} \quad (\text{Ref. 74, p. 113})$$

where μ = absolute viscosity of helium in the pipe
 ν = kinematic viscosity of helium in the pipe

The next step is to calculate the Reynolds number of the helium in the pipe by:

$$\text{Re} = \frac{2 \rho \nu R_1}{\mu} = 3.71 \times 10^6 \quad (\text{Ref. 74, p. 115})$$

This confirms that the helium is in a turbulent flow condition. Next calculate the film conductance of the helium in the pipe using:

$$\begin{aligned} h &= 0.625 K_h (\text{Re Pr})^{0.4/2} R_1 \\ &= 59.2 \text{ BTU/hr}\cdot\text{ft}^2\cdot^\circ\text{F} \end{aligned} \quad (\text{Ref. 74, p. 180})$$

The next step is to define the film conductance coefficient for the air surrounding the pipe. This is defined by h_w :

$$\begin{aligned} h_w &= 0.18 (T_w - T_a)^{1/3} \\ &= 0.995 \text{ BTU/hr}\cdot\text{ft}^2\cdot^\circ\text{F} \end{aligned} \quad (\text{Ref. 74, p. 199})$$

where T_a = temperature of surrounding air
 T_w = temperature of outside edge of insulation

T_w is assumed to be a maximum of 100°F for this case. Thus with the thermal resistance of the pipe and the insulation and the film conductances of the inside fluid and the outside air defined, the actual heat being transferred or lost radially per foot of pipe length can be calculated using

$$Q = \frac{2 \pi (T_{s4} - T_a)}{\frac{1}{hR_1} + r + \frac{1}{h_w R_3}} = 0.2 \text{ MW} \quad (\text{Ref. 74, p. 23})$$

where Q = the actual heat lost divided by the pipe length.

This then is one of the two parameters that are used to define the insulation thickness. The criterion is that if the value of Q exceeds 1/10 of one percent of the actual q being transferred to the engine, another inch is added to the insulation thickness and the entire calculation is reaccomplished beginning with the redefinition of R_3 .

The other criterion used to define the insulation thickness is the maximum outside insulation temperature. To calculate this, use the fact that the temperature changes are proportional to the thermal resistances via

$$\frac{T_w - T_a}{r_o} = \frac{T_{s4} - T_a}{r_T}$$

where

$$r_o = 1/h_w R_3$$

$$r_T = r_o + r + 1/h R_1$$

This proportion when solved for T_w yields

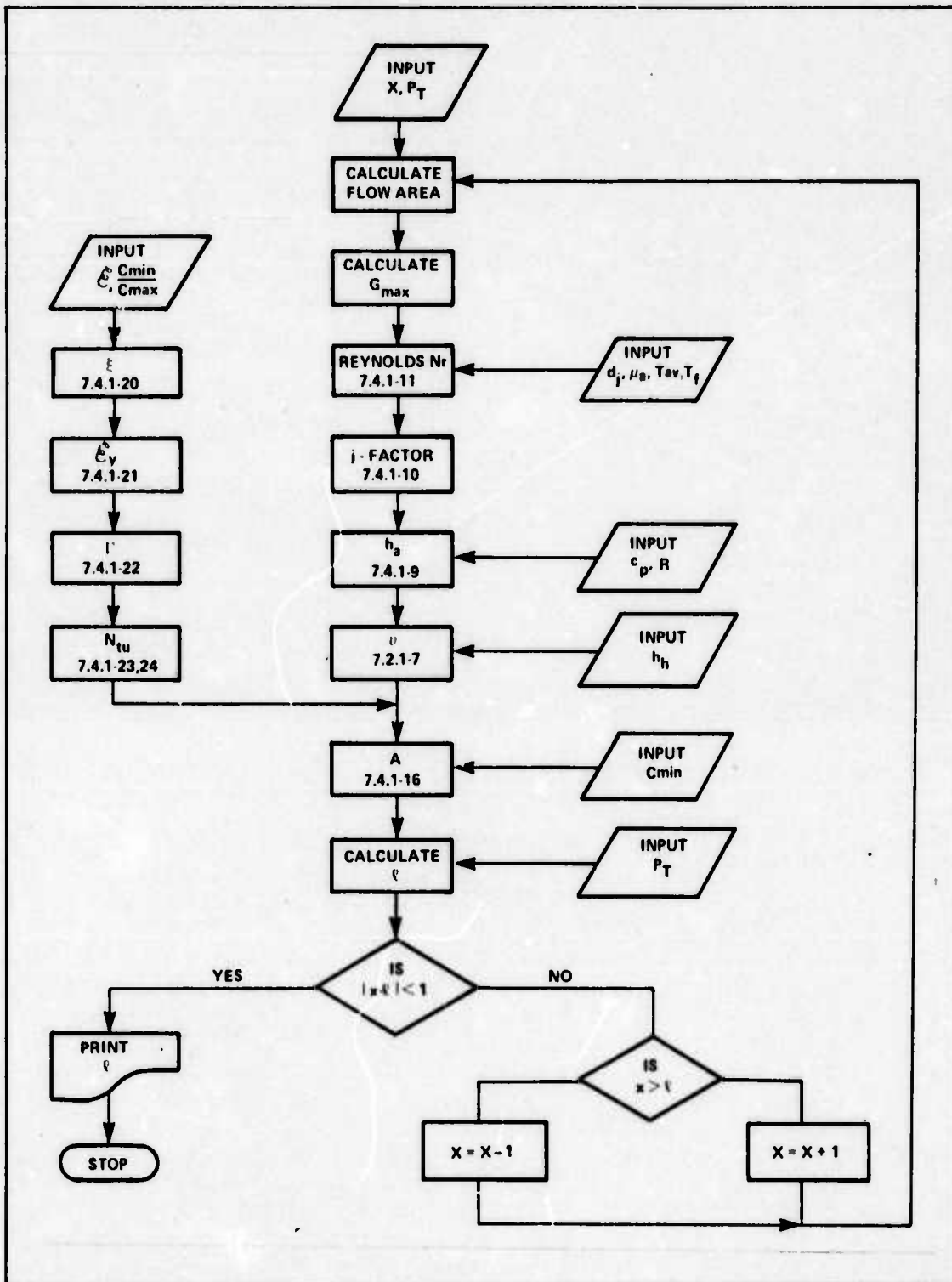
$$T_w = T_a + \frac{r_o}{r_T} (T_{s4} - T_a) = 561^\circ\text{F}$$

This value of T_w is then compared to the maximum allowable temperature at the surface of the insulation of 100°F and if it exceeds that value, another inch of insulation is added and the entire calculation is redone.

For the case in point of helium as the heat transfer fluid, here is a summary of the values obtained after the insulation is increased to the point where both criteria are satisfied.

Maximum allowable q — 0.05 MW
 Actual radial q lost — 0.05 MW
 Maximum allowable T_w — 100°F
 Actual T_w — 94°F
 Insulation thickness — 8 in.

A.7.2 TUBE LENGTH CALCULATION COMPUTER LOGIC



APPENDIX A.8 SAFETY ANALYSIS

A.8.0 INTRODUCTION

This appendix is a supplement to Section 8. Sections A.8.1.1 through A.8.1.4 deal with collection and modeling of the data used in obtaining the failure rates for Section 8.1. Section A.8.2 deals with the consequence models of both the WASH-1400 report and this study. Section A.8.2.1 through A.8.2.4 include the validation of the WASH-1400 model. Section A.8.2.5 gives a numerical example of calculations leading to one K factor. The product of a K factor and a population density give the number of deaths for a particular weather condition.

The final Section A.8.3 contains the computer logic diagrams used in modeling all aspects of Section 8.

A.8.1 RELEASE PROBABILITY DATA

A.8.1.1 CRASH DATA

A.8.1.1.1 CRASH RATES: Aircraft crash rate data were taken from Reference 183 for 1961 through 1973. In all cases, the data are a combined figure for the two major aircraft categories, bomber and cargo. The crash rate data are shown in Table A.8.1.1.1-1 where the rate is the number of crashes divided by the number of flying hours.

The 13 estimates of crash rate shown in Table A.8.1.1.1-1 were modeled using standard statistical techniques to determine the underlying probability function. Estimators for the mean and standard deviation were obtained from:

$$\text{Mean} = \bar{\lambda} = \frac{1}{N} \sum_{i=1}^N \lambda_i \quad (\text{A.8.1.1.1-1})$$

$$\text{Standard deviation} = S = \left[\frac{1}{N-1} \sum_{L=1}^N (\lambda_i - \bar{\lambda})^2 \right]^{1/2} \quad (\text{A.8.1.1.1-2})$$

The estimates so derived are.

$$\text{mean} = 1.42 \times 10^{-5} \text{ crashes/hour}$$

$$\text{std dev} = 4.26 \times 10^{-6}$$

A standard normal distribution with Z statistic

$$Z = \frac{\lambda - 1.42 \times 10^{-5}}{4.26 \times 10^{-6}} \quad (\text{A.8.1.1.1-3})$$

where λ = crash rate

TABLE A.8.1.1.1-1. AIRCRAFT CRASH RATES

YEAR	NUMBER OF CRASHES	NUMBER OF FLYING HOURS	CRASH RATE
1961	77	3,787,155	2.03×10^{-5}
1962	82	3,599,941	2.30×10^{-5}
1963	51	3,511,129	1.45×10^{-5}
1964	58	3,527,498	1.64×10^{-5}
1965	53	3,434,601	1.54×10^{-5}
1966	60	3,490,596	1.71×10^{-5}
1967	60	3,530,227	1.69×10^{-5}
1968	59	4,116,823	1.43×10^{-5}
1969	51	3,561,022	1.43×10^{-5}
1970	33	3,064,790	1.07×10^{-5}
1971	27	2,768,109	9.75×10^{-6}
1972	33	2,630,359	1.25×10^{-5}
1973	11	1,998,098	5.50×10^{-5}

was hypothesized as the underlying probability distribution and was tested using the Kolmogorov-Smirnov (K-S) test at a significance level $\alpha = 0.20$, and the normal distribution was accepted. Table A.8.1.1.1-2 shows the ordered values of failure rate; their observed cumulative probability, $\frac{i}{n}$; the predicted cumulative probability, P ; and the absolute difference between observed and predicted probabilities, d . The maximum value of d is 0.124, and the critical value of d from K-S tables (Ref. 97, p. 300) is 0.190. Since 0.124 is less than 0.190, the hypothesis of normality is accepted.

TABLE A.8.1.1.1-2. K-S TEST OF FAILURE RATES

i	$\frac{i}{n}$	$\frac{i}{13}$	P	d
1	5.50×10^{-6}	0.076	0.020	0.053
2	9.75×10^{-6}	0.153	0.149	0.004
3	1.07×10^{-5}	0.230	0.206	0.023
4	1.25×10^{-5}	0.307	0.344	0.037
5	1.43×10^{-5}	0.384	0.508	0.124
6	1.43×10^{-5}	0.461	0.508	0.047
7	1.45×10^{-5}	0.538	0.472	0.066
8	1.54×10^{-5}	0.615	0.610	0.005
9	1.64×10^{-5}	0.692	0.696	0.004
10	1.69×10^{-5}	0.769	0.736	0.033
11	1.71×10^{-5}	0.846	0.751	0.095
12	2.03×10^{-5}	0.923	0.923	0.000
13	2.30×10^{-5}	1.000	0.980	0.020

In addition to the crash rates, the frequency of occurrence by location was determined. Crashes during takeoff, initial climb after takeoff, final descent for landing, and landing were grouped into a category called airport crashes. All other crashes were denoted cruise crashes. The relative frequency of these two categories was found to be 80 percent for airport crashes and 20 percent for cruise crashes, or:

$$P(\text{airport crash} | \text{crash occurred}) = 0.8$$

$$P(\text{cruise crash} | \text{crash occurred}) = 0.2$$

The frequency with which aircraft crashed with electrical power failed was also determined. Of 439 crashes, only three had electrical failure, or

$$P(\text{electrical power failed crash}) = 6.83 \times 10^{-3}$$

A distribution of electrical failure probabilities was formulated by utilizing the methodology and error factor values given in WASH-1400 (Ref. 185, Appendix III, p. 104). The failure probability of 6.83×10^{-3} was taken as the median value, and an upper bound was found by multiplying by an error factor of ten. The lower bound was found by dividing the median value by an error factor of ten. This methodology generates a log-normal distribution of values and the computed upper value of 6.83×10^{-2} and the computed lower value of 6.83×10^{-4} were taken as the 95th and 5th percentiles, respectively.

A.8.1.1.2 CRASH IMPACT SPEED: The crash impact speeds for large multi engine aircraft crashes were compiled in a NASA study (Ref. 55, p. 10-27) and were used in this report as a probability distribution.

The crashes were grouped into categories of airport crash and cruise crash, and the speeds for both cases were modeled as in Section A.8.1.1.1. The impact speed probability distributions for both cases were found to be normally distributed with Z statistic as follows:

For airport crash

$$Z = \frac{V_A - 195}{66} \tag{A.8.1.1.2-1}$$

For cruise crash

$$Z = \frac{V_C - 583}{269} \tag{A.8.1.1.2-2}$$

V_A = airport crash velocity

V_C = cruise crash velocity

The data used are given in Table A.8.1.1.2-1 for airport crashes and in Table A.8.1.1.2-2 for cruise crashes. All impact speeds are given in units of ft/sec.

TABLE A.8.1.1.2-1. AIRPORT CRASH IMPACT SPEEDS

CRASH NUMBER	IMPACT SPEED FT/SEC	CRASH NUMBER	IMPACT SPEED FT/SEC
1	34	17	186
2	60	18	186
3	132	19	200
4	135	20	209
5	140	21	220
6	145	22	220
7	160	23	257
8	169	24	270
9	169	25	270
10	169	26	270
11	169	27	270
12	169	28	275
13	169	29	290
14	169	30	300
15	170	31	317
16	186	—	—

TABLE A.8.1.1.2-2. CRUISE CRASH IMPACT SPEEDS

CRASH NUMBER	IMPACT SPEED FT/SEC
1	270
2	340
3	500
4	680
5	710
6	1000

A.8.1.1.3 CRASH IMPACT ANGLES: In addition to the impact velocity, the angle of impact measured between the terrain and the impact velocity vector was compiled in Reference 55, p. 10-27. These were also grouped into categories of airport and cruise crashes. The impact angle data for airport crashes are given in Table A.8.1.1.3-1 and for cruise crashes in Table A.8.1.1.3-2.

TABLE A.8.1.1.3-1. AIRPORT CRASH IMPACT ANGLES

CRASH NUMBER	IMPACT ANGLE	CRASH NUMBER	IMPACT ANGLE
1	1	12	8
2	1	13	8
3	1	14	10
4	1	15	15
5	1	16	25
6	1	17	30
7	2	18	45
8	5	19	50
9	5	20	50
10	5	21	65
11	6	—	—

TABLE A.8.1.1.3-2. CRUISE CRASH IMPACT ANGLES

CRASH NUMBER	IMPACT ANGLE	CRASH NUMBER	IMPACT ANGLE
1	10	7	60
2	20	8	80
3	20	9	80
4	30	10	90
5	57	11	90
6	60	—	—

These data were used in the SIMPAK computer program and the distribution statistics are summarized in Table A.8.1.1.3-3.

TABLE A.8.1.1.3-3. CRASH IMPACT ANGLE PROBABILITY DISTRIBUTION

CRASH LOCATION	ANGLE			
	0.05	0.50	0.95	MEAN
AIRPORT	1.00	6.00	44.5	14.9
CRUISE	18.5	60.0	81.0	54.9

A.8.1.2 AIRCRAFT SYSTEM FAILURE RATES

A.8.1.2.1 ELECTRICAL SYSTEMS: Aircraft primary electrical system failure data are based on historical data from the C-5 data base and were provided by the Lockheed Corporation (Ref. 156). The C-5 electrical system data are broken into two broad categories, Generator and Generator Subsystem. These two categories make up one independent electrical system and the failure rates were given as 8.387×10^{-5} failures/hour for the Generator and 1.51×10^{-3} failures/hour for the Generator subsystem. These rates were taken as an upper bound and the possibility of improved reliability was incorporated by setting a lower bound one order of magnitude lower and skewing a log-normal distribution between the bounds (Ref. 185, Appendix III, p. 17).

The distribution statistics are summarized in Table A.8.1.2.1-1.

TABLE A.8.1.2.1-1. AIRCRAFT ELECTRICAL SYSTEM FAILURE RATES

COMPONENT	FAILURE RATE		
	.05	.50	.95
GENERATOR	8.38×10^{-6}	5.89×10^{-5}	8.38×10^{-5}
GENERATOR SUBSYSTEM	1.51×10^{-4}	1.06×10^{-3}	1.51×10^{-3}

A.8.1.2.2 ENGINES: Engine failure rates were taken from Reference 60, p. 132. These rates are current and projected rates for the General Electric CF-6 engine and were given as 9.5×10^{-5} failures/hour and 4×10^{-5} failures/hour. These values were taken as the end points of a Beta distribution with parameters (4,2). This was done to favor the higher failure rate end of the distribution during Monte Carlo random sampling. The Beta (4,2) distribution is similar to the log-normal used in Reference 185, but is skewed in the opposite direction. The distribution statistics are given in Table A.8.1.2.2-1.

TABLE A.8.1.2.2-1. ENGINE FAILURE RATES

COMPONENT	FAILURE RATE		
	0.0	0.50	1.0
ENGINE	4.00×10^{-5}	7.68×10^{-5}	9.50×10^{-5}

A.8.1.3 NUCLEAR SYSTEM DATA

A.8.1.3.1 NUCLEAR SYSTEM FAILURE RATES: The failure rates for all components in the nuclear system are given in Table A.8.1.3-1. All failure rates are distributed with a log-normal distribution. Most of the data were taken directly from Reference 185.

TABLE A.8.1.3-1. NUCLEAR SYSTEM FAILURE RATES

COMPONENT OR FUNCTION	FAILURE RATE			REFERENCE
	.05	.50	.95	
AUX GEN START	$1.00 \times 10^{-2}/D$	$3.00 \times 10^{-2}/D$	$1.00 \times 10^{-1}/D$	185, p. 19-20
AUX GEN RUN	$3.00 \times 10^{-4}/HR$	$3.00 \times 10^{-3}/HR$	$3.00 \times 10^{-2}/HR$	185, p. 19-20
SWITCHES (ELEC)	$3.00 \times 10^{-5}/D$	$1.00 \times 10^{-4}/D$	3.00×10^{-4}	185, p. 19-20
MONITOR AND CONTROL	$1.00 \times 10^{-7}/HR$	$1.00 \times 10^{-6}/HR$	$1.00 \times 10^{-5}/HR$	185, p. 19-20
PUMP	$3.00 \times 10^{-6}/HR$	$3.00 \times 10^{-5}/HR$	$3.00 \times 10^{-4}/HR$	185, p. 19-20
PIPE (3 IN)	$3.00 \times 10^{-12}/H$	$1.00 \times 10^{-10}/H$	$3.00 \times 10^{-9}/H$	185, p. 19-20
ACCUMULATOR	$1.00 \times 10^{-4}/D$	$3.00 \times 10^{-4}/D$	$1.00 \times 10^{-3}/D$	185, p. 19-20
VALVES, OPERATE	$1.00 \times 10^{-4}/D$	$3.00 \times 10^{-4}/D$	$1.00 \times 10^{-3}/D$	185, p. 19-20
VALVES, REMAIN	$3.00 \times 10^{-5}/D$	$1.00 \times 10^{-4}/D$	$3.00 \times 10^{-4}/D$	185, p. 19-20
MOTORS	$3.00 \times 10^{-6}/HR$	$1.00 \times 10^{-5}/HR$	$3.00 \times 10^{-5}/HR$	185, p. 19-20
EXPLOSIVE CHARGE	$1.00 \times 10^{-4}/D$	$1.00 \times 10^{-3}/D$	$1.00 \times 10^{-4}/D$	156
CONTROL DRUMS	$6.00 \times 10^{-5}/D$	$1.80 \times 10^{-4}/D$	$5.40 \times 10^{-4}/D$	176

Data for control drums were provided by the Westinghouse Corporation (Ref. 176), and were found to be identical with that given in Reference 52, p. 453. These data were then bounded by the same error factor applied to control rods in Reference 185.

Data for explosive charges were provided by Mound Laboratories (Ref. 156). There was no information at all upon which to estimate the data variance, so the given data were taken as the median and a one order of magnitude variance either side of the median was used.

Valve data are from Reference 185, and include several types of valves. The median value was checked against handbook values for isolation valves in Reference 52, p. 354-408, and was found to be identical.

Pipe failure rates are based on historical data from both nuclear and industrial applications and are defined to be average values for rupture of pipe sections between major discontinuities such as valves, welds, etc. The averaging process utilizes a constant value for pipe failure rate regardless of pipe length.

A.8.1.3.2 TRANSIENT EVENT RATES: The transient event rate was taken from Reference 185, Appendix V, p. 56, where transient is defined as a condition imposed on the reactor coolant system that results in a demand for reactor shutdown. The rate is based on historical data of such shutdowns in ground-based power generating systems, and is given as log-normally distributed with 5th, 50th, and 95th percentiles of 5.70×10^{-4} , 1.14×10^{-3} , and 2.28×10^{-3} , transients per hour, respectively

A.8.1.4 CONTAINMENT VESSEL IMPACT DATA

A.8.1.4.1 CONTAINMENT VESSEL IMPACT RUPTURE DATA: Impact tests of simulated containment vessels were conducted by the National Aeronautics and Space Administration (NASA) (Ref. 144) and the Air Force Weapons Laboratory (AFWL) (Ref. 75) to test the impact rupture survivability. The tests simulated containment vessels of approximately 20 ft diameter and approximately 500,000 lbs impacted against concrete obstacles at various speeds. Results of those tests are given in Table A.8.1.4-1.

TABLE A.8.1.4-1. CONTAINMENT VESSEL IMPACT TESTS

TEST	AGENCY	IMPACT SPEED FT/SEC	RESULTS
1	NASA	241	NO RUPTURE
2	NASA	392	NO RUPTURE
3	NASA	413	NO RUPTURE
4	NASA	467	NO RUPTURE
5	NASA	580	NO RUPTURE
6	AFWL	641	NO RUPTURE
7	AFWL	915	RUPTURE
8	AFWL	1000	NO RUPTURE
9	AFWL	1055	NO RUPTURE
10	AFWL	1080	RUPTURE
11	AFWL	1100	RUPTURE

An assumption was made, based on References 125 and 89, that the failure probability of the containment vessel as a function of impact speed was normally distributed. Graphical modeling techniques yielded a mean of 980 ft/sec and standard deviation of 90 ft/sec. However, a slightly more conservative approach was used by setting $P(\text{failure}) = 0.33$ at $V = 914$ ft/sec (1/3 of total failures) and $P(\text{failure}) = 0.95$ at $V = 1100$ ft/sec.

Utilizing the normal Z statistic

$$Z_{0.33} = \frac{915 - \bar{S}}{\sigma}$$

$$Z_{0.95} = \frac{1100 - \bar{S}}{\sigma}$$

the solution yields a mean (\bar{S}) of 954 ft/sec and a standard deviation (σ) of 88 ft/sec giving a Z statistic of

$$Z = \frac{S - 954}{88}$$

S = impact rupture speed

(A.8.1.4-1)

This distribution gives the probability of rupture for a given impact speed. For example, if

$$S = 1000 \text{ ft/sec}$$

then

$$Z = 1.07$$

and from normal probability tables

$$P(\text{rupture}) = 0.857$$

In order to find the probability of rupture, the impact speed must be known, but the impact speed is a random variable as shown in Section A.8.1.1.2. To find the probability of rupture, the technique employed in Reference 125, pp. 152-158, was used. The method computes the probability of rupture as a normal distribution with Z statistic:

$$Z = \frac{\bar{S} - \bar{V}}{\sqrt{\sigma_S^2 + \sigma_V^2}}$$

\bar{S} = mean impact rupture speed

\bar{V} = mean impact speed

σ_S = impact rupture speed variance

σ_V = impact speed variance

Utilizing Eqs. A.8.1.1.2-1 and A.8.1.4-1 gives the probability of rupture for an airport crash:

$$Z = \frac{954 - 195}{\sqrt{88^2 + 66^2}} = 6.9$$

$$P(\text{rupture} | \text{airport crash}) = 2 \times 10^{-12}$$

and Eqs. A.8.1.1.2-2 and A.8.1.4-1 give

$$Z = \frac{954 - 583}{\sqrt{88^2 + 269^2}} = 1.31$$

$$P(\text{rupture} | \text{cruise crash}) = 9.51 \times 10^{-2}$$

It is to be noted that these figures apply only to impacts against hard surfaces (concrete). Further modeling to account for different weights and impact surfaces is performed in Section A.8.1.3.6.

A.8.1.4.2 CONTAINMENT VESSEL IMPACT BURIAL DATA: Testing was conducted by NASA (Ref. 143) to determine burial characteristics of a simulated containment vessel when impacted against soil. The results yielded the following empirical equation:

$$D = 0.0031 S N \left(\frac{W}{A} \right)^{1/2} (V - 100) \quad (\text{A.8.1.4.2-1})$$

where

- D = penetration depth (ft)
- V = impact velocity (ft/sec)
- W = containment vessel weight (lbs)
- A = frontal area (sq in)
- N = nose performance coefficient
- S = soil constant

The penetration depth, D, is measured along the velocity vector (Figure A.8.1.4.2-1) and the depth of burial was defined as:

$$H = D \times \sin(\theta)$$

θ = impact angle

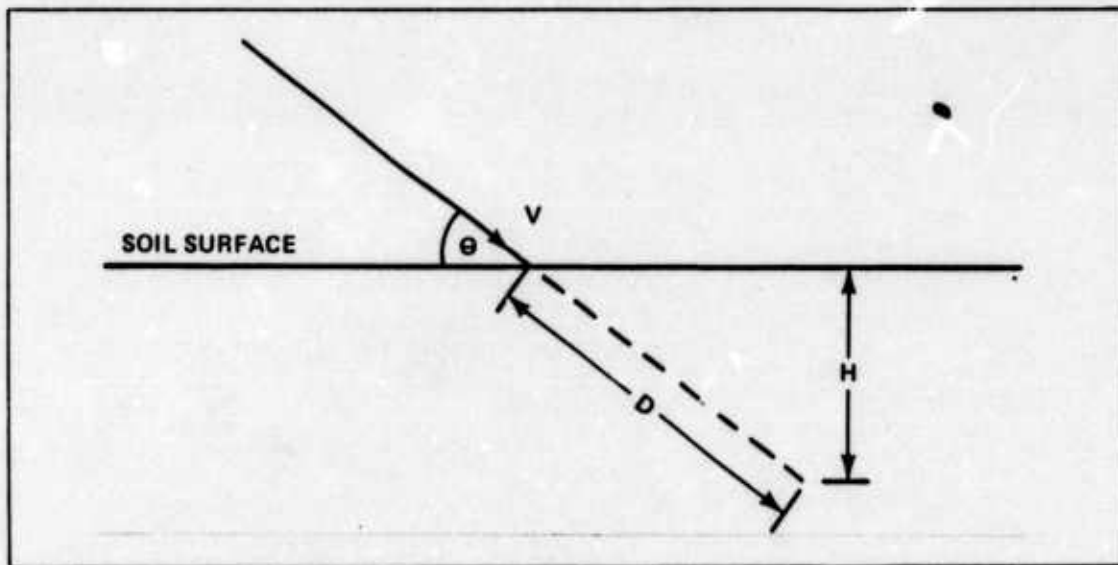


Figure A.8.1.4.2-1. Soil Impact Burial

The nose performance coefficient, N, uses a value of 0.7 for a sphere and for this study the soil constant was chosen to be 7.5 (packed soil). For a 20 ft diameter containment vessel weighing 1,000,000 lbs, the expression for H is:

$$H = 0.0765 \times (V - 100) \times \sin(\theta) \quad (\text{A.8.1.4.2-2})$$

in which both impact velocity and impact angle are random variables. A depth of burial probability distribution was generated via Monte Carlo simulation using random selections of impact velocity and impact angle. The results are summarized in Table A.8.1.4.2-1.

TABLE A.8.1.4.2-1. DEPTH OF BURIAL PROBABILITY DISTRIBUTION

BURIAL DEPTH (FT)			
0.05	0.50	0.95	MEAN
0.066	1.250	49.00	9.340

A.8.2 REACTOR SAFETY STUDY VALIDATION

The WASH-1400 report contains a consequences model that is constructed for a large fixed nuclear reactor. Since this model appeared to be applicable in most parts to a movable reactor, it was decided to validate the model. After each of the equations was researched as to its source, one particular ground reactor accident sequence was followed through to determine its associated number of immediate deaths. The sequence was divided into four basic sections: first, determine the amount of radioactivity released; second, model the dispersion of the release; third, a population model to estimate the exposed people; last, to approximate the number of deaths using a medical effects model. The particular sequence chosen was the one resulting in the maximum number of deaths.

A.8.2.1 MAGNITUDE OF RELEASE: The accident with the highest number of fatalities was a category 2 release for a pressurized water reactor (PWR) (Ref. 185, Appendix VI, p. 90). This accident assumes that the core melts and the released fission products can readily escape to the outside atmosphere. The products leak out at ground level, but approximately one-fourth of them are trapped in the containment building.

Table A.8.2.1-1 shows the activity of all the fission products produced by a 3200 megawatt reactor using UO₂ fuel. When the core melts, however, not all of these are released. Only the products that are in a gaseous state will escape from the molten mass (See Table A.8.2.1-2).

All releases are grouped by similar magnitudes of release into nine categories for the PWR and six for the boiling water reactors (BWR). Category 2 release for both reactors assumes that a near maximum amount of fission products are released at ground level. Each sequence in a category will release slightly different amounts because the circumstances for each are different. WASH-1400 used a computer code to figure the exact amount released for each sequence. The percentages used in this validation are slightly higher than WASH-1400 report used for a category 2 release because the details of the computer code were not available. The WASH-1400 report assumed that approximately 17% of the fission products will plate out on the cooler parts of the reactor, containment, etc.

**TABLE A.8.2.1-1. SET OF INITIAL ACTIVITY OF FISSION PRODUCTS
USED IN MODEL**

NUMBER	NAME	SOURCE (CURIES X 10 ⁹)	HALF-LIFE (DAYS)
1	KR-85	0.006	3.900E 03
2	KR-85*	0.26	1.800E-01
3	KR-87	0.52	5.300E-02
4	KR-88	0.76	1.160E-01
5	SR-89	1.1	5.060E 01
6	SR-90	0.052	1.050E 04
7	SR-91	1.3	4.000E-01
8	Y-90	0.052	2.700E 00
9	Y-91	1.4	5.900E 01
10	ZR-95	1.6	6.550E 01
11	ZR-97	1.6	7.000E-01
12	NB-95	1.6	3.500E 01
13	MO-99	1.6	2.800E 00
14	TC-99*	1.4	2.500E-01
15	RU-103	1.0	4.000E 01
16	RU-105	0.58	1.800E-01
17	RU-106	0.19	3.680E 02
18	RH-105	0.58	1.500E 00
19	TE-129	0.28	4.800E-02
20	TE-129*	0.10	3.410E 01
21	TE-131*	0.15	1.250E 00
22	TE-132	1.2	3.250E 00
23	I-131	0.85	8.050E 00
24	MI-131	0.85	8.050E 00
25	I-132	1.2	1.000E-01
26	I-133	1.7	8.750E-01
27	I-134	2.0	3.600E-02
28	I-135	1.5	2.800E-01.
29	MI-135	1.5	2.800E-01
30	XE-133	1.7	5.300E 00
31	XE-135	0.26	3.800E-01
32	CS-134	0.017	7.520E 02
33	CS-136	0.06	1.290E 01
34	CS-137	0.058	1.100E 04
35	BA-140	1.6	1.280E 01
36	LA-140	1.6	1.660E 00
37	CE-141	1.6	3.280E 01
38	CE-143	1.5	1.370E 00
39	CE-144	1.1	2.850E 02
40	PR-143	1.5	1.360E 01
41	ND-147	0.6	1.100E 01
42	PM-147	0.17	9.600F 02
43	PM-149	0.4	2.200E 00
44	PU-238	0.001	3.200E 04
45	PU-239	0.0001	8.700E 06

**TABLE A.8.2.1-2. AMOUNT OF RADIOACTIVE ISOTOPES RELEASED
WHEN FISSIONIZED UO₂ MELTS**

FISSION PRODUCTS	PERCENTAGE RELEASED
Kr, Xe, I, Br,	90
Cs, Rb,	83
Te, Se, Sb,	15.1
Sr, Ba,	10
Ru, Mo, Pd, Rh, Tc,	3
La, Nd, Y, Ce, Pr } Pm, Np, Pu, Zr, }	0.3

Each percentage from Table A.8.2.1-2 was multiplied by the activity available from Table A.8.2.1-1. Their total shows that 13.3×10^8 curies are available immediately after shutdown. This is 0.336 of the activity of all 45 isotopes listed in Table A.8.2.1-1. The release time was assumed to be one hour.

Using a simplified version the Way-Wigner formula:

$$A = A_0 t^{-0.2} = 13.3 \times 10^8 (3600)^{-0.2} = 2.59 \times 10^8 \text{ curies.}$$

are available at one hour but, only 3/4 of the total escapes

so, $3/4(2.59 \times 10^8) = 1.94 \times 10^8$ curies

is the total activity that escapes to the atmosphere.

A.8.2.2 DISPERSION MODEL: As the cloud of radioactivity is moved from the reactor site by the wind, its concentration is changed. The concentration is reduced by the cloud expanding and by minute particles falling from the cloud. The activity of the fission products is constantly decreasing with time, so the level of concentration of activity in the cloud is also time varying. This model attempts to determine the concentration of the escaping radioactive cloud in curies per cubic meter. The concentration problem is a complex, three dimensional, time varying one, but there are approximations available for its solution (Ref. 160, p. 403).

To calculate the concentration of the cloud of radioactive particles that escaped, WASH-1400 used the Pasquill expression:

$$X(x) = \frac{Q}{c Au + \sqrt{2\pi} \pi f x \sigma_z(x) u \exp(h^2/2\sigma_z^2)} \quad (\text{A.8.2.2-1})$$

where $\chi(x)$ = cloud concentration at radial position x (curie-sec/m³)
 Q = source (curies)
 f = angular sector width (fraction of circle)
 u = wind velocity (m/sec)
 $\sigma_z(x)$ = standard deviation for vertical diffusion (m)
 h = release height (m)
 cA = effective area of building (2000 m²)—used only when $h = 0$ and $u \geq 1$ m/sec

This expression was adapted from the cross-wind integrated equation by assuming the cloud was uniformly distributed across an arc of a particular width (Ref. 160, p. 113). To facilitate the calculations the cloud movement was broken into intervals. Since the interval length used by WASH-1400 was not given, x was incremented in 500 meter intervals, as illustrated in Figure 8.2.2-1.

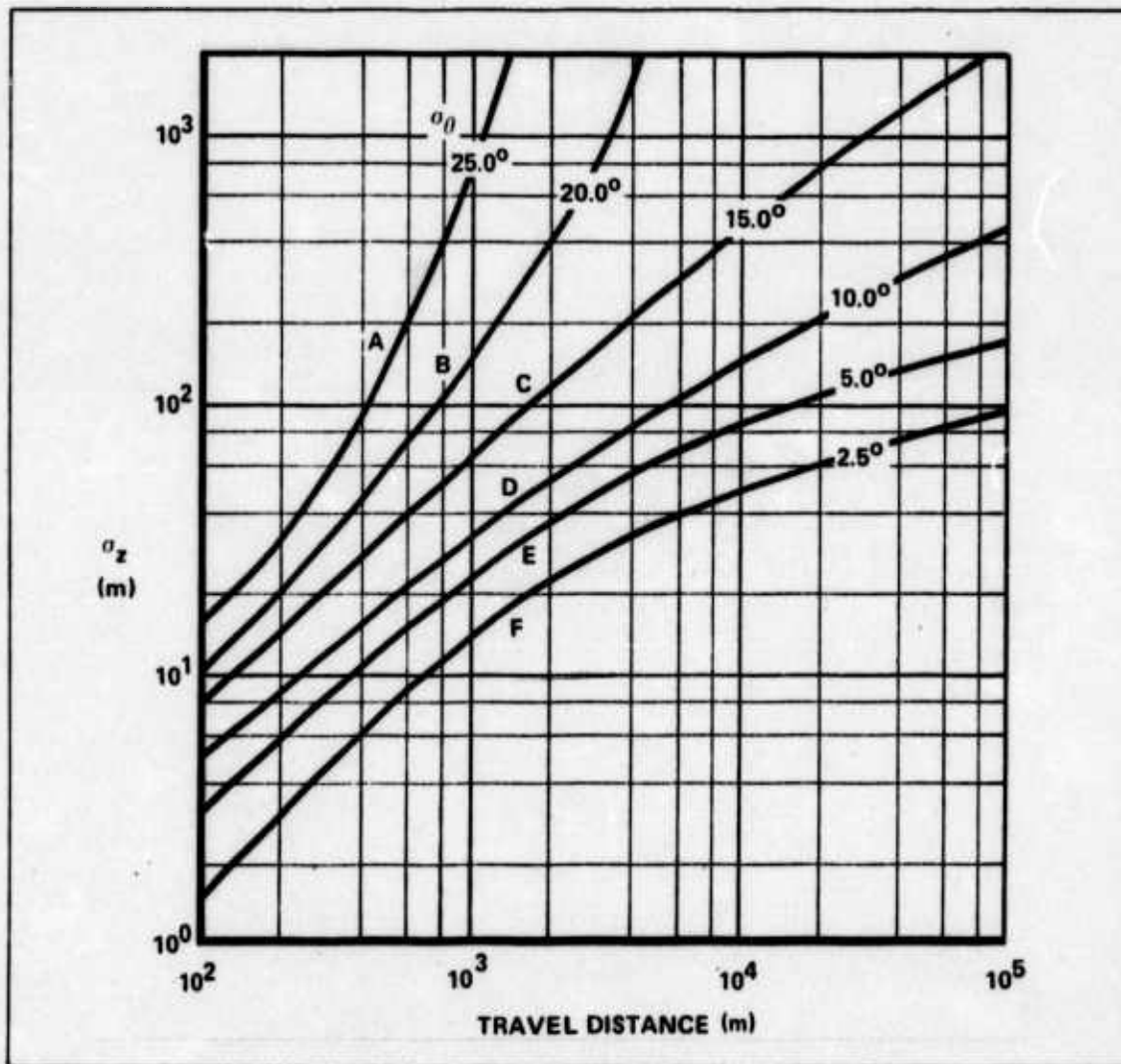


Figure A.8.2.2-1. Vertical Concentration Distribution

A.8.2.2.1 WIND STABILITY: The angle of the arc and the vertical diffusion of the cloud are determined by the stability of the wind. Pasquill classifies wind into six categories of stability. Figure A.8.2.2-1 shows the vertical diffusion for all the categories while Table A.8.2.2-1 has the arc of lateral dispersion specified in fractions of a circle and degrees. Table A.8.2.2-1 also shows the probability of each combination of wind velocity and stability classification. These probabilities come from averaging the weather of 39 reactor sites located in 27 different states.

TABLE A.8.2.2-1. METEOROLOGICAL PARAMETERS

NUMBER	STABILITY CLASSIFICATION	RELATIVE PROBABILITY	WIND VELOCITY (M/SEC)	SECTOR (FRACTION OF CIRCLE)
1	A	1.02E-02	8.00E-01	1.11E-01
2	A	1.94E-02	2.50E-00	1.11E-01
3	A	1.41E-02	4.50E 00	1.11E-01
4	A	0.96E-02	7.00E 00	1.11E-01
5	B	6.72E-03	8.00E-01	8.30E-02
6	B	0.98E-02	2.50E 00	8.30E-02
7	B	8.10E-03	4.50E 00	8.30E-02
8	B	8.60E-03	7.00E 00	8.30E-02
9	C	1.10E-02	8.00E-01	5.50E-02
10	C	2.95E-02	2.50E 00	5.50E-02
11	C	3.00E-02	4.50E 00	5.50E-02
12	C	2.15E-02	7.00E 00	5.50E-02
13	D	3.23E-02	8.00E-01	4.20E-02
14	D	7.00E-02	2.50E 00	4.20E-02
15	D	7.70E-02	4.50E 00	4.20E-02
16	D	7.20E-02	7.00E 00	4.20E-02
17	E	5.60E-02	8.00E-01	2.80E-02
18	E	0.98E-01	2.50E 00	2.80E-02
19	E	7.96E-02	4.50E 00	2.80E-02
20	E	6.22E-02	7.00E 00	2.80E-02
21	F	7.30E-02	8.00E-01	2.10E-02
22	F	5.91E-02	2.50E 00	2.10E-02
23	F	3.11E-02	4.50E 00	2.10E-02
24	F	2.12E-02	7.00E 00	2.10E-02
25	D(RAIN)	0.91E-01	2.50E 00	4.20E-02

A.8.2.2.2 DEPOSITION: As the cloud moves from the site, it deposits minute radioactive particles along its path. The depletion of the cloud was computed in the WASH-1400 report at each interval using

$$\text{where } fr_k = \frac{v \delta x_k}{\bar{z}_k U}$$

fr_k = fraction deposited in interval k.

$$\bar{z}_k = \sqrt{\pi/2} \sigma_z \exp(h^2/2\sigma_z^2)$$

v = the particles falling velocity.

δx_k = 500 meters (Ref. 185, Appendix VI, p. 20)

By assuming that the release height is always zero, then

$$\bar{z}_k = 1.25 \sigma_z$$

The falling velocities (v) were assumed to be 0.5 cm/sec for iodine and 0.2 cm/sec for all other particles. These are approximate values and are considered to be conservative (Ref. 46, p. 109).

The total activity released as calculated in Section A.8.2.1 has 23.7% Noble Gas (Xenon and Krypton), 65% iodine, and 11.3% of all others. The Noble Gases do not fall out like the other two groups. Substituting these percentages into the previous equation yields:

$$fr_k = \frac{0.65 (0.005) 500}{\bar{z}_k U} + \frac{0.113 (0.002) 500}{\bar{z}_k U} = \frac{1.39}{\sigma_z U}$$

To obtain an accurate measure of the total fraction remaining in the cloud the following equation was used:

$$FM_k = \exp \left\{ - \sum_{i=1}^{K-1} fr_i \right\}$$

This gives the amount of the cloud over interval k as the negative exponential of the sum of the previous fractions.

A.8.2.2.3 DISPERSION SUMMARY: Following through the maximum credible accident, the wind is given as classification F (See Table A.8.2.2-1) with velocity 0.8 meters/sec. (Ref. 185, Appendix VI, p. 90).

Using Eq. A.8.2.2-1

$$X(x) = \frac{1.94 \times 10^8}{0.338 + 7.87 (0.021) 500 (7.8) 0.8} = 3.76 \times 10^5 \frac{\text{curie-sec}}{\text{cubic meter}}$$

The fraction of the cloud deposited is given by

$$fr_k = \frac{1.39}{7.8 (0.8)} = 22\%$$

This leaves

$$FM_k = e^{-22} = 80\%$$

of the fission products still in the cloud.

Therefore at the end of 500 meters of travel the concentration of the cloud is 3.02×10^5 curies per cubic meter. The effective area of the building term (cAu) becomes insignificant as the cloud moves over 100 meters away from the building. The only new inputs in each interval were the σ_z , x , and the decayed value of Q . The σ_z comes from Table A.8.2.2-1 and the Q is computed using the cumulative elapsed time from cloud release to the start of the interval.

For example for 1000 meters:

$$\sigma_z = 12.8 \text{ meters}$$

and

$$Q = \frac{13.31 \times 10^8}{(4100)^{0.2}} = 1.89 \times 10^8 \text{ curies}$$

A.8.2.3 POPULATION MODEL: This model is divided into a population distribution and evacuation scheme. It first computes the number of people that could be exposed, then it allows for some to escape exposure or to receive partial exposure.

A.8.2.3.1 POPULATION DISTRIBUTION: Population data from 66 reactor sites were used in the WASH-1400 Report to form a distribution. The area surrounding each site was divided into 16 equal sectors. All the data were ordered in descending order by sector and averaged. The averages of all the sites are shown in Table A.8.2.3-1.

The worst accident, of course, assumes the highest population density which is the top line on Table A.8.2.3-1. The 160 people in the first two miles were assumed to be uniformly spread throughout the two miles of the sector. Since stability classification F covers only $7\frac{1}{2}^\circ$, only 1/3 of the sector is covered by the cloud. So within 2 miles only 53 people are exposed and out to 5 miles only 1266 are exposed. At 10 miles (16,000 meters) the normal 500 meter interval contains 0.78 sq mi with 1643 people per sq mile for a total of 1287 people.

**TABLE A.8.2.3-1. CUMULATIVE POPULATION (THOUSANDS) OF CATEGORIES
AT SELECTED DISTANCES FOR A 22½° SECTOR**

CATEGORY	DISTANCE (MILES)				
	2	5	10	20	50
1 (99-100%)	0.16	3.8	28.0	279	1057.9
2 (97-99%)	0.2	2	15.6	136	1341.5
3 (95-97%)	0.45	2.1	11.8	92.1	895.8
4 (90-95%)	0.22	2.8	11.5	52.9	279.1
5 (80-90%)	0.21	2	7.6	26.1	220.0
6 (70-80%)	0.2	1.1	3.6	13.2	151.8
7 (60-70%)	0.06	0.5	2.3	8	119.5
8 (50-60%)	0.07	0.5	1.6	5.3	65.8
9 (40-50%)	0.03	0.2	1.1	3.6	39.8
10 (30-40%)	0.01	0.1	0.75	2.3	52.5
11 (20-30%)	0.1	0.09	0.3	1.3	29.9
12 (10-20%)	0.1	0.04	0.2	0.5	19.6
13 (0-10%)	0	0	0	0	0

A.8.2.3.2 EVACUATION MODEL: In most reactor accidents there will be at least an hour of warning time before the majority of the fission products are released. This time could be effectively used to evacuate a large number of people. The expression used by WASH-1400 was that in each specified interval i , the population was reduced by the factor F_i where:

$$F_i = a + (1 - a) \exp \{ - \lambda (t_i - TL + T_j) \}$$

and

- a = fraction of population unaffected by evacuation = 0.1
- λ = measure of evacuation rate = 8.3 days⁻¹
- t_i = time for cloud transport to mesh point i = 0.26 days
- T_j = time between awareness of impending core melt and leakage for accident type j = 1.5 hours or 0.063 days
- TL = time lag associated with interpretation of data and issuance of warning to evacuate = 0.02 day.

a , λ , and TL are constant for all accidents but T_j depends on the accident type.

At the interval ending at 10 miles (16,000 meters)

$$\begin{aligned} F_{16} &= 0.1 + (0.9) \exp \{ -8.3(0.26 - 0.02 + 0.063) \} \\ &= 0.17 \end{aligned}$$

The number of people in this interval was calculated at the end of the previous section as being 1287. Therefore 1287 (0.17) or 1073 people are left to evacuate with the half life of two hours. So two hours later 537 people remain, at four hours later 268 people remain, etc.

A.8.2.4 MEDICAL EFFECTS: This model was used to translate the number of people exposed to varying levels of radiation into the statistics of acute deaths, illness, and property damage. Acute deaths were defined as any deaths in the 30 days following the accident. WASH-1400 considered the vulnerability of the lungs, GI tract, and whole body to a radioactive dose. Of these, the whole body dose was found to be the major contributor. For the validation, this study considered only the acute deaths resulting from a whole body dose (WBD).

The WBD includes the radioactive dose received from particles inhaled from the cloud, from the cloud itself, and from the particles deposited on the ground. The probability distribution used by WASH-1400 to compute deaths from the dose received is shown in Figure A.8.2.3-1.

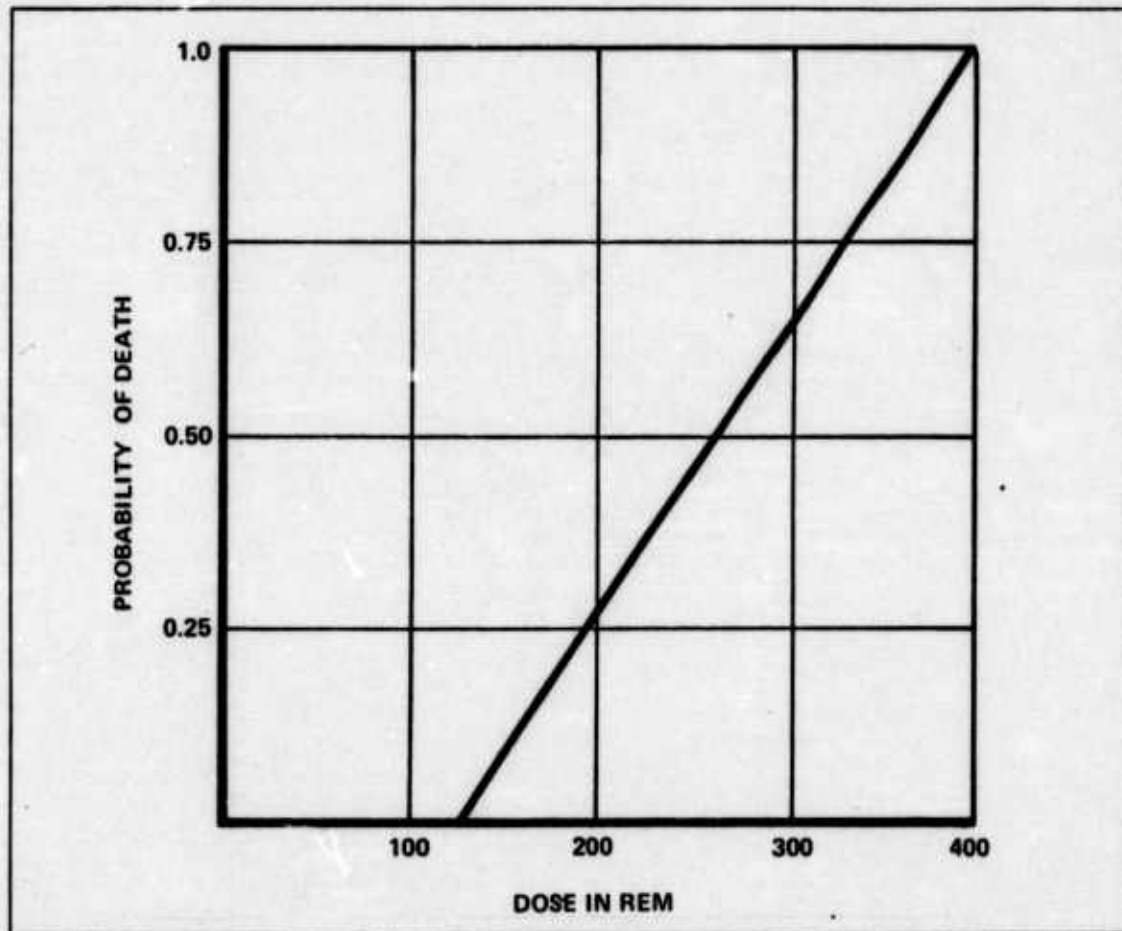


Figure A.8.2.3-1. Dose vs Probability of Death

A.8.2.4.1 INHALATION: As a cloud of minute fission products passes, everyone engulfed in the cloud would inhale an amount of radioactive material that depends on the concentration of the cloud. The concentration in 500 meter intervals has been computed, but

needs to be converted to a dose in REM. Table A.8.2.4-1 assists in making this conversion. Several values from this table were picked at random and verified (Ref. 46, p. 95). Each value was multiplied by the percentage it contributed to the total and then summed. For example I_{132} contributes 9.6% of the clouds activity so its WBD for a 30 day total would be 11 REM per curie. The total of all the isotopes came to 560 (REM per curie).

A breathing rate of 2.2×10^{-4} cubic meters per second was assumed and multiplied times the WBD_{30} total to complete the conversion factor of 0.12 REM cubic meters/curie-sec.

A.8.2.4.2 CLOUD SHINE: When exposed to a radioactive source, which in this case, is a cloud, a person will receive a dose that is proportional to the concentration of the cloud. Using the values from Table A.8.2.4-2 and the same procedure as in Section A.8.2.4.1, a conversion factor for cloud shine of 0.274 REM cubic meters/curie-sec was computed. This was reduced to one third its value due to the fact that people spend the vast majority of their time indoors. The final cloud shine conversion was 0.0913 REM cubic meters/curie-sec.

A.8.2.4.3 GROUND DEPOSITION: The passing cloud left radioactive particles which are assumed to be evenly distributed over a 500 meter interval. To complete the dose of these particles, the values from Table A.8.2.4-2 were multiplied by their percentage of the total activity and then summed. This yields 13.17 REM square meters/curie/hour. This is corrected for the effect of shelter by multiplying by 1/3 to yield 4.39 REM square meter/curie-hour. By multiplying the fraction of the cloud deposited in each interval (from Section A.8.2.2.2) by the curies available at the time, one obtains the initial deposition activity for that interval. The activity per unit area is obtained by dividing by the area of the interval. This multiplied by the 4.39 REM square meters/curie-hour yields REM/hour for the ground deposition dose rate.

A.8.2.4.4 SUMMARY: To obtain the number of deaths, each interval must be considered separately. The WBD from inhalation and cloud shine could be immediately computed by assuming the cloud concentration remained constant through the interval and that no one left while the cloud was passing. The WBD from ground deposition depends almost completely on the evacuation model. The people evacuated in each two hour period following cloud passage were assumed to receive the average ground dose for that period. This dose was then added to the WBD for inhalation and cloud shine for the total WBD. With this total WBD in REM, Figure A.8.2.3-1 will give the probability of death for those people evacuated in that two hour period. The acute deaths for that two hour period became simply the product of the number of people evacuated and the probability of death. Each two hour period was computed until everyone was evacuated; then all periods were totaled. This total is for one 500 meter interval so all intervals were so computed and totaled. This was the grand total of people killed by that particular accident sequence for those weather and population combinations.

The interval ending at 8000 meters (approximately 5 miles) was chosen to illustrate the procedure of computing the acute deaths due to WBD.

1. From the top line of Table A.8.2.3-1, the people in the $22\frac{1}{2}^\circ$ sector from 2 to 5 miles is $(3800 - 160) = 3640$.

TABLE A.8.2.4-1. INHALATION DOSE FACTORS (REM/CI) X 10³

NAME	WBD (30d)
KR-85	0.0
KR-85*	0.0
KR-87	0.0
KR-88	0.0
SR-89	3.90E 00
SR-90	1.60E 00
SR-91	3.52E-01
Y-90	6.00E-01
Y-91	2.60E 00
ZR-95	4.90E 00
ZR-97	3.90E-01
NB-95	2.00E 00
MO-99	6.61E-01
TC-99*	8.40E-03
RU-103	7.71E-01
RU-105	6.44E-02
RU-106	2.85E 00
RH-105	9.75E-02
TE-129	2.00E-02
TE-129*	4.40E 00
TE-131*	7.32E-01
TE-132	1.96E 00
I-131	2.40E 00
OI-131	2.40E 00
I-132	1.30E-01
I-133	5.70E-01
I-134	4.00E-02
I-135	2.90E-01
OI-135	2.90E-01
XE-133	0.0
XE-135	0.0
CS-134	1.50E 01
CS-136	5.50E 00
CS-137	8.20E 00
BA-140	7.20E 00
LA-140	8.35E-01
CE-141	8.10E-01
CE-143	3.37E-01
CE-144	6.60E 00
PR-143	1.13E 00
ND-147	1.16E 00
PM-147	3.60E-01
PM-149	3.11E-01
PU-238	3.04E 02
PU-239	2.83E 02

TABLE A.8.2.4-2. AVERAGE DECAY ENERGIES AND DOSE FACTORS
FOR GROUND DEPOSITION AND CLOUD SHINE

NUMBER	NAME	GROUND (REMS/HR)/(CI/m ²)	CLOUD REMS/(CI-SEC/m ³)
1	KR-85	0.0	0.0
2	KR-85*	3.0	0.036
3	KR-87	10.0	0.36
4	KR-88	30.0	0.42
5	SR-89	0.0	0.0
6	SR-90	0.0	0.0
7	SR-91	14.2	0.16
8	Y-90	0.01	0.002
9	Y-91	0.01	0.002
10	ZR-95	10.0	0.19
11	ZR-97	11.9	0.06
12	NB-95	10.2	0.18
13	MO-99	3.6	0.06
14	TC-99*	2.0	0.035
15	RU-103	7.2	0.11
16	RU-105	9.0	0.20
17	RU-106	3.0	0.05
18	RH-105	1.4	0.005
19	TE-129	1.5	0.018
20	TE-129*	1.5	0.025
21	TE-131*	16.8	0.375
22	TE-132	3.4	0.05
23	I-131	5.6	0.09
24	MI-131	5.6	0.09
25	I-132	34.0	0.55
26	I-133	7.4	0.12
27	I-134	32.0	0.60
28	I-135	24.0	0.42
29	MI-135	24.0	0.42
30	XE-133	1.0	0.007
31	XE-135	3.0	0.060
32	CS-134	24.0	0.36
33	CS-136	30.0	0.46
34	CS-137	8.4	0.13
35	BA-140	4.2	0.06
36	LA-140	30.0	0.52
37	CE-141	1.1	0.016
38	CE-143	4.4	0.085
39	CE-144	0.6	0.004
40	PR-143	0.0	0.0
41	ND-147	2.0	0.045
42	PM-147	0.0	0.0
43	PM-149	0.05	0.012
44	PU-238	0.002	0.0
45	PU-239	0.002	0.0

2. This sector contains 4.12 sq mi, so if the population is spread uniformly, there are 882 people per sq mi.

3. The area of the 500 meter interval ending at 8000 meters is 0.196 sq mi.

4. In the interval of interest are:

$$882(0.196) = 173 \text{ people}$$

5. This number is reduced thru evacuation by a factor of $F_B = 0.36$, leaving 111 people exposed to the cloud.

6. All of these people received a WBD from inhalation and cloud shine of

Conversion factors		Cloud concentration	
(0.12 + 0.09)	x	988	= 207 REM

7. The activity of the cloud at the beginning of the interval is obtained using Eq. 8.2.1-2

$$A = \frac{A_0}{t^{0.2}}$$

where A_0 is 3/4 of the released fission products and t is the time in seconds from reactor shutdown until the cloud reaches the interval.

$$A = \frac{9.98 \times 10^8}{(12975)^{0.2}} = 1.50 \times 10^8 \text{ curies}$$

8. The fraction of the initial activity remaining in the cloud at the beginning of the interval is 34%; however, at the end of the interval it is 32%. This difference gives a fraction dropped of 2%.

9. The fraction of activity dropped is therefore $1.50 \times 10^8(0.02) = 3.0 \times 10^6$ curies.

10. This was spread uniformly over the interval by dividing by the area:

$$3.0 \times 10^6 / 507,000 = 5.92 \text{ curies per sq meter.}$$

11. The initial dose from the ground is found by using the conversion factor

$$5.92 \frac{\text{curies}}{\text{sq meter}} \left(4.39 \frac{\text{REM sq meter}}{\text{curie hour}} \right) = 26 \text{ REM/hour}$$

12. The dose two hours later is 24 REM/hour so the average dose is:

$$(26 + 24)/2 = 25 \text{ REM per hour}$$

Therefore the people evacuated in the first two hour period receive a dose from the ground of 50 REM.

13. In the first two hours, one-half of the remaining 111 people leave. These 56 people receive a dose of

$$207 + 50 = 257 \text{ REM.}$$

From Figure A.8.2.3-1 they have a 0.45 probability of dying or $0.45(56) = 25$ people of this group will die.

14. In the next two hours the ground dose decreases to 22 REM/hour so the 28 people that are evacuated receive a total dose of 303 REM. This means $(.62)(28) = 17$ people from this group will die.

15. Continuing in that manner leads to a total of 63 people who received a lethal dose. By stepping through each interval in that manner, a total of 2178 people were killed by the chosen accident conditions. This is very comparable to the 2300 deaths in WASH-1400, so it was concluded that the method used was a valid one.

A.8.3 COMPUTER LOGIC DIAGRAMS: Figure A.8.3-1 shows the computer logic diagram for solution of the fault trees and Figure A.8.3-2 shows the computer logic diagram for solution of the event trees. Included in the computer program was the SIMPAK subroutines for generation of probability distributions and random sampling therefrom.

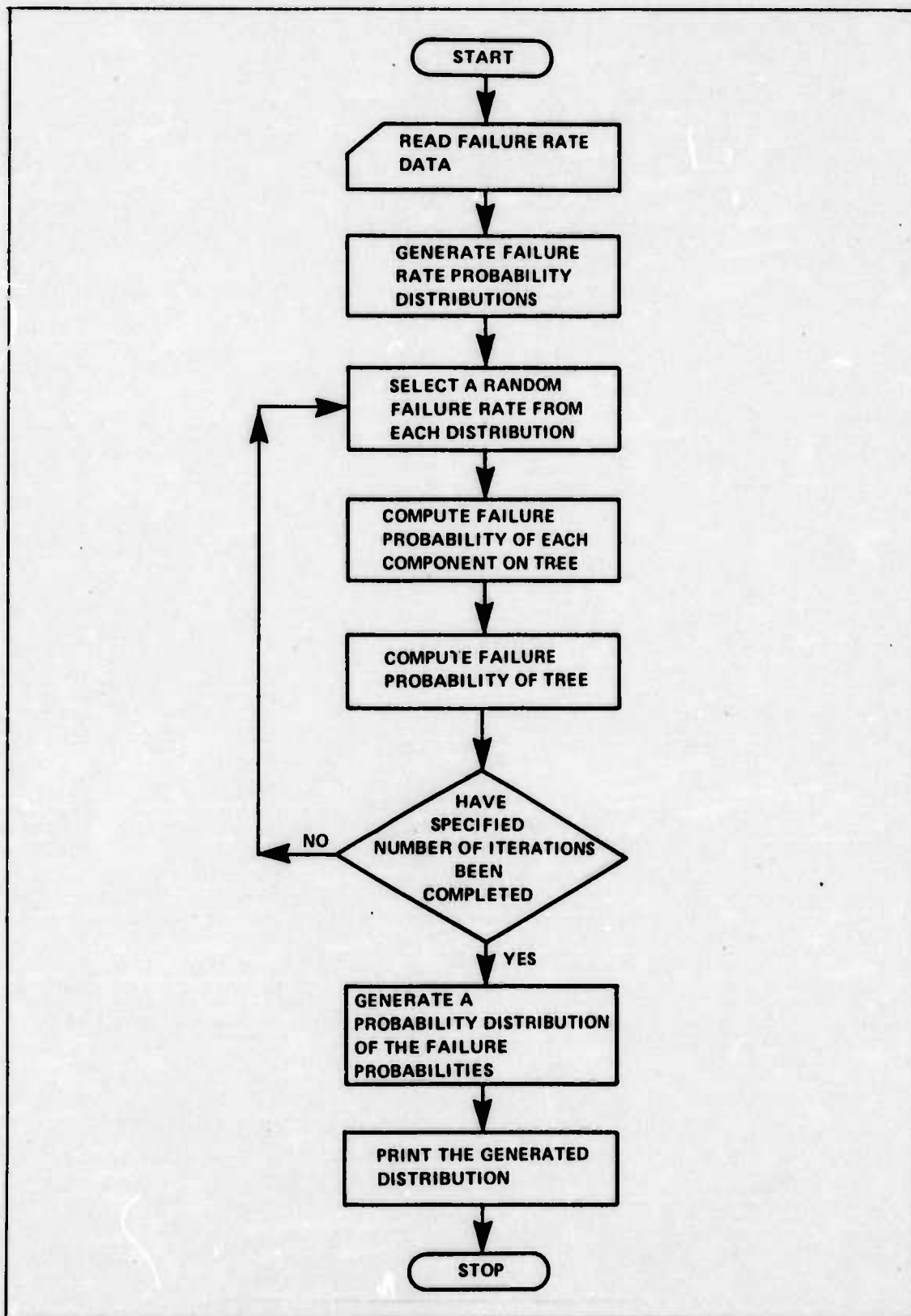


Figure A.8.3-1. Fault Tree Logic

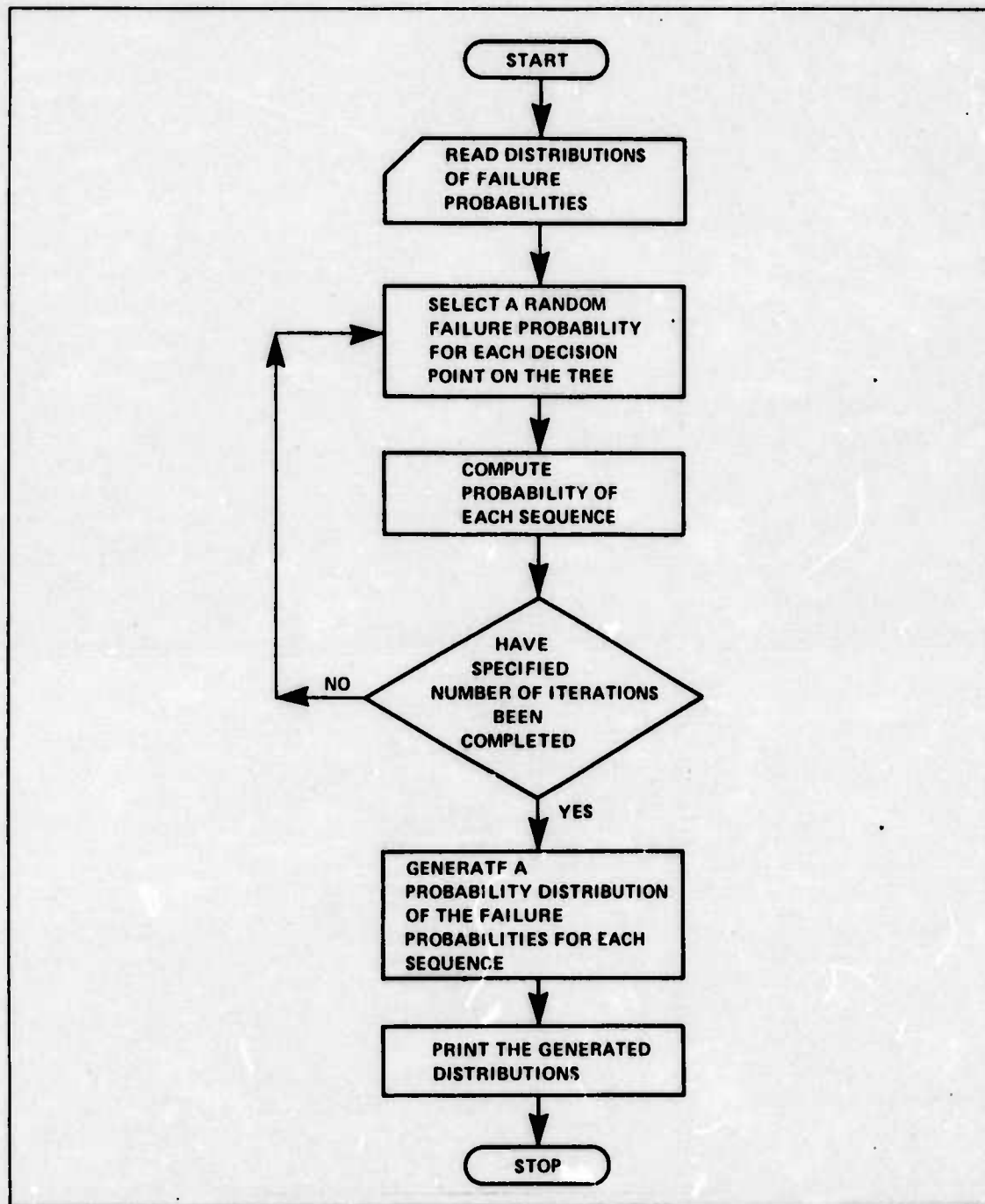


Figure A.8.3-2. Event Tree Logic

APPENDIX A.9 LIFE CYCLE COST

A.9.1 REACTOR

The nuclear reactor production cost was obtained by contacting organizations with reactor expertise. The following is a copy of the letter to these contractors.

Dear

This letter is a follow-up on the telephone conversation with _____ I had on 20 November 1974. At that time we discussed the problem faced by the Graduate Systems Engineering class in costing a proposed lightweight reactor for a nuclear airplane. As I mentioned at the time, any help we receive has to be on an unfunded basis.

Our method of costing is to break the reactor down into as many parts as feasible at this time and obtain estimates from experts in the field. These estimates are in the form of high, low, and most probable cost. The opinions will be combined statistically to obtain an estimate of the system cost.

By high cost we mean a cost that you feel is realistic and yet a zero probability of the component exceeding that cost. For the low cost we imply a cost that is realistic but with probability of one of the price exceeding. The most likely cost is, of course, your best guess.

We are aware of the "risk" involved with an estimate of reactor cost, especially with an undesigned, high technology reactor. Our approach can be presented in our study in such a way that the individual cost estimate will not be associated with the expert who gave them. Our study will list the estimates that were provided as one portion and list the experts as a group.

Since there is no hard design for the reactor, our description is, we hope, sufficient for cost estimates, and yet does not constrain the experts to any unfeasible points. The reactor as we envision it will be in the 200-400 Megawatt (thermal) range. We hope that fuel technology will have progressed to give us 500 w/cc as a core power density. The containment vessel should fit inside a 25 ft diameter aircraft hull. For safety reasons, we are leaning toward a helium cooled reactor.

In closing, I must stress that this is an academic study, not an official Air Force report, and that there are no funds available for this study and no contracts to be let. If you cannot afford to give us the breakdown, we would appreciate any unfunded help you could provide.

We do not envision this requiring an inordinate amount of your time, nor do we envision your having to do this immediately. Getting the results prior to 5 December 1974 will give us plenty of time to use them.

Attached is a breakdown sheet for your convenience.

Sincerely

RALPH J. LUCZAK
Captain, USAF
GSE-75M, Student
School of Engineering

Atch: a/s

BREAKDOWN OF ESTIMATES

COMPONENT	HIGH	MOST PROBABLE	LOW
core			
shielding			
circulation and power supply			
intermediate heat exchange			
engineering			
reactor vessel			
ducting and valving			
core reflector and control structure			
refurbishment			
allowance for auxiliaries			

ATTACHMENT 1

A.9.2 AVIONICS

The distribution of cost for a 0.95 reliable system to accomplish a 14 day mission is given in Section 9.6. Table A.9.2-1 illustrates cost distributions for reliable system other than 0.95.

**TABLE A.9.2-1. AVIONICS COST VS RELIABILITY
FOR A 14 DAY MISSION**

RELIABILITY	MILLIONS				
	0.00	0.25	0.50	0.75	1.00
0.10	8.04	8.73	9.08	9.33	9.77
0.30	10.11	11.06	11.41	11.75	12.73
0.50	11.41	12.53	12.98	13.31	13.92
0.70	13.66	15.04	15.64	15.99	16.77
0.90	17.29	18.95	19.62	20.14	21.09